UCRL 3131

UNIVERSITY OF CALIFORNIA

Radiation Laboratory

BERKELEY, CALIFORNIA

DISCLAIMER

UCRL-3131

UNIVERSITY OF CALIFORNIA

Radiation Laboratory
Berkeley, California

Contract No. W-7405-eng-48

VAPOR-LIQUID EQUILIBRIA IN THE SYSTEM HYDROGEN-NITROGEN

Arturo Maimoni

(Thesis)

September 1, 1955

Printed for the U. S. Atomic Energy Commission

VAPOR-LIQUID EQUILIBRIA IN THE SYSTEM HYDROGEN-NITROGEN

Contents

Contents (continued)

VAPOR-LIQUID EQUILIBRIA IN THE SYSTEM HYDROGEN-NITROGEN

Arturo Maimoni

Radiation Laboratory
University of California
Berkeley, California

September 1, 1955

ABSTRACT

A recirculation-type apparatus with a novel liquid-sampling system was used to obtain liquid-vapor equilibrium data for the system hydrogen-nitrogen at 90° and 95° K and pressures up to 700 psia. The data obtained show an average scatter in liquid compositions of the order of 0.01 %, thus proving the feasibility of the new liquid-sampling system.

The vapor samples are shown by thermodynamic analysis to scatter less than 0.1 % and may have a systematic error smaller than 0.2 %. Several possible methods of gas analysis capable of giving high accuracies in a minimum time are carefully examined.

Data on other systems were also obtained and will be found in a forth-coming University of California Radiation Laboratory Report.

INTRODUCTION

This report is divided into three main sections dealing, respectively, with details of the experimental technique used to obtain the liquid–vapor equilibrium data, with presentation of the data obtained and their thermodynamic analysis, and a detailed discussion of the methods used for gas analysis.

The section on equipment describes an apparatus of the recirculation type, designed for the operating range 14.5 to 2000 psia and 80° to 180° K, together with the considerations leading to its design and details of the experimental technique. It also describes the necessary auxiliary equipment, which includes a sensitive liquid-level indicator.

The presentation of the data is followed by a discussion of the possible methods for testing thermodynamic consistency, which points out the difficulty in analyzing liquid-vapor equilibrium data when the vapor cannot be treated as an ideal gas and one of the components is much above its critical temperature, leading to questionable extrapolations of its vapor pressure curve. An inferential method is developed, in which the limiting behavior of the activity coefficient of the heavy component is examined, and the data are considered to be thermodynamically consistent if the activity coefficient follows a simple relationship with concentration.

The section on analytical techniques deals with the different methods for obtaining accurate analysis of hydrogen–nitrogen mixtures and examines in detail the technique of gas analysis by optical interferometry.

EQUIPMENT

Vapor-Liquid Equilibria Equipment

The accurate measurement of liquid-vapor equilibrium compositions is not a simple experimental problem. Attempts to solve this problem have resulted in a number of designs of experimental equipment, designs which vary a great deal in their intrinsic capabilities as to type of system that may be handled and in their accuracy. Thus, it is not unusual to find deviations of ± 10% between different investigators using essentially the same techniques on the same system. This lack of consistency between data of different investigators, which may be due in part to basic design faults of their equipment and in part to individual factors, has led gradually to the development of basic thermodynamic methods to check the internal consistency of the data, until it is now becoming standard practice to test the data for thermodynamic consistency before accepting them.

Most of the equipment described in the literature is adapted for operation on binary mixtures not much above room temperature, since the experimental problems are greatly enhanced by operation on ternary and multicomponent mixtures and temperatures farther removed from room temperature. These, however, are regions of potential industrial practice.

The equipment to be described is well adapted to obtaining binary and ternary liquid-vapor equilibrium data at low temperatures and moderately high pressures; it has a novel liquid-sampling system and the data thus far obtained with it are thermodynamically consistent to the limit of accuracy of the equations of state used to test them. Some of the considerations leading to its design are described in the following sections.

Equipment and techniques adaptable to obtaining liquid-vapor equilibrium data at low temperatures and for systems above the critical temperature of one of the components may be divided into three main groups, as follows:

(a) Equipment of constant total volume charged with a known amount of mixture of known composition, which allows obtaining the PVT data

for the mixture, and from these data the boundaries of the liquid-vapor curve. For a binary mixture, the compositions of the equilibrium phases can be obtained graphically from the intersections of the phase-boundary curves. Although this method is basically sound, it is limited by the accuracy of graphical techniques, especially since the phase-boundary curves are difficult to smooth accurately.

(b) Equilibrium-bomb techniques, in which samples are obtained of the coexisting phases in equilibrium. This method involves several experimental difficulties which are met with varying degrees of success by the different investigators.

The contents of the equilibrium bomb must be agitated to reduce the time required for a given approach to equilibrium, but extensive testing is required to determine empirically if the time allowed is sufficient. This is further complicated because the time of approach to equilibrium varies with the experimental conditions, especially with the relative volatility, the viscosity, and other transfer properties of the phases. During sampling there are pressure changes due to the removal of material, and these pressure changes can be large in magnitude, thus affecting the composition of the phases being sampled. It will be shown in another section that the hydrogen-nitrogen liquid-vapor equilibria obtained by Verschoyle[46] give consistently low hydrogen concentrations in the liquid at low pressures, a fact that could be explained if it were assumed that flashing of the liquid occurred during sampling of the vapor phase. Some investigators operating near room temperature avoid this difficulty by introducing mercury into the system while the samples are being removed, but this technique is not applicable below -40°C. Another difficulty with the method is that in most cases it is necessary to use sampling lines of small cross sections. These may fill up with liquid during the initial part of the operation and introduce an error into the concentration of the liquid or of the vapor samples. It is then necessary to purge the sampling lines to remove such liquid, or to design the equipment so as to avoid dead volumes in the sampling lines.

(c) Dynamic methods, in which a means is provided for circulating the gas in the equipment. The dynamic method may be further sub-

divided into recirculation methods in which the gas is recirculated over the liquid, or once-through methods in which the gas is made to bubble through successive vessels filled with liquid. In either case the basic principle is the gradual approach of the two phases to equilibrium, and subsequent sampling of the phases for analysis.

The once-through method is more suited to low-pressure operation, wherein the number of moles of any component in the vapor phase is negligible compared to the amount in the liquid, resulting in very slow changes in the composition of the liquid phase. Very often the vapor pressure of the solution is low compared with the total pressure over the system which is supplied with an inert carrier gas. As the total pressure is increased, and with it the solubility of the carrier gas in the liquid, the method can give erroneous results if the true liquid-vapor equilibria for the mixture without carrier gas are desired.

For operations without carrier gas, the once-through method is well adapted to determinations of multicomponent liquid-vapor equilibria, since it allows control of the temperature, the pressure, and the composition of the liquid phase; however, for binary systems the method is overdefining, because temperature and pressure are in general sufficient to define the state of the system, and it may be extremely difficult to obtain a true approach to equilibrium.

The recirculation method, which was the method used in this investigation, is now considered in more detail.

The recirculation method, in which the vapor is repeatedly pumped through the liquid, is better adapted to binary and ternary than to multicomponent systems, because in the latter case it is difficult to fix the composition variables according to the Phase Rule to obtain a completely defined system.

In the determination of the liquid-vapor equilibrium compositions in binary mixtures the system is loaded with a given amount of gas of given composition, and the temperature is controlled while the pressure is the free variable. For ternary mixtures it is more convenient to control the temperature and the total pressure, and let the composition variables adjust themselves.

After a given amount of time has been allowed for the system

to come to equilibrium, samples of the liquid and vapor phases are taken. While the system appears simple, in actual practice it involves a number of complications:[37]

(1) The system must be completely leakproof, otherwise the total quantity of material in the system will vary and with it the equilibrium compositions. (Of course, this condition also applies to any of the methods described above.)

(2) This type of system is best applied when the vapor does not condense at room temperature, otherwise it may be necessary to heat the pumping system to a high temperature to avoid condensation of the vapor, and difficulties may be encountered due to vapor pressure of mercury (pump fluid) or any other pump-sealing material. Also, it is always necessary that the pumping section be at a higher temperature than the equilibrium section, which contains the liquid, otherwise local condensation in the vapor line after the pumps may occur.

(3) The quantities of liquid and vapor, when equilibrium is obtained, must remain constant and should not vary during the circulation. To assure this condition it is necessary to keep constant the total volume of the system and the temperatures in the different sections of the vapor lines. In particular, the pump design should preferably be one that does not introduce volume changes in the system, and the reservoir from which the vapor sample is taken should be thermostated.

(4) It is necessary to ensure that there is no entrainment of the liquid by the vapor leaving the equilibrium chamber, otherwise the vapor sample will be contaminated. This calls for low vapor velocities and baffles to reduce entrainment, and is a factor that contributes materially to the nonapplicability of this type of equipment to regions close to the critical conditions of the mixture, when the density differences between liquid and vapor phases become small.

(5) The choice of pumping equipment is somewhat difficult. Although a double-acting reciprocating mercury-piston type pump is perhaps the easiest to achieve experimentally and maintains a constant total volume for the system, it introduces undesirable fluctuations in the pressure and flow rate of the gas. The effect of these fluctuations is twofold; the pressure fluctuations change the distribution of gas in

the different sections of the system and may have some effect on the material balance relationships that should apply at equilibrium, and also, these pressure fluctuations of the vapor in contact with the liquid may lead to slightly different values for the equilibrium compositions than will be obtained if the pressure is maintained steadily at the arithmetic mean pressure, which is the value measured by the pressure transducers.

The above effects would be especially noticeable at low pressures, where the fluctuation is an appreciable fraction of the total pressure, and in the critical region where the properties of the phases change very rapidly with slight changes in experimental conditions.

By proper design of the pumping system it may be possible to "filter" most of the fluctuations before they reach the liquid, and thus eliminate some of the above objections.

(6) A definite advantage of the recirculation equipment is that the time required for a given approach to equilibrium is short and can be predicted for the different experimental conditions, a matter which is discussed in a later section.

(7) There is another small uncertainty connected with the measurement of the pressure at equilibrium which arises from the bubbling of the vapor through the liquid. This bubbling action implies that the pressure of the gas coming in contact with the liquid is higher than the pressure of the gas leaving the liquid by the amount of liquid head. Under most experimental conditions this effect can be neglected, but limits the operation of the equipment in the region of low pressure or very near the critical region.

(8) Probably the greatest disadvantage of recirculation equipment is its complexity, which is enhanced by all the auxiliary equipment, such as that for purification and storage of the raw gases, the vacuum system for withdrawing and handling the vapor and liquid samples, and the analytical equipment. The above considerations are perfectly general and apply to all the types of recirculation equipment reported in the literature, including the one to be described shortly.

Perhaps the only claim for novelty of the equipment used in

this work is the liquid-sampling system. Most of the equipment described in the literature follows the design of Dodge and Dunbar,[8] which avoids the complication of having a valve in the low-temperature section for sampling the liquid by having a long capillary line immersed in the liquid in the low-temperature section, and having the liquid-sampling valve outside the cold thermostat. This procedure introduces uncertainty in the composition of the liquid sample due to purging and the possibility of flashing of the liquid in the capillary line.

The liquid-sampling system used in this work is discussed with reference to Fig. 1, which is a simplified flow diagram of the recirculation equipment. The equipment is filled with gas by opening valve V-15 leading to the purification and storage manifold. Once the desired amount of gas is inside the equipment, the double-acting mercury-piston pump is turned on, forcing the gas to circulate along the path indicated by the heavier line in Fig. 1. Meanwhile all the bypass valves V-6, V-10, and V-11 are closed. After the gas leaves the pump it passes through a rotameter to the cold thermostat, where the cooling coil cools it to the operating temperature of the thermostat. The gas then follows the path through V-7, PV-3, V-8, the liquid-sampling valve V-1, and V-9, and bubbles through the liquid in the equilibrium cell PV-1. After the vapor leaves the liquid, it goes through a series of baffles inside PV-1, which remove the liquid entrained. The gas leaving PV-1 goes through V-3 and then outside the cold thermostat to a heating coil in the intermediate water bath. From there it goes back into the main water bath and through V-4, V-2, PV-4, and V-5 back to the inlet of the pumps.

After sufficient time has been allowed for the vapor and liquid phases to come to equilibrium, the bypass valves V-6, V-10, and V-11 are opened to flush the small amount of gas present in those lines with equilibrium gas. After about two minutes of flushing the normal circulating path is resumed for another five minutes, and again the bypass valves are flushed. Then, after sufficient time is allowed for the system to go back to equilibrium conditions, the liquid and vapor samples are taken as follows:

1. Valves V-11, V-10, and V-6 are opened consecutively.

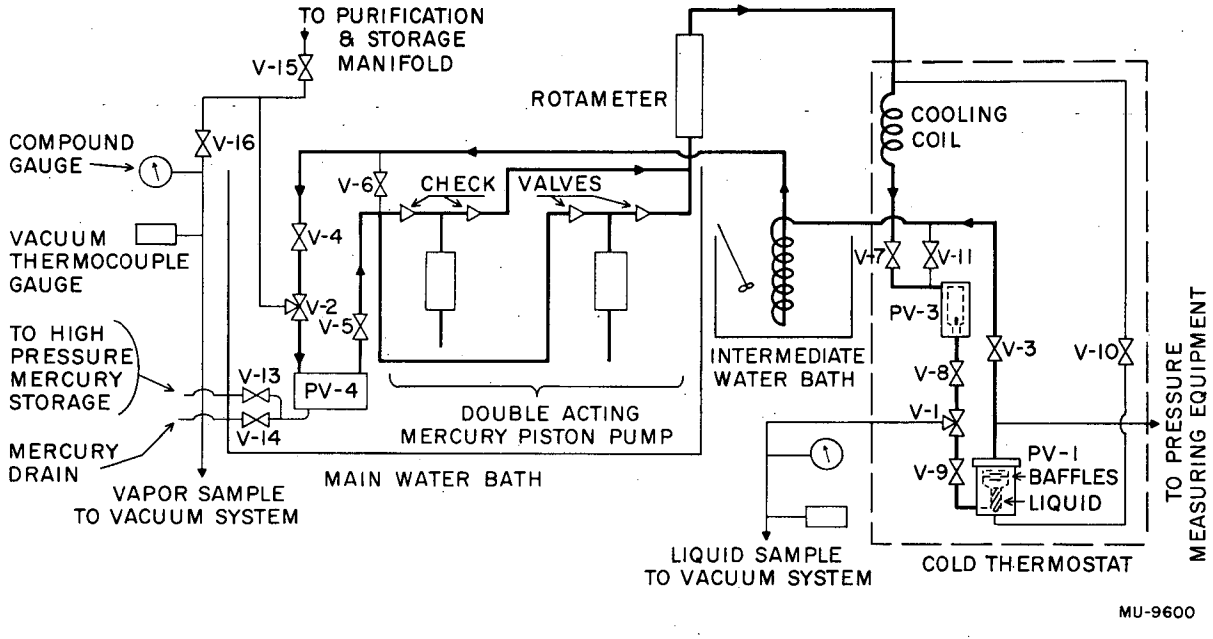

Fig. 1. Simplified flow diagram of recirculation equipment.

2. The Gas sample. Valves V-4 and V-5 are closed which isolates the equilibrium vapor in PV-4. This vapor is sent later to the vacuum system for analysis by opening V-2 and V-16. Of course the line between V-15, V-16, and V-2 is pumped out of raw gas before the gas sample is sent to the vacuum system.

3. The Liquid sample. The liquid-level indicator in PV-3 is turned on and adjusted as described in the section on liquid-level indicators, then V-7 is closed, forcing the gas to circulate through V-10. The line coming from V-10 into PV-1 terminates well above the liquid surface, so that no active mixing of the liquid and vapor occurs during sampling. Then V-3 is partially closed and the pressure drop through it forces the liquid at the bottom of PV-1 into the line leading to PV-3. When the liquid reaches PV-3, as indicated by the liquid-level indicator, valves V-8 and V-9 are closed, trapping about 2 ml of liquid in the line. The liquid sample is sent to the vacuum system for analysis by opening V-1. The valves V-1, V-8, and V-9 were specially designed to minimize the possibility of trapping small bubbles of vapor in the line as the liquid flows up the line into PV-3, and are described in another section.

While this liquid-sampling procedure is certainly more complicated than the method used by Dodge, it removes all the uncertainties in the composition of the liquid sample mentioned before.

It introduces uncertainties of its own, however, because of the possibility of having a vapor bubble trapped in the liquid-sampling line. This actually occurred before the correct adjusting procedure for the controls of the liquid-level indicator in PV-3 was found. Fortunately, the composition of the liquid samples thus obtained was in error by quite a few percent, whereas the usual scatter in liquid-sample compositions was of the order of 0.01%, so that these off samples were very easy to identify. Some of the other features of the equipment shown in Fig. 1 are as follows:

The gas sample reservoir PV-4 is a vessel of adjustable total volume, which allows for making small pressure adjustments in the system when running ternary or multicomponent mixtures. The volume adjustment is made with mercury, which comes from a

high-pressure mercury reservoir located inside of the main water bath, and can be drained to the outside. Also, since PV-4 is located very near the inlet of the reciprocating pump, its capacitance acts to damp the pulsations originating in the pump.

The main water bath is used to keep a constant temperature in the gas reservoir and adjacent gas lines. It is also used to keep the resistance bridge of the temperature controller for the cold thermostat at constant temperature so as to eliminate slow drifts in the control point.

The intermediate water bath is used to warm the gases coming from the cold thermostat to room temperature, especially the vent lines from the liquid nitrogen cooling tanks located inside the cold thermostat.

The high-pressure rotameter was used as a qualitative indication of flow through the equipment.

The section of equipment comprising the main and intermediate water baths and the high-pressure rotameter is shown in Fig. 2.

The equilibrium cell PV-1 is shown in more detail in Fig. 3. The vapor coming from the bottom of the cell bubbles through the liquid and leaves through a fitting in the cap of the vessel. The temperature of the liquid is measured with a two-junction copper-constantan thermopile, which has at least two inches of bare wire in contact with the liquid to ensure a true reading of liquid temperature. The normal liquid leavel, as determined by the liquid-level indicator, is about 1 cm above the inlet holes for the thermocouple wires, corresponding to an operating liquid volume of about 20 ml. The gas tube coming from V-10 ends just below the baffles.

The remaining sections of the equipment require a more detailed description:

Pumps

As mentioned above, the pumping system for recirculating the gas used mercury pistons to avoid contamination of the gas with oil from the packing of the pump. The pump used was a double-acting reciprocating Hills-McCanna type U* proportioning pump. It was

* Manufactured by the Hills-McCanna Co., 2438 W. Nelson St., Chicago 18, Ill.

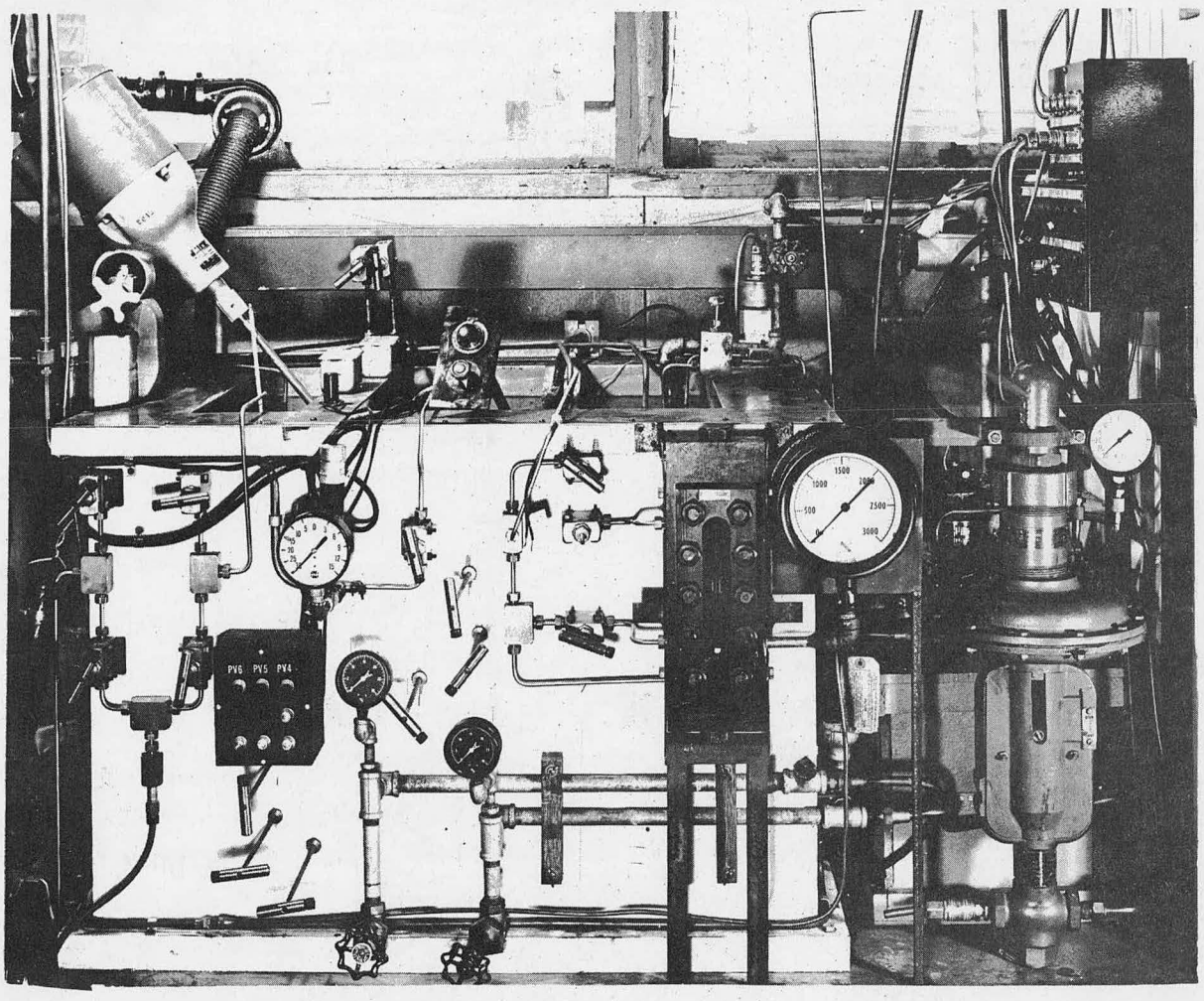

ZN-1307

Fig. 2. Main water bath.

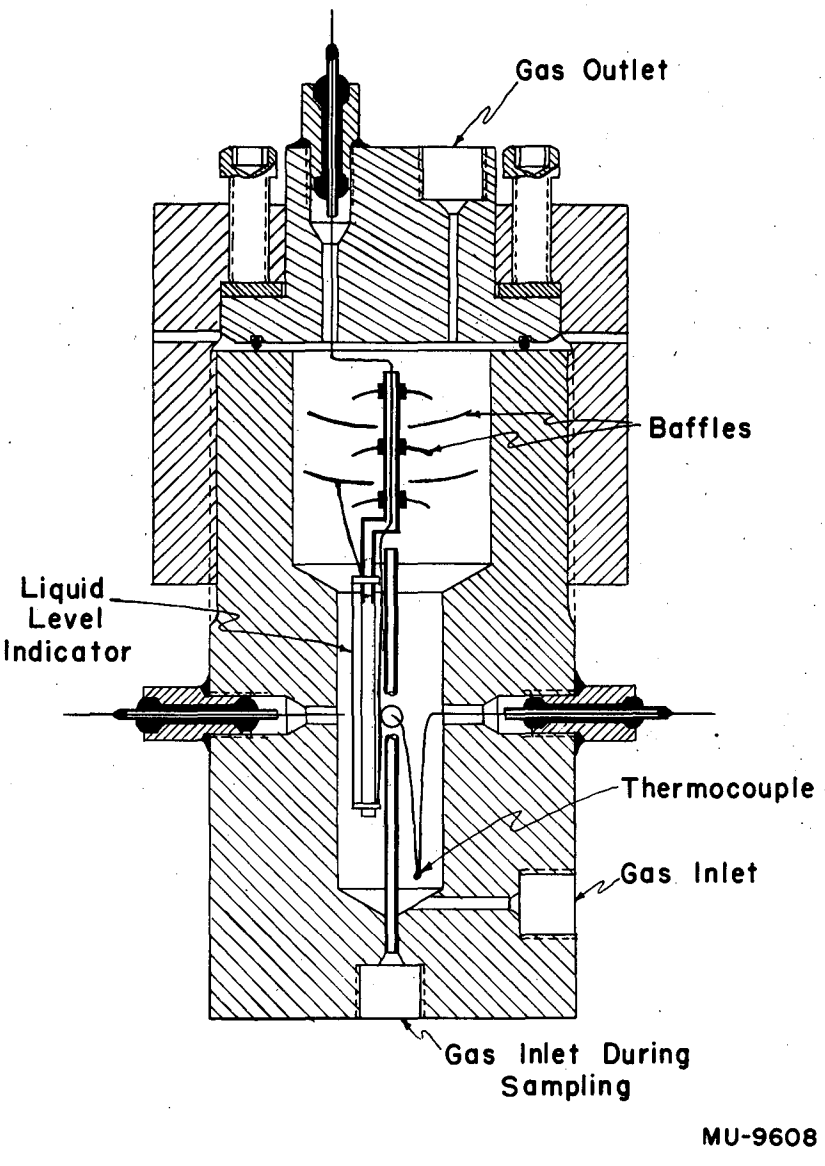

Fig. 3. Equilibrium cell.

connected to the system as indicated in Fig. 4, in which only one side of the pumping equipment is shown. The mercury displaced by the piston of the pump goes into the tempering vessel PV-9 and then to the pumping vessel PV-14, where it pushed the gas through the outlet check valve. The tempering vessel is used to prevent cold mercury from coming in contact with the thermostated gas. V-21 is the mercury fill valve for the pumping system.

The operation of the pumping equipment was not very satisfactory for two reasons: First, it was not possible to develop an entirely trouble-free pump packing, and mercury leaks through it were very common. These leaks increased the volumetric clearance of the pump, which decreased the pumping rate below its design value of 100 ml/min per piston, thus increasing the time required for a given approach to equilibrium.

Second, the liquid-vapor equilibrium equipment was always completely evacuated before the purified gases were admitted after a shutdown. Since the highest section of the mercury line is above the level of the gas lines in the water bath, these lines filled with mercury which had to be blown out before the operation of the equipment was started, so as to avoid mercury plugs in the lines leading to the cold thermostat. This problem was accentuated by any air leaks into the section of line leading to V-21.

After the mercury present in the gas lines was blown out from the equipment, the pumps were refilled with mercury to their operating level (indicated by an electrical contact located in PV-14.)

For future operation of the equipment, it would be desirable to replace the present pumping system by an electromagnetic high-pressure reciprocating pump, which would eliminate the above objections. From the standpoint of filtering the pulsations, it would be advantageous to have a small volume displacement per stroke and a relatively high number of strokes per unit time. The upper limit would be dictated by the maximum operating speed of the check valves.

Cold Thermostat

The choice of type of thermostat to be used in this investigation had to be made very early in the design. The main requirements

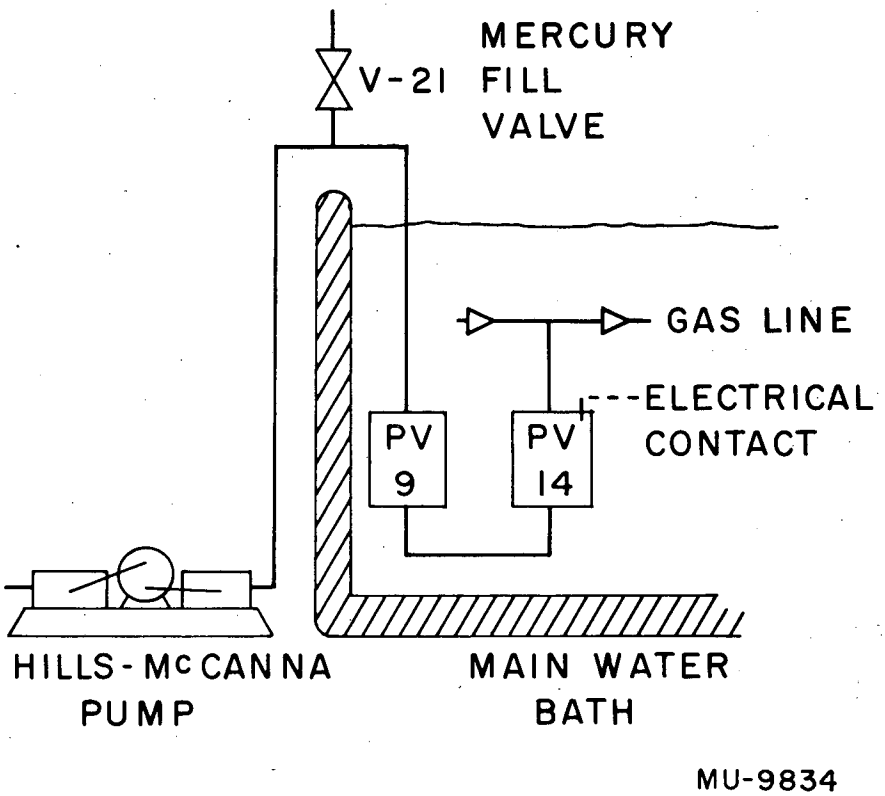

Fig. 4. Mercury piston pump.

desired of the thermostat were a large operating temperature range, which was later restricted to the region between 80° and 180° K; a large thermostated volume, of the order of 3 ft.^{3}; small temperature gradients across the thermostat; and good temperature control. In addition, it was desired to have a relatively fast-moving thermostat, to allow for changes in the operating temperature and for shutdown at night to minimize the consumption of refrigerant. The main characteristics of liquid and gas thermostats adaptable for operation in this temperature region are as follows.

Temperature gradients. Since the liquid has a larger heat capacity than the gas, smaller heat leaks produce larger temperature gradients in a gas thermostat. Vigorous stirring or a well-defined flow path is a necessity for either type of thermostat if it is desired to minimize random temperature fluctuations.

Heat transfer. The heat transfer to equipment located inside the thermostat is much better in a liquid thermostat. The temperature of the liquid in a well-designed bath is a good measure of the temperature of any piece of equipment submerged in the bath--with no heat dissipation inside the equipment--whereas this may be far from true in a gas thermostat.

Temperature control. Liquid baths are in general much easier to control, because the larger heat capacity and density of the liquid results in a larger time constant for the bath, while the better heat-transfer coefficient decreases the time constant of the control elements. The problem of temperature control in a gas thermostat is discussed in greater detail later in this section.

The above conditions favor the use of a liquid rather than a gas thermostat; however, a liquid thermostat to be used in this temperature region has a number of operating disadvantages.

Substances that remain liquid in this temperature region have large vapor pressures at room temperature, therefore, the thermostat has to be built as a pressure vessel, or suitable provisions have to be made for draining and storage of the thermostat liquid. If the operating pressure of the thermostat is not to exceed one atmosphere, a number of different thermostat liquids may have to be selected, thus complicating

the storage problem. Probably the best liquid for operation in the region between 80° and 180° K is a mixture of propane and propene, which would have vapor pressure below 1 atmosphere up to about -45°C, and a melting point very close to 80° K; however, this is a highly flammable mixture and very careful design would be required to avoid air contamination during low-temperature operation.

The liquid-vapor equilibrium equipment has a large number of valves, high-pressure vapor lines, and electrical lead wires leading to the cold thermostated section, and provision has to be made to obtain adequate seals. For high-pressure tubing and electrical lead wires the problem is not so complicated as for the valve stems, which have to be free to rotate. An experimental study was made of a number of possible valve packings for operation at low temperatures,* but none was found adequate. This difficulty could perhaps be circumvented by bringing up all the lines and valve stems through the top of the thermostat and making all the necessary seals at room temperature, but this was not considered a very practical solution, since it would involve a number of gears or flexible shafts, leading to a very complicated mechanical assembly.

The cooling of thermostat liquid could be achieved by an external heat exchanger, or if a liquid of high vapor pressure such as oxygen or nitrogen were used, the necessary cooling could be obtained by controlling the vaporization rate. For a gas thermostat the cooling problem is much simplified, since it is then possible to cool the gas by direct injection of liquid nitrogen. The larger heat capacity of liquids requires larger cooling and heating elements if it is desired to have a relatively fast-moving thermostat. After considerable discussion of the above considerations, it was decided to build a gas thermostat.

There is very little information available in the literature concerning the design of gas thermostats,[12] consequently the design of the present thermostat proceeded almost by trial and error, with progressive changes in design as increasing operating experience at low temperatures was accumulated.

---

* Section on valves, pp 46

The layout of the thermostat is shown in Figs. 5, 6, 7, and 8. Figures 5 and 6 show the thermostat as it was before the last modification, while Figs. 7 and 8 are photographs of the present equipment.

The thermostated region, about 11 x 12 x 36 in., is completely surrounded by a thickness of at least 12 in. of Fiberglas insulation.* The gas inside the thermostat is circulated in a closed loop by a blower. Cooling is obtained by direct injection of liquid nitrogen into the gas stream at the inlet of the blower, which breaks up the liquid nitrogen jet into a fine spray. The excess nitrogen vapor is vented from the thermostated region into a heat shield at the right of the thermostat (Fig. 6) where the sensible heat of the vapor is used to decrease the heat leak into the thermostated region. The ducting below the blower has a reversal section (Fig. 5), which increases the contact time between liquid nitrogen and the vapor to avoid having any liquid nitrogen in contact with the temperature-control element or inside the thermostated region. Below the duct-reversal section is the control heater and right after it, but shielded from direct radiation, the temperature-sensing element of the temperature controller.

The liquid nitrogen tanks F and G located at the top of the thermostat served for storage of liquid nitrogen coolant; they are provided with centrifugal vapor-liquid separators for use during filling and have an approximate capacity of 14 liters each.

At the time Figs. 5 and 6 were drawn, tank F was used to provide the main thermostat cooling and tank G for the auxiliary cooling of the return gas stream. This arrangement was later found to be unsatisfactory and the thermostat was modified by operating tanks G and F in parallel, thus providing additional storage capacity and therefore longer operating times before refilling. The vent line from tank F leads to a pressure gauge and a 16 psig back-pressure-regulating valve, which kept constant the pressure in the vapor space of tank F and thus also the pressure drop across the liquid nitrogen control valves C.

In order to decrease the heat leak into the thermostated region, a set of three heat shields was placed around it, which when operated in conjunction with the shield at the right of the thermostat completely

* Manufactured by the Owens-Corning Fiberglas Corporation.

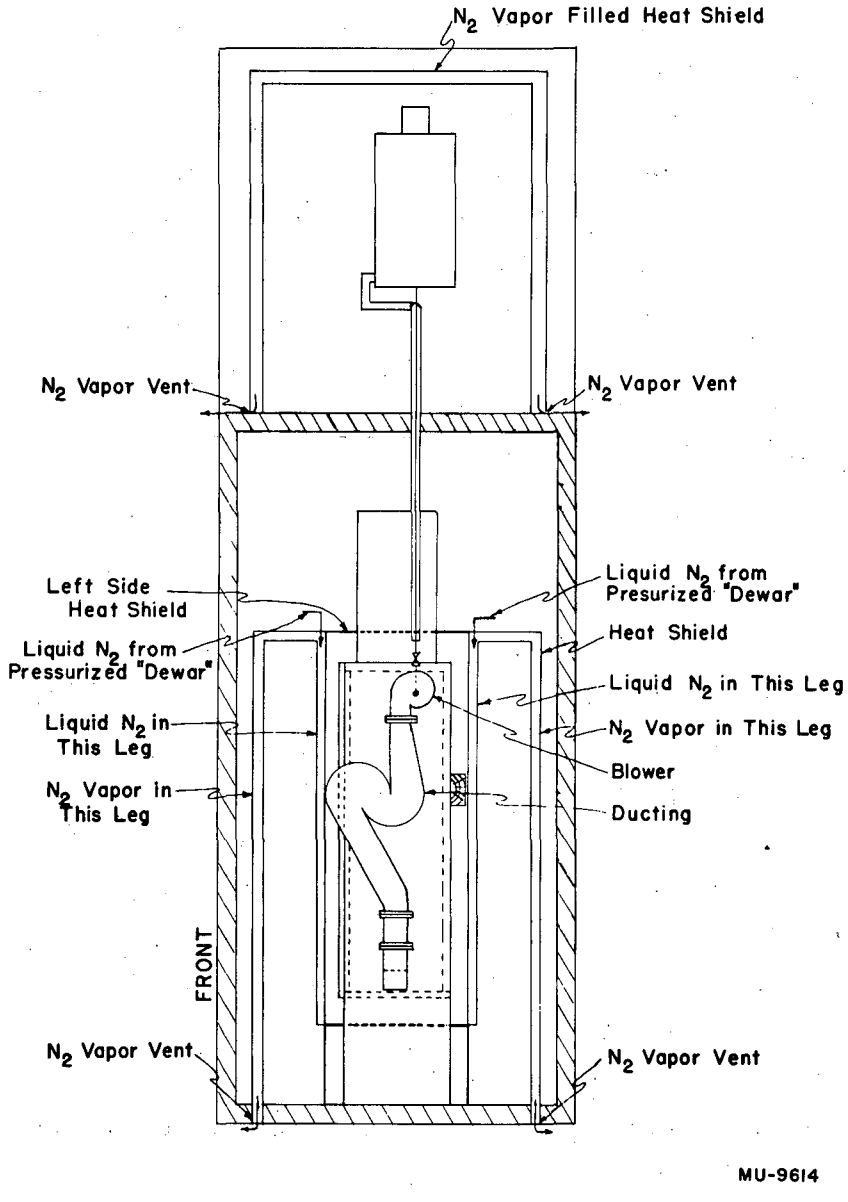

Fig. 5. Cold thermostat, side view.

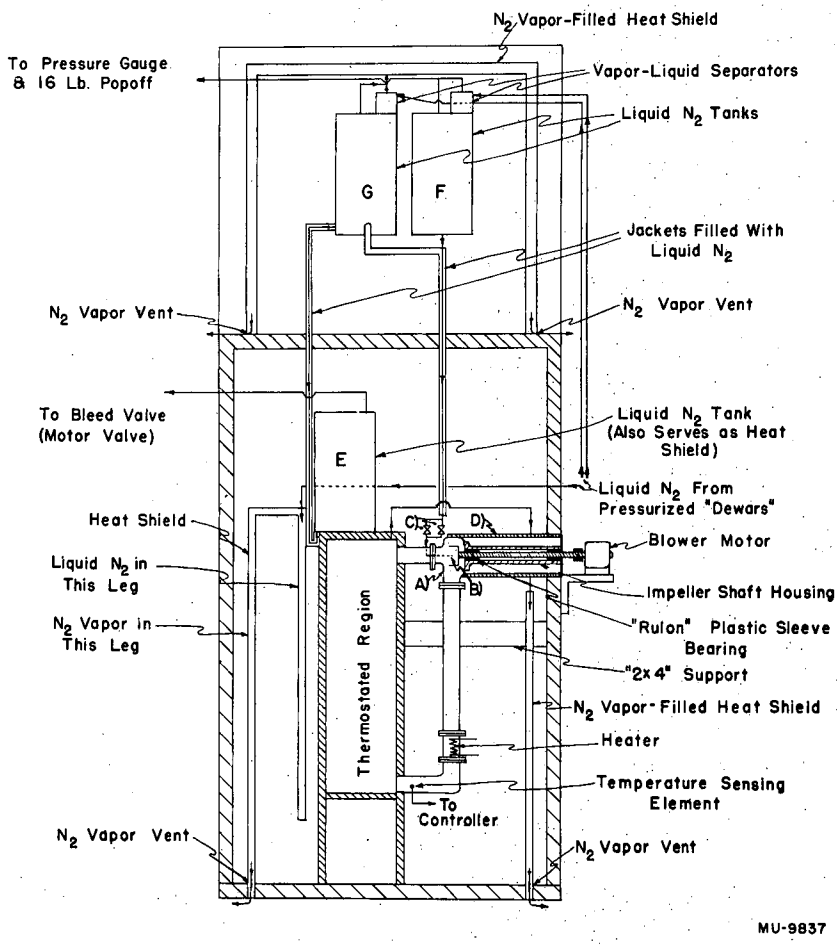

Fig. 6. Cold thermostat, elevation. A-Stainless steel centrifugal blower. B-Liquid nitrogen jet. C-Coarse and fine control valves for liquid nitrogen coolant. D-Access box for blower, impeller, bearing, etc. E-Liquid nitrogen tank confining cooling coil for high-pressure gas return. F-Liquid nitrogen "pressure" tank, provides liquid nitrogen for thermostat cooling. G-Liquid nitrogen "atmospheric" tank, provides liquid nitrogen for tank E.

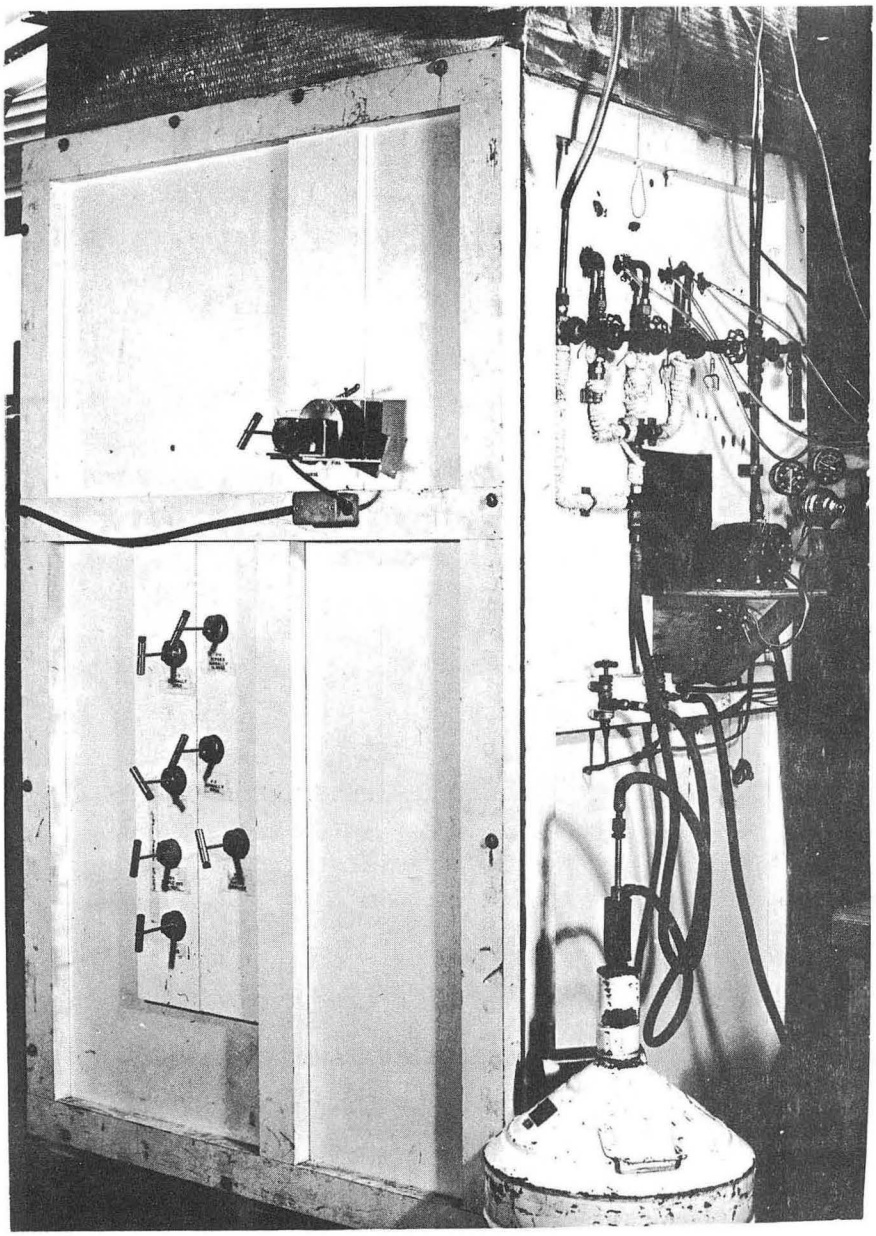

ZN-1305

Fig. 7. The cold thermostat.

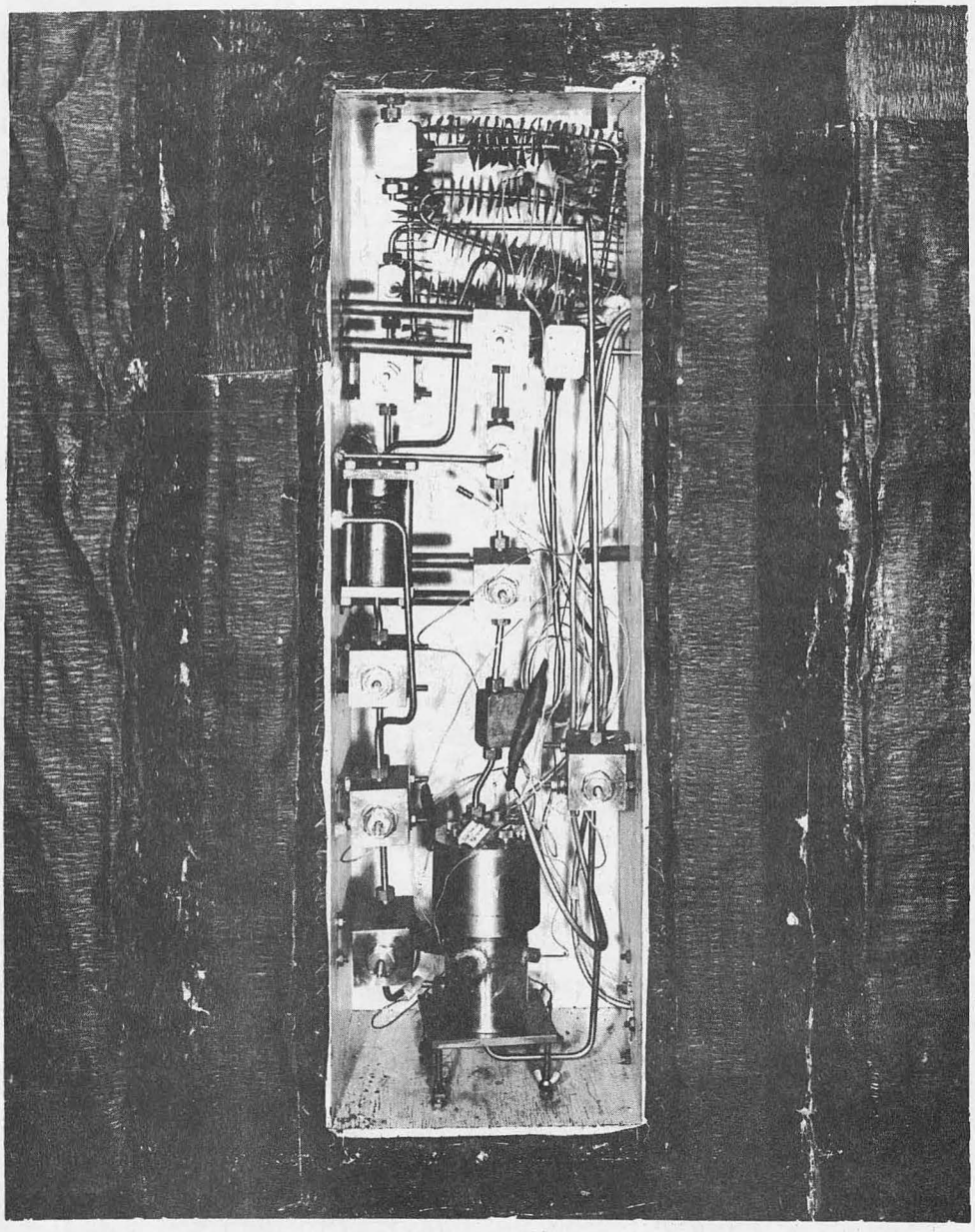

ZN-1300

Fig. 8. Cold thermostat, thermostated region.

enclosed the thermostated region. The inner section of each shield, located about 2 in. from the thermostated region, was a long rectangular can which contained liquid nitrogen. The nitrogen vapors originating in the can were taken to the outer section of the shield, located 2 in. inside the outer walls, where some of the sensible heat of the nitrogen vapor was used to decrease the heat leak. The shields were very effective in decreasing the liquid nitrogen consumption of the main cooling system, but were not used when the operating temperature of the thermostat was above 85°K, because it was found that they introduced undesirable temperature gradients in the thermostated region. The cooling action derived from the shield was sufficient to maintain the thermostat at -125°C(148°K), with the blower on and no additional cooling from the main cooling system. When in use, the shields were refilled every 7 hours.

Cooling of the return gas stream. The first design for cooling the high-pressure return gas is shown in more detail in Fig. 9. Tank E is a hollow tank of minimum capacity which houses the cooling coil. The cooling coil was wound with a logarithmic taper to have equal controllability for all levels of liquid nitrogen inside the tank. The high-pressure gas leaving the coil went through a ten-junction thermopile, which had the cold junction inside the thermostated region, immediately adjacent to the equilibrium cell PV-1 (Fig. 1). The signal from the thermopile went to a Brown* circular-chart temperature recorder controller, which actuated the control valve regulating the flow of nitrogen vapor coming from tank E, and thus the level of liquid nitrogen. The storage tank G was vented to the atmosphere, and was located about four feet above E, to provide a relatively constant liquid nitrogen head independent of the level in G. With this control system it was hoped that the temperature of the return gas stream could be controlled slightly above the temperature at the bottom of the thermostat, where the equilibrium cell was located. This control system was very unstable, however, and it was not possible to obtain the desired results.

It was found, though, that the cooling of the return gas by heat conduction from the insulation and longitudinal heat conduction along

*Minneapolis-Honeywell Regulator Co., Philadelphia, Pa.

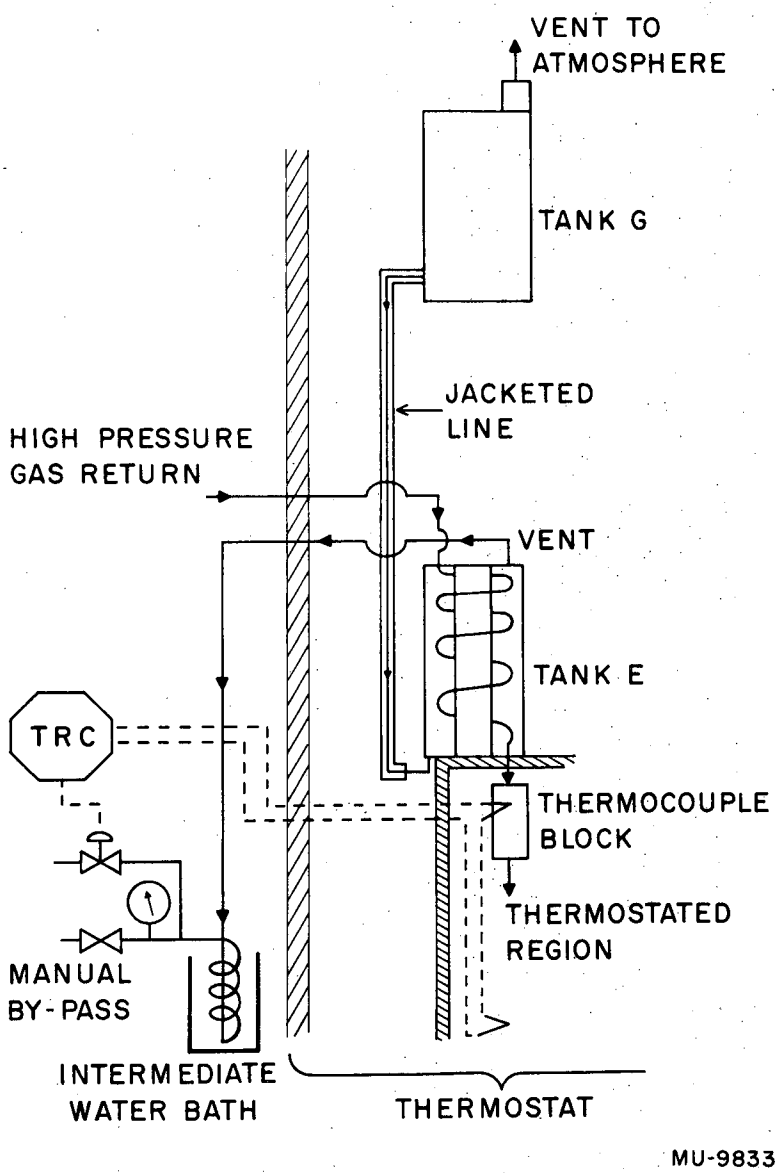

Fig. 9. Cooling of the return gas stream, early design.

the high-pressure tubing was quite effective. Thus, for a nitrogen flow rate of 200 ml/min and without any additional cooling, the temperature of the incoming gas as measured in the thermocouple block was 8.1°C higher than the bottom when the thermostat was operated at about 151°K and 1112 psig gas pressure, and 6.5°C at 90°K and 38 psig. Therefore, the next few degrees of cooling could well be taken care of by heat transfer from the gas inside of the thermostated region, and a nine foot long section of finned tube was installed at the top of the thermostated region, in the space formerly occupied by the thermocouple block, as seen in Fig. 8.

Blower. The blower was used to circulate the thermostat gas at the rate of about 60 cfm through the thermostated space.

Some difficulty was experienced in selecting the bearing material for the cold side of the blower shaft, which had to operate at 3600 rpm unlubricated, throughout the entire operating temperature range. The most satisfactory bearing material found was Rulon* plastic, which showed no appreciable wear after more than six months' operation.

Temperature gradients in the thermostated region. Most of the measurements on temperature gradients inside the thermostated region were obtained very early in this investigation, before the temperature controller for the cold thermostat was properly adjusted and the temperature-measuring equipment was entirely reliable. Therefore, the information that follows is mostly qualitative.

The temperature gradients inside the thermostat vary with changes in operating conditions and degree of approach of the thermostat to steady state. Operation at 90°K, with the shields full of liquid nitrogen and with cooling of the high-pressure return gas by the coil in tank E, resulted in temperature differences of the order of 0.03°C at steady state between the outlet and inlet gas; while operation without external cooling from the shields and the additional heat load of cooling the return gas in the finned section of tube, increased the temperature difference to a maximum value of 1.5°C. The temperature at the center

* Manufactured by Dixon Lubricating Saddle Co. Bristol, Rhode Island.

of the thermostat was practically independent of gas flow in the high-pressure tubing, and was of the order of 0.1°C above inlet for operation without the shields.

Temperature control. The temperature of the thermostat was controlled with a proportional reset controller, devised by the Electronics Section of the Laboratory, which is represented in a block diagram in Fig. 10. The temperature of the thermostated gas stream is measured by the change in resistance of the sensing element located in the path of the gas stream, after the heater. The resistance of the sensing element is measured with a resistance bridge and the error signal from the bridge goes to the amplifier, which controls the heat dissipated in the heater. The output from the amplifier also goes to a set of relays which control the motor valve regulating the flow of liquid nitrogen coolant.

The sensing element is a Globar type 304B resistor, chosen because it has a large temperature coefficient of resistance in the range 80° to 180°K.

The resistance bridge was wound with manganin wire and had coarse and fine adjustments for range. It was enclosed in a watertight box immersed inside the main water bath, which kept its temperature constant.

The amplifier regulated the phase shift in a gas tube providing up to 100 watts power to the heater.

The reset feature was incorporated into the control system through the control of the liquid nitrogen cooling rate, which was adjusted with the motor valve to keep the power output to the heater, and thus the operating range of the amplifier, within narrow limits.

The liquid nitrogen control valve was a Hoke needle valve No. 2RB280 which requires 23 turns to open and provides for good flow-rate control in the range 4 to 900 ml/min. with a maximum flow rate of 1300 ml/min at 14.5 psi pressure drop (tested with water). It was driven with a 1-rpm reversible motor, shown in Fig. 7.

The operation of the control system was not very satisfactory, due to the following reasons;

(a) Time constants. It was mentioned earlier that a gas thermostat

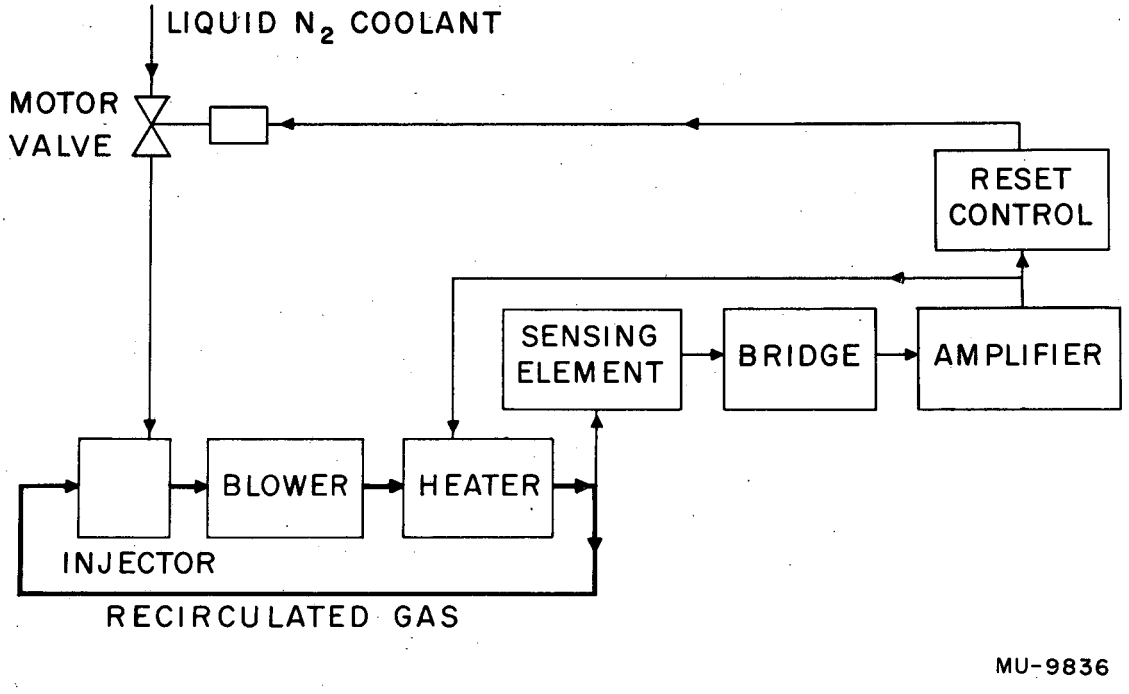

Fig. 10. Cold thermostat, temperature controller.

has adverse control characteristics owing to the low heat capacity of the gas and its poor heat-transfer properties, which increase the time constants of the control elements, the heater, and the Globar. This factor, when coupled with the need for a very close temperature control--that is, a very high gain in the amplifier-- results in an unstable system which requires very elaborate feedback loops in the amplifier to obtain good proportional control.

The development of the temperature controller took a great deal of time and effort, and delayed appreciably the completion of the project; however, it finally gave satisfactory operation, except as noted below.

(b) Noise originating in the sensing element. The choice of a Globar resistor as sensing element was unfortunate because its resistance at constant temperature drifted with time in a random fashion, thus upsetting the control.

The data obtained with the equipment were taken when the resistance of the Globar remained fairly steady, resulting in a temperature control which was at best within $0.002^{\circ}C$, but usually drifted up and down by about 0.01 or $0.02^{\circ}C$ during a few minutes, resulting in a temperature drift in the equilibrium cell of about $0.005^{\circ}C$.

Access to the thermostated region. The thermostat was designed for easy access to the thermostated region. The insulation was laid out in three separate sections; port of access to the bearing of the blower, thermostat door and insulation leading to the thermostated section, and the insulation of the main body of the thermostat. The main body of the thermostat was insulated with four-inch horizontal sections of Fiberglas, separated by wax paper to minimize the vertical convection currents inside the insulation.

Each section was mechanically separated from the others, as may be seen in Figs. 6 and 8, so that repairs could be easily carried out in the blower or in the thermostated sections.

Proposed modifications. The present thermostat is unsatisfactory because of the difficulties experienced with the temperature controller and the relatively large temperature gradients present in the thermostated region owing to heat leak from the outside and the cooling of the

high-pressure return gas stream.

The proposed scheme would retain the flexibility of a gas thermostat, while incorporating the ease in controllability and the small temperature gradients of a liquid thermostat; however, it would require larger capacity for the liquid nitrogen storage tanks to provide for longer operating periods between fillings.

The high-pressure equipment now located inside the thermostated region is to be soldered to 3/8-in.-thick copper plate in such a way that it will be completely enclosed by copper. The thermostat gas is to circulate on the outside of the copper plates, which will have to be provided with fins for additional area for heat-transfer to the gas. The problem of cooling the high-pressure return gas stream would be solved by soldering the coil directly onto the copper plates. By the use of this device, the entire thermostated region would be essentially isothermal.

The problem of instability of the temperature controller would be solved by attaching a nickel or platinum resistance thermometer to the copper plate somewhere in the vicinity of the inlet of the thermostat gas stream. This would make the temperature of the sensing element identical with the temperature of the equipment and would give a very long time constant for the sensing element, which is very advantageous for control.

Since the thermal mass of the high-pressure equipment plus copper plates will be very large compared with the heat-transfer coefficients between the gas and the copper, it would be advantageous to have very long operating periods between fillings of the liquid nitrogen storage tanks, because small temperature upsets occur during filling.

The present liquid-nitrogen-filled heat shields would be removed and supplanted by vacuum jackets, which should be very efficient in reducing the heat leak at the low operating temperature of the thermostat.

Auxiliary Equipment

Temperature Measurement

Temperatures at various locations were measured with copper-constantan thermocouples and read with a Leeds-Northrup type K-2 potentiometer. The constantan wire was continuous from the hot to the cold junction, while the copper wire was interrupted by the thermocouple selector switch, from which the wires went to the potentiometer. The switch was a Leeds-Northrup 12-position, 2-pole thermocouple switch, which was properly shielded and thermally insulated from the surroundings to minimize thermal emf's.

While techniques and methods used for reading thermocouple emf's are hardly in need of further description, some related aspects, such as thermocouple shielding and ice-bath temperature have not been emphasized as much in the literature as perhaps they should. The reproducibility of the ice-bath temperature is known[43] to be about $\pm 0.0001^{\circ}C$, if corrections are applied for pressure. However, most ice baths do not maintain this degree of reproducibility over long periods of time, owing to the melting of the ice and convection currents originating at the walls of the Dewar. These effects were quite noticeable during the testing of the temperature controller for the cold thermostat, appearing as slow drifts of the emf values obtained when a simple ice bath consisting of a Dewar filled with finely crushed ice and distilled water was used. The amount of drift was decreased by stirring the ice bath or by pumping the water from the bottom to the top of the ice bath, but was still quite noticeable. Finally an ice bath was designed according to the suggestions of White;[48] it is shown in Fig. 11.

It consists of two separate ice baths, one inside the other. The thermocouple junctions are made with 24-gauge constantan wire and 36-gauge copper wire wound in a coil such that at least 10 inches of thermocouple wire are inside a tube filled with a low-viscosity organic liquid, which is located inside the inner ice bath. The long length of wire immersed reduced the effect of thermal conduction along the wire to the point where a change of 1 inch in the length of wire immersed did not change the potentiometer reading. The inner ice bath is completely surrounded by the outer, and the only heat leak coming into it

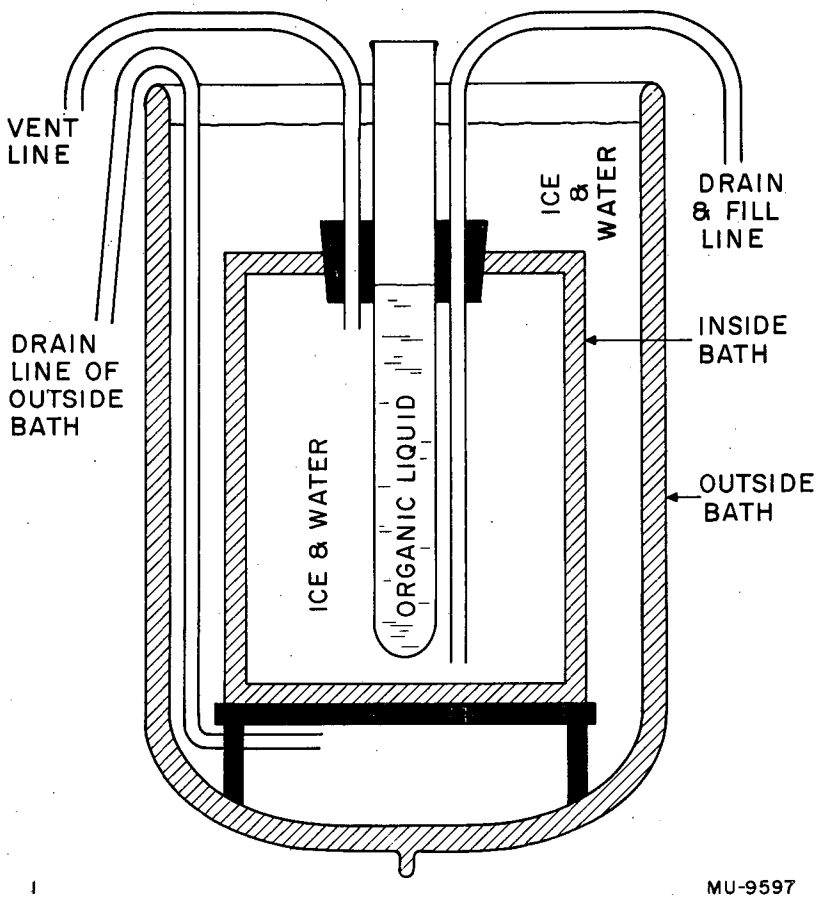

Fig. 11. Ice bath.

arises from the relatively small amount of heat flowing along the thermocouple wires. White recommended that the water in the inside bath be changed frequently. Accordingly, the inner bath has provision for draining and filling with fresh air-saturated distilled water without removal from the outer bath. The ice in the inner bath does not melt appreciably over periods as long as a week, provided the outer bath is always kept filled with ice. This design of ice bath seems to be very stable and reproducible, as evidenced by tests in which the water in the inner bath was drained after remaining undisturbed for 24 hours, and the bath filled again with precooled air-saturated distilled water. The thermocouple readings before and after filling were identical, to the limit of accuracy of the potentiometer, which for this test was reading a 2-junction thermopile with a reading error of about 0.1 μv, which corresponds to ± 0.001°C. Good thermocouple shielding and the use of a common electrical ground for the entire experimental equipment were found essential to eliminate noise in the thermocouple circuits.

Pressure Measurement.

The operating pressure for each run was determined to the nearest 0.02 psia with the dead-weight gauge shown in Figs. 12 and 13.

Figure 12 is a photograph of the pressure- and temperature-measuring station, showing the dead-weight gauge, three pressure gauges for the different ranges, the control panel and the K-2 potentiometer, ice baths, and galvanometer. Figure 13 is a schematic flow diagram of the pressure-measuring system. The piston of the dead-weight gauge was connected to a rocking mechanism to reduce the static friction and drag in the vertical movement of the piston.

The ultimate limit of sensitivity of the gauge was about 0.002 psia, equivalent to less than 50 mg vertical drag on the piston. The reproducibility of the gauge, as shown by repeated calibrations, was better than 0.02 psia, and the maximum measurable pressure about 2200 psia. The set of stainless steel weights used with the gauge was calibrated at the Standards Laboratory of the University.

The piston-cylinder combination was operated and aged for about one year before final calibration of the gauge, which was carried out at low pressures against a mercury manometer and at the carbon

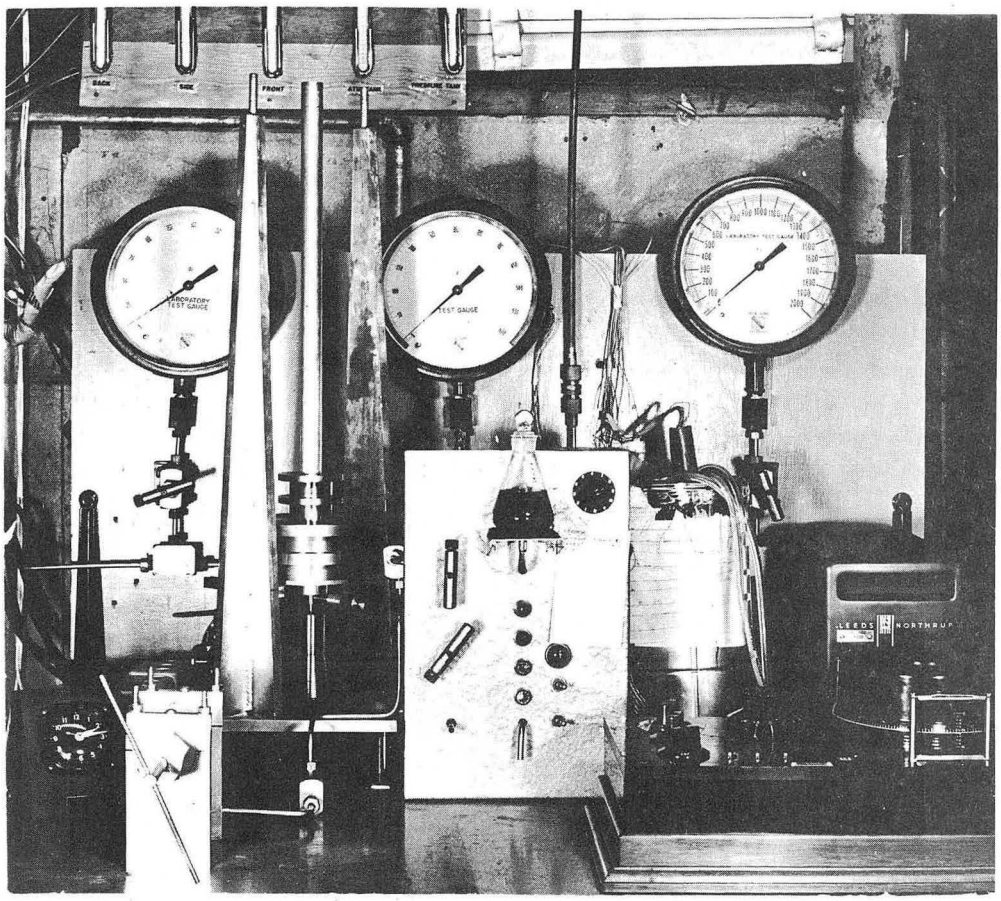

ZN-1306

Fig. 12. Equipment for measuring temperature and pressure.

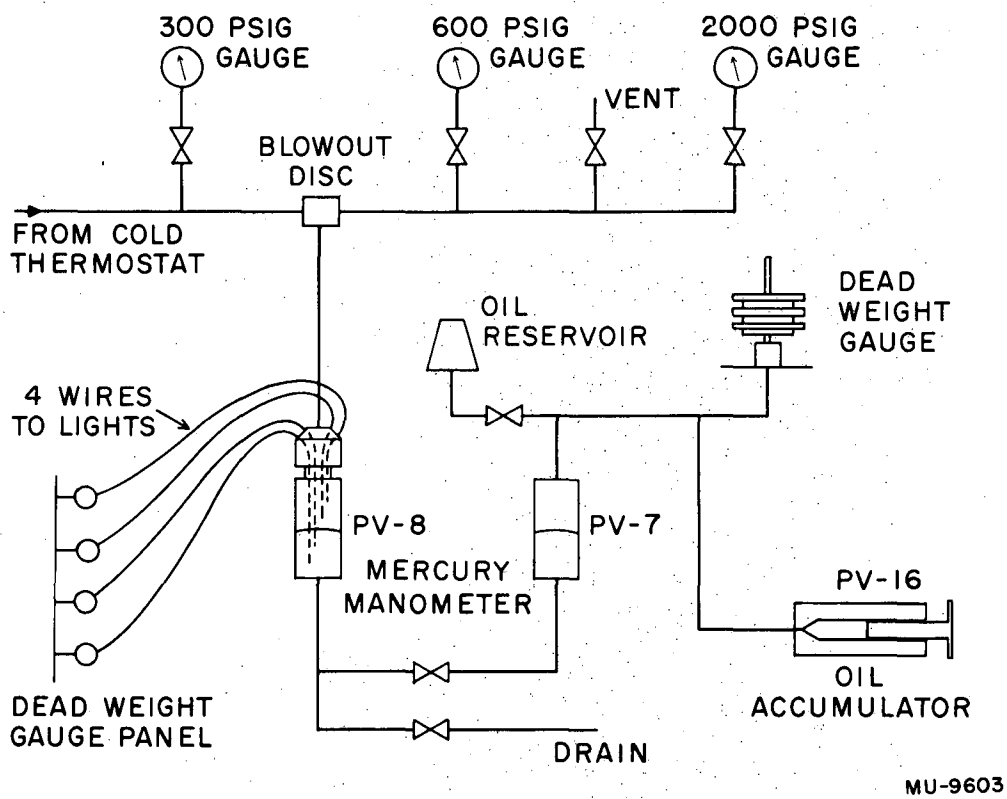

Fig. 13. The dead weight gauge.

dioxide point (505.557 psia). The carbon dioxide used in the calibration was specially purified, analyzing better than 99.993% by mass spectrographic analysis. A further check of its purity was the reproducibility of several gauge calibrations made with different carbon dioxide samples.

Equipment for Purification and Storage of Gases.

The section used for purification and storage of the gases used in this investigation was built in as a permanent part of the equipment. The piping manifold, purification equipment, Toepler pump, and storage cylinders for the purified gases are shown in Fig. 14. It may be noted that the piping arrangement allows for three raw-gas cylinders and three purified-gas cylinders, together with an additional storage cylinder to be used for mixture storage. This arrangement was built in for future use in running ternary systems. Figure 15 is a photograph of the equipment. The purification of the gases, in this case hydrogen and nitrogen, was accomplished by passing the raw gas at high pressure and a slow rate through a bed of activated charcoal held at a low enough temperature to remove most of the higher-boiling impurities of the raw gas; thus, for nitrogen purification the bed was held at dry ice temperature, while for hydrogen purification the bed was cooled with liquid nitrogen. The purification vessel PV-23 was heated to 100°C to help in outgassing the charcoal while the entire manifold and purification systems were evacuated before starting the purification procedure.

This method of purification seemed to be quite effective, as evidenced by the following mass spectrographic analysis of a typical sample of purified gases. It should be noted that the amounts of impurities recorded below are the maximum limits of impurities in the sample, assuming that the mass spectrograph has zero background.

Gas	H_2	N_2
A	--	0.022
O_2	0.004	0.004
N_2	0.009	99.974
H_2	99.970	
D_2	0.002	
HD	0.015	
	100.	100.

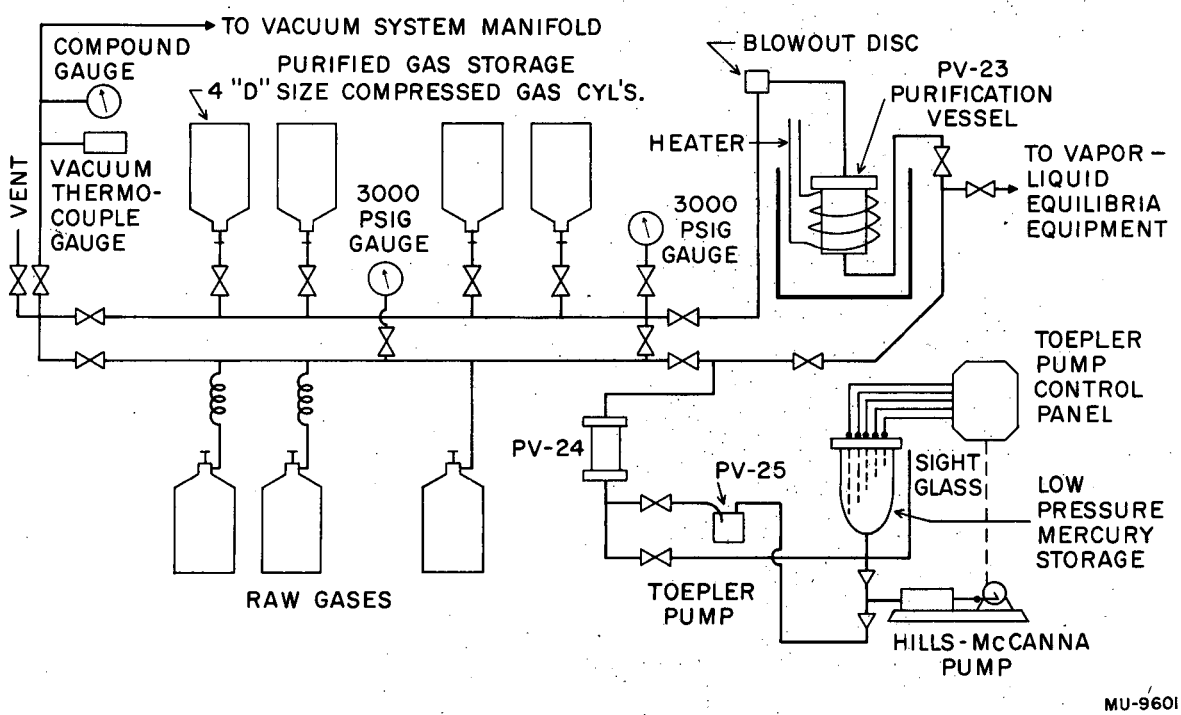

Fig. 14. Gas manifold and purification equipment.

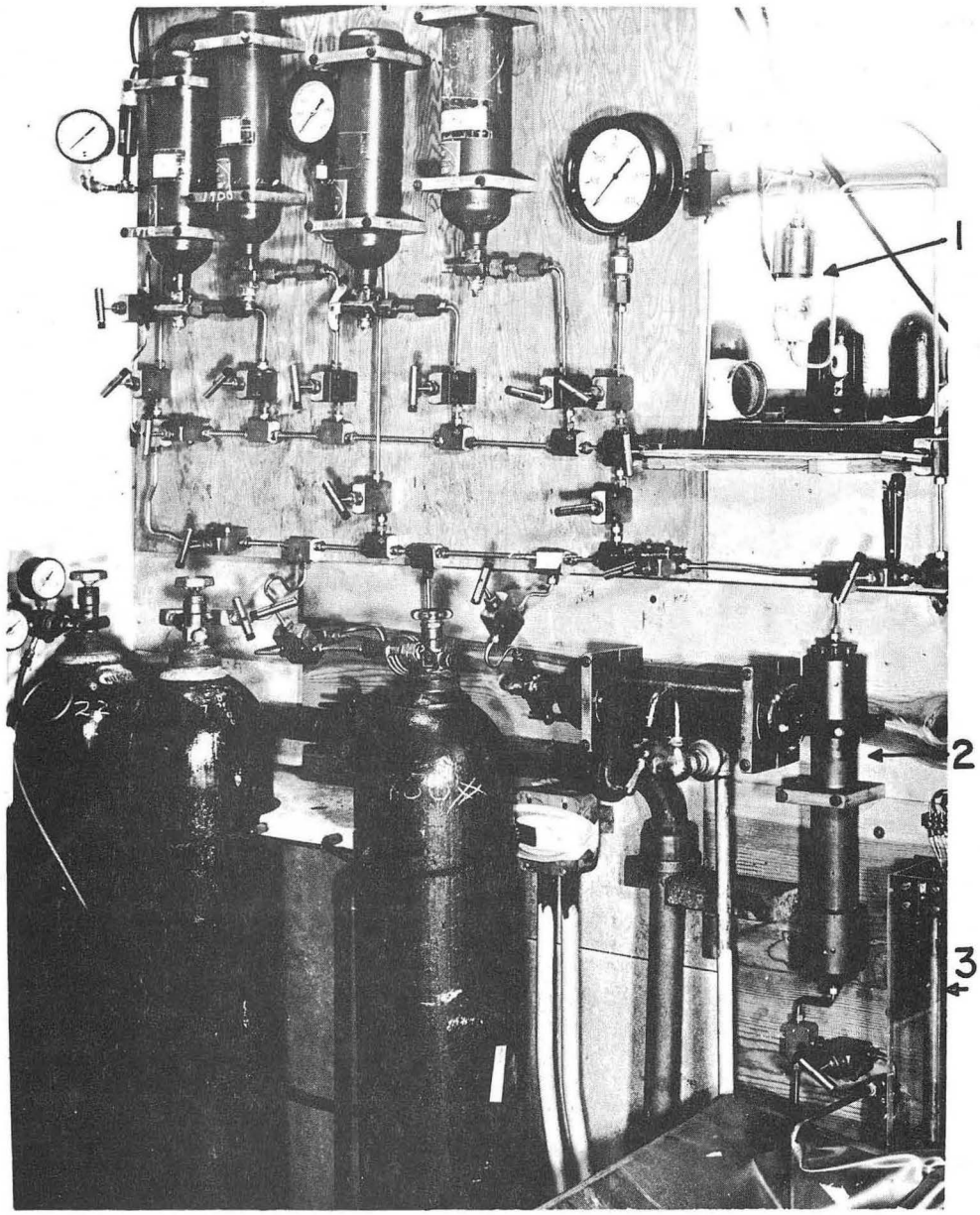

ZN-1264

Fig. 15. Gas manifold and purification equipment.
1- PV-23. 2- PV-24. 3- Low-pressure mercury reservoir.

The Toepler pump was used to pump gases from the raw- to the purified-gas cylinders and to pump pure gases into the liquid-vapor equilibrium equipment when the latter was operated at higher than cylinder pressure. The main consideration in the design of the Toepler pump was avoiding contamination of the gases with pump packing. For this reason the Toepler pump principle was used, in which the gases are pumped by mercury displacement.

In this case the pump was designed for semiautomatic operation; all the high-pressure valves have to be operated manually, but the low-pressure mercury-storage tank has built-in electrical contacts that shut off the pump at the end of each pumping cycle. An oil trap, PV-25, is built into the inlet mercury line to avoid any carry-over of oil into the gases.

Vacuum System.

The vacuum system designed for the liquid-vapor equilibrium equipment is adapted to the handling of individual components and mixtures that exist as vapors at room temperature, and is shown in Fig. 16.

The vapor sample coming from the main water bath is held in a 500-ml receiver for further analysis. Operation of the manual Toepler pump allows for pumping gas into the line leading to the analytical equipment. The liquid sample coming from the cold thermostat is pumped with an automatic Toepler pump into a 2-liter receiver, where it is held for analysis.

Since the liquid sample is obtained by flashing the liquid contained in the section of tubing between two valves, the composition of the first vapor reaching the sample reservoir is richer in the lower-boiling component, while the remaining vapor is richer in the higher-boiling one. For this reason it is desirable to have some provision for mixing the liquid sample before analysis. This mixing was done as follows:

The Toepler pump was operated until the pressure in the line leading to the cold thermostat was below 35 microns, as indicated by a thermocouple vacuum gauge located near the cold thermostat. Then the bypass around the pump was opened, allowing the gas from the

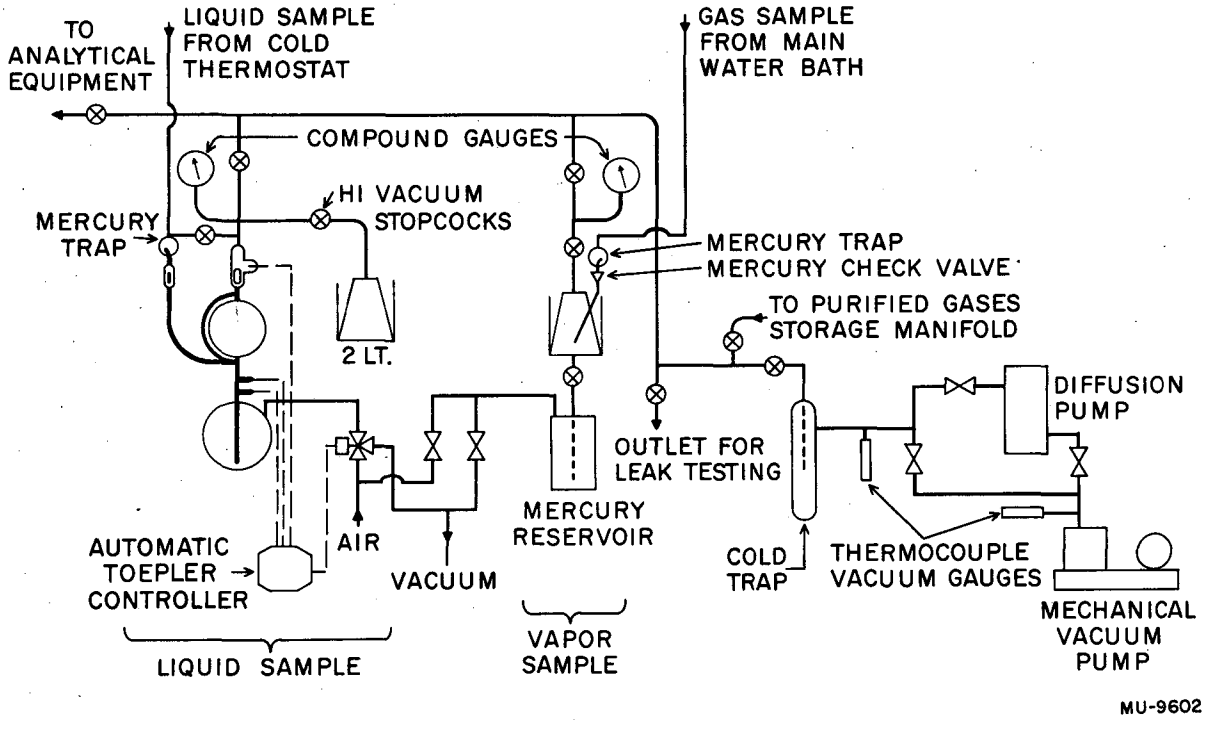

Fig. 16. Vacuum system.

reservoir to fill the line. The pumping operation was again started, until the pressure in the line dropped below 50 microns. At this stage valve V-1 in the cold thermostat was closed and the bypass around the pump opened.

The liquid sample was held in the reservoir and line until it was sent to the analytical equipment by proper operation of the stopcocks and the automatic Toepler pump, operation which provides additional mixing.

The vacuum system has connections to the purified-gas cylinder manifold and to the analytical equipment, and an additional outlet for leak testing or sending gas samples for mass spectrographic analysis.

Electrical Connectors

Suitable means of introducing thermocouple lead wires inside pressure vessels had to be developed, once it was found that the soapstone cones supplied by the American Instrument Company gave a much higher leak rate than could be tolerated.

For temperatures in the vicinity of room temperature it was easy to find adequate seals. Thus, the design shown in Fig. 17 can be machined out of polyethylene or Teflon or leather, giving a seal which is tight to the helium mass spectrograph leak detector under vacuum or 2000 psig pressure.

The development of an electrical connector that could be cooled repeatedly to liquid nitrogen temperatures without developing leaks proved to be considerably more difficult.

The design finally adopted, shown in Fig. 18, consists of a glass-to-Kovar type of seal, which seems to be stable to slow temperature changes. The outer nut is soft-soldered to the body of the pressure vessel, for which reason it is preferable to have the pressure vessel made out of brass rather than stainless steel. This type of electrical connector requires skillful glass blowing and careful outgassing of the Kovar before the glass is bonded to it, but those connectors which were satisfactory on an initial vacuum test before assembling into the pressure vessels were satisfactory thereafter. The weakest part of the assembly is the soldered joint between the

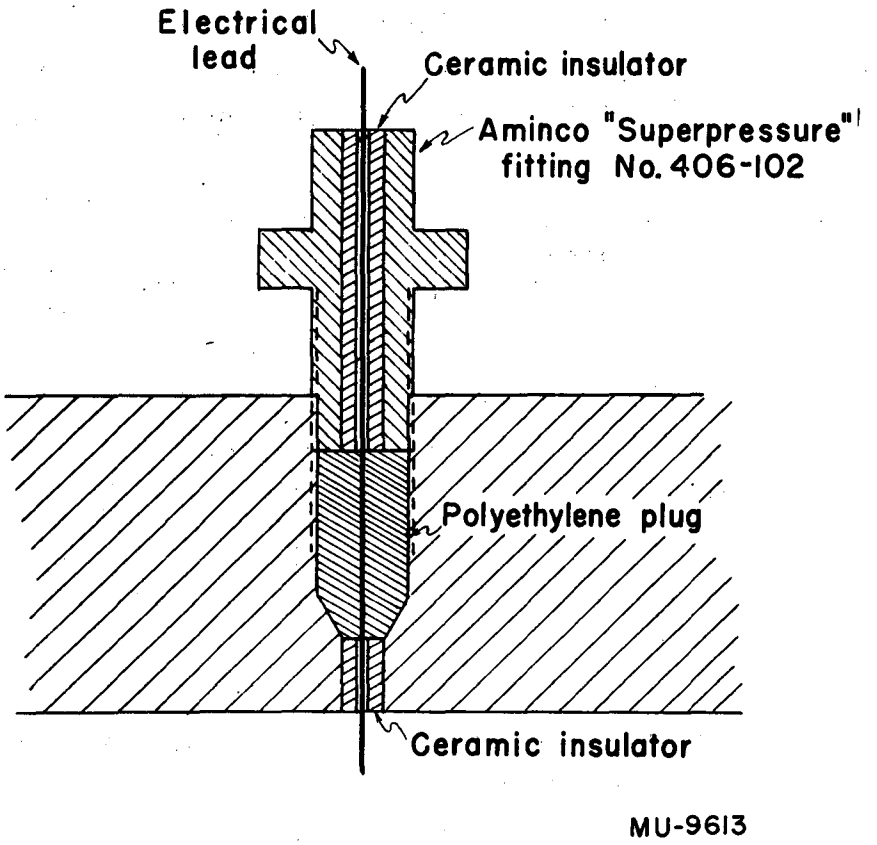

Fig. 17. Electrical connector for room-temperature operation.

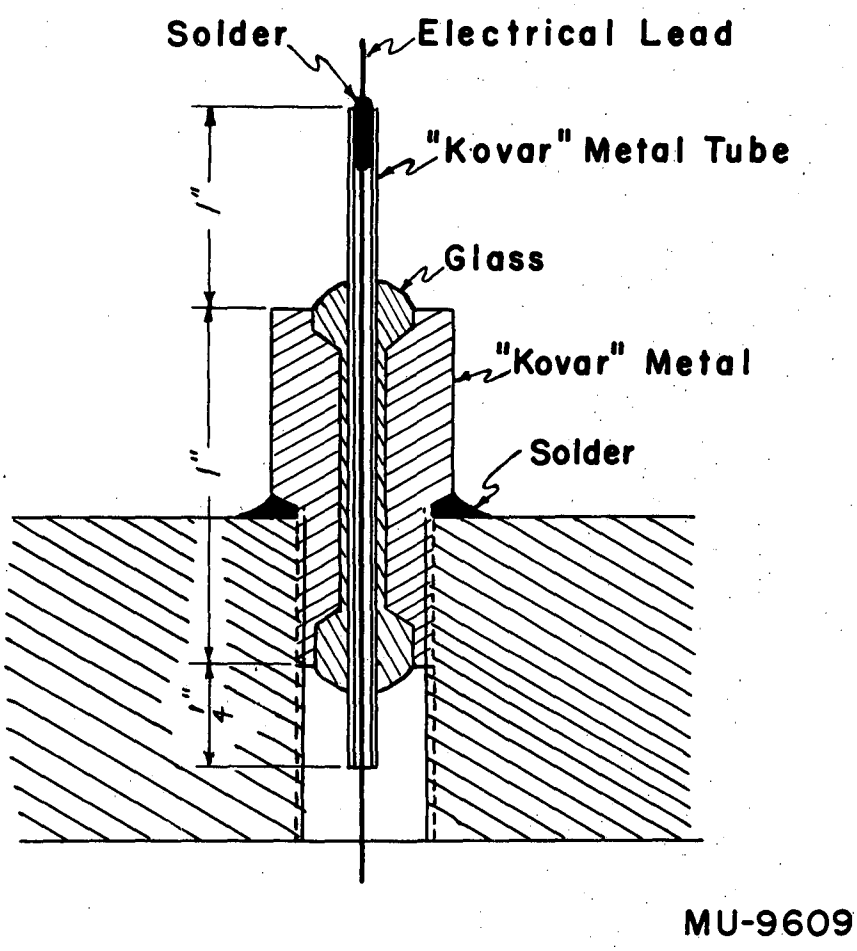

Fig. 18. Electrical connector for low-temperature operation.

electrical lead wire and the inside of the Kovar tube, as evidenced by the occasional appearance of pinhole leaks, which fortunately can be easily repaired.

Other types of glass-to-metal seals for use at low temperatures have been described by Corak and Wexler.[6]

Valves.

All the sections of the equipment operating at room temperature used the high-pressure valves supplied by the American Instrument Co., which gave very satisfactory service. It was not possible, however, to develop a suitable packing for operation at liquid nitrogen temperatures, therefore the bellows valves shown in Fig. 19 were developed, using 1/4-inch i.d. "Supraflex" stainless steel tubing, of the U.S. Flexible Metallic Tubing Company.

As may be seen in Fig. 19 , the three-way valve offered a straight-through passage with no dead volume to trap vapor bubbles, which was a very important consideration in the design of the liquid-sampling system. The bellows valves were the most common source of leaks in the entire apparatus, and are in need of further development work. The leaks appeared in the solder joints between the bellows tube and the stainless steel parts serving as gasket and point of the valve and were probably due to the combined effects of temperature and pressure stresses, since extensive testing showed that leaks did not appear when only one of these sources of stress was present.

Improvement in the valves might result from using welded and annealed type of construction instead of the solder joint presently used, or by using soldered construction with brass rather than stainless steel for the gasket and the point of the valve.

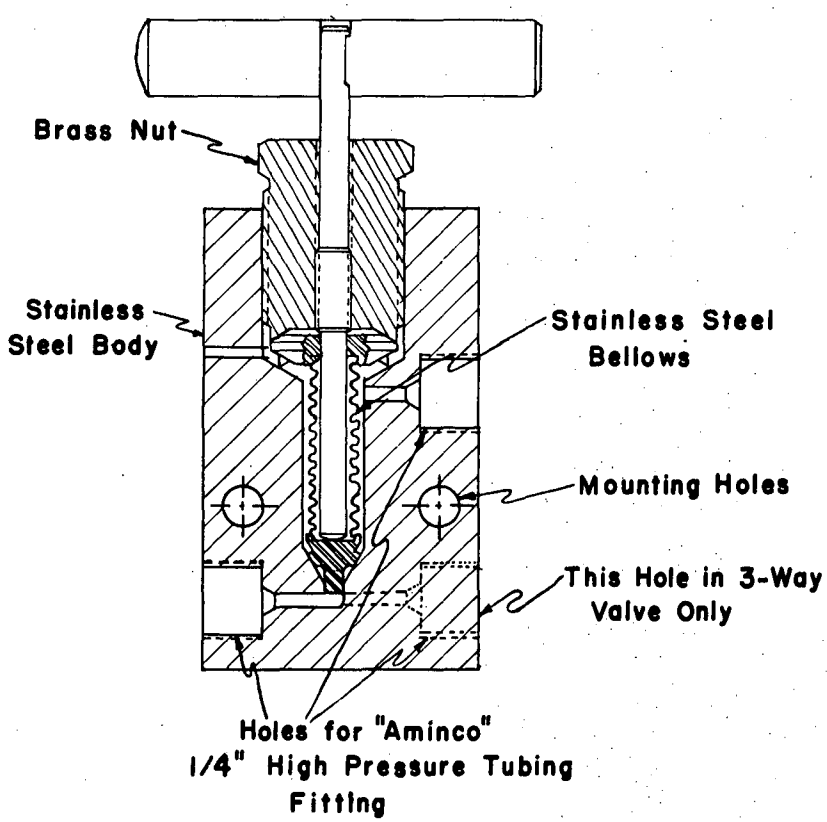
Brass Nut
Stainless Steel Body
Stainless Steel Bellows
Mounting Holes
This Hole in 3-Way Valve Only
Holes for "Aminco" 1/4" High Pressure Tubing Fitting
MU-9588

Fig. 19. Valve.

Liquid-Nitrogen-Level Indicators

A number of ways have been developed for controlling the level of low-boiling liquids as applied to automatic filling of cold traps. Of the proposed devices, perhaps the simplest is a commercial bimetallic thermoregulator[24] used to control a solenoid valve. Most of the other devices measure the change in resistance of a wire or a carbon resistor when immersed in the liquid.

Equipment for measurement of level, rather than an on-off indication, may use the change in resistance of a wire,[47] the change in capacity of a condenser having the two-phase fluid as dielectric,[49] or the scattering of x-rays.[19]

Of the above methods, the measurement of change in resistance is perhaps the simplest. It was used to measure the level of liquid in the equilibrium cell, and to indicate when liquid nitrogen reached PV-3 during sampling.

The sensing element is usually a fine wire heated by a small electric current so that it rides at a temperature slightly above ambient temperature. The magnitude of this temperature difference between the wire and the medium is a function of the thermal properties of the medium surrounding it; and for a liquid-vapor interphase, it is a definite function of the liquid level.

The variations in average temperature of the wire with variations in liquid level are reflected in changes in the resistance of the wire, which can be measured with a sensitive bridge circuit, or can give a direct indication of level if an unbalanced bridge is used.

Theory. Consider a section of heated wire dissipating a certain amount of heat, q, surrounded uniformly by a fluid of heat-transfer coefficient h. From a heat balance on a section of the wire we can write

$$\frac{\partial U}{\partial \theta} + \frac{q}{\rho C_p A_c} - \frac{A_s h}{\rho C_p A_c} U + \frac{K}{\rho C_p} \left(\frac{\partial^2 U}{\partial x^2}\right) = 0, \qquad (1)$$

where

U = temperature difference between wire and medium,

θ = time,

q = heat dissipation per unit length,

ρ = density,

C_p = specific heat,

A_c = cross-sectional area,

A_s = surface area per unit length,

h = heat-transfer coefficient of the fluid,

K= thermal conductivity of the wire,

x = distance along wire.

For steady-state conditions we have $(\partial U/\partial \theta) = 0$, and the equation simplifies to

$$\frac{\partial^2 U}{\partial x^2} - a^2 U = -b, \tag{2}$$

where $a^2 = A_s h/KA_c$ and $b = q/KA_c$.

For a semi-infinite wire, with one end clamped so that at $x = 0$ $U = 0$, Eq. (2) can be integrated to

$$U(x) = U\,\infty\,(1 - e^{-ax}), \tag{3}$$

$$U\,\infty = b/a^2 = q/A_s h, \tag{4}$$

where $U\,\infty$ is the steady-state temperature difference between the wire and the medium at $x = \infty$.

For a finite wire of length L, with both ends clamped; $U = 0$ at $x = 0$ and at $x = L$,

$$U(x) = U\,\infty\,\left(1 - \frac{1}{1+\alpha}\, e^{ax} - \frac{\alpha}{1+\alpha}\, e^{-ax}\right), \tag{5}$$

where

$$\alpha = e^{aL}, \tag{6}$$

and the average temperature of such a wire is given by

$$U_{av} = U\,\infty\,\left(1 + \frac{2}{aL}\,\frac{1-\alpha}{1+\alpha}\right). \tag{7}$$

The general case, when a wire of length L is immersed in liquid to a depth l, requires separate equations for the vapor and liquid phases, which have to meet the following boundary conditions:

$x = 0$	$U = 0$
$x = L$	$U' = 0.$
$x = l$	$U = U'$
$x = l$	$dU/dx = dU'/dx,$

and the resulting coefficients for equations of the form

$$U = U\,\infty + C_1 e^{ax} + C_2 e^{-ax} \qquad (8)$$

are functions of L, l, a, a', U ∞, U'∞, where the primed quantities apply to the vapor phase.

Design considerations, however, require only the solutions for the finite and semi-infinite wires surrounded by a uniform medium.

Design considerations. The liquid-level indicator for the equilibrium cell was required to indicate liquid level to better than 0.1 in., in a total span of 2 in., with a very small power dissipation.

Table I is a comparison of calculated values for several possible sensing elements, operating on the system acetone-air at room temperature.

The sensing elements were compared under conditions which gave the same values of temperature difference between the element and the fluid, conditions which also yield approximately the same values for the heat-transfer coefficients.

Under these conditions, Eq. (4) indicates that the power required to obtain a given temperature difference at a large distance from one of the terminals is directly proportional to the surface area; thus we see it is advantageous to operate with a very fine wire.

The sensitivity of the liquid-level indicator, however, depends not only on the power dissipated, but also on the ratio of heat transferred to the fluid to heat transferred longitudinally along the wire--a factor which appears exponentially in Eq. (3) through (8). This factor "a" was calculated for the different sensing elements and appears in Table I together with its reciprocal, which for the semi-infinite wire is the distance along the wire necessary for a 63% approach to U ∞. On the same table appears the average temperature that the 2-in. sensing element would assume in contact with air under the same conditions.

Thus it appears that either a 0.0005-in. platinum wire or a platinum ribbon would be the most advantageous sensing elements. The 0.5-mil wire requires a smaller power input than the ribbon to maintain the same temperature difference, but the ribbon gives a more linear response near the ends of the filament, an effect which is more noticeable in short sensing elements. The platinum wire should not

Table I

Characteristics of different liquid-level indicators for the system acetone-air at room temperature

Sensing Element	$(U)_L$ (°C)	$(U)_G$* (°C)	q (watts/in)	a ft^{-1}	"Sharpness" (1/a in.)	$(U_{av})_G$
No. 40 copper wire	1	39	1.1×10^{-3}	8.3	1.45	5.2
2-mil platinum wire	1	39	7.1×10^{-4}	24.4	0.51	19.8
1-mil quartz, silver-plated	1	39	2.6×10^{-4}	46.8	0.25	29.2
1-mil platinum wire	1	39	2.6×10^{-4}	34.5	0.35	25.5
0.5-mil platinum wire	1	39	1.8×10^{-4}	48.9	0.25	29.2
platinum ribbon 0.001 by 0.0002 in.	1	39	2.5×10^{-4}	61-81.0	0.19-0.15	31.6

* Calculated using h = 1 Btu/hr x sq. ft. x °F, which is approximately the gas-film heat-transfer coefficient.

be silver coated (Wollaston wire), however, because the thermal conductivity of silver is about six times that of platinum, thus offsetting some of the advantage of the small diameter.

A platinum ribbon approximately 1 mil x 0.2 mil was used as the sensing element and was made by rolling 3-mil Wollaston platinum wire into a ribbon 1 mil thick. This ribbon was wound on a glass tube and the silver dissolved with nitric acid. The resulting ribbon has a resistance of about 22 Ω/inch at room temperature and is very uniform throughout its length.

The liquid-level indicator was mounted as indicated in Fig. 20 and its resistance was measured by means of the bridge circuit shown in Fig. 21. The 20-μa full-scale meter was calibrated directly in inches.

Although the bridge was operated with rectified ac, it is shown battery-operated, because the reading is very sensitive to variations in operating current and battery operation probably would be more satisfactory.

Calibration and results. The instrument is calibrated by adjusting the Helipot R-4 so that ME-1 reads zero when the sensing element is completely immersed in liquid, then, by adjusting the current and the sensitivity, the 20-μa meter can be made to read full scale when totally outside the liquid. It may be necessary to readjust the settings until the meter reads correctly at the two ends of the scale.

The calibrating procedure given above is satisfactory when the instrument is to operate always in the same liquid and the same gas, under identical conditions of temperature and pressure; however, it was desired to obtain a method of calibration whereby the instrument could be calibrated rapidly, without resort to visual indications, and under widely different conditions of pressure, temperature, and composition of the phases.

The procedure adopted, which gave satisfactory results for the systems acetone-air at room temperature and liquid nitrogen-nitrogen vapor at 1 atmosphere pressure, is as follows:

(a) Adjust R-5 for maximum sensitivity.

(b) With the sensing element totally immersed in liquid, and the lowest current (about 1.5 ma), adjust the Helipot R-4 to balance the

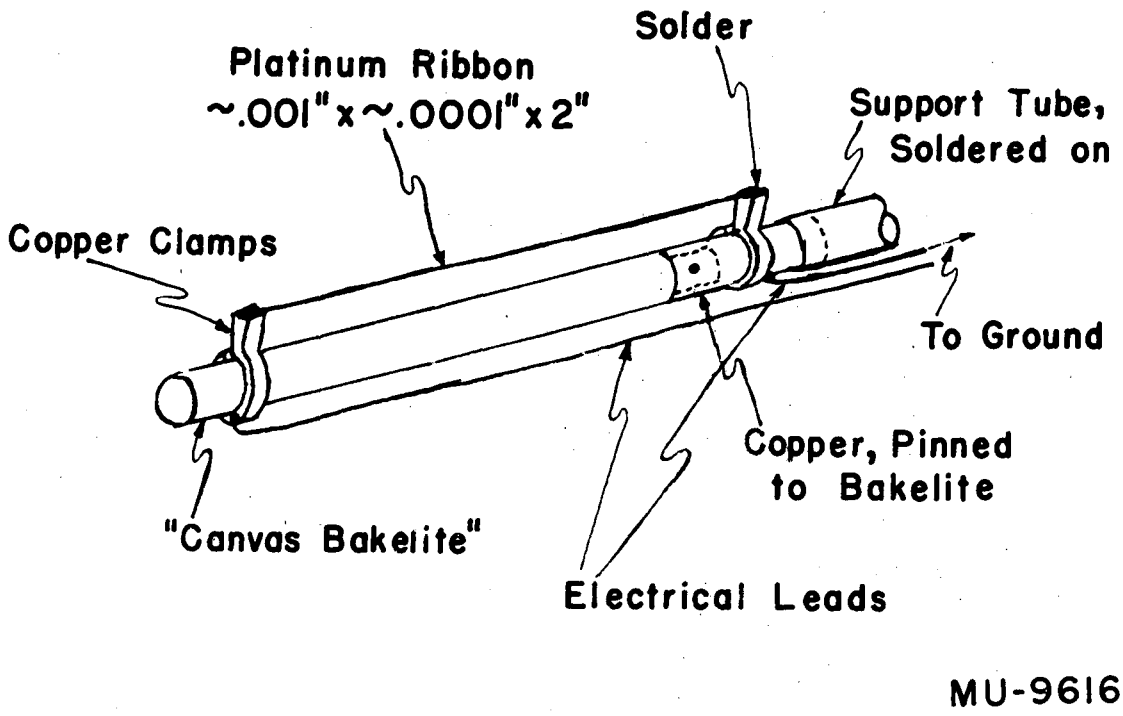

Fig. 20. Liquid-level indicator.

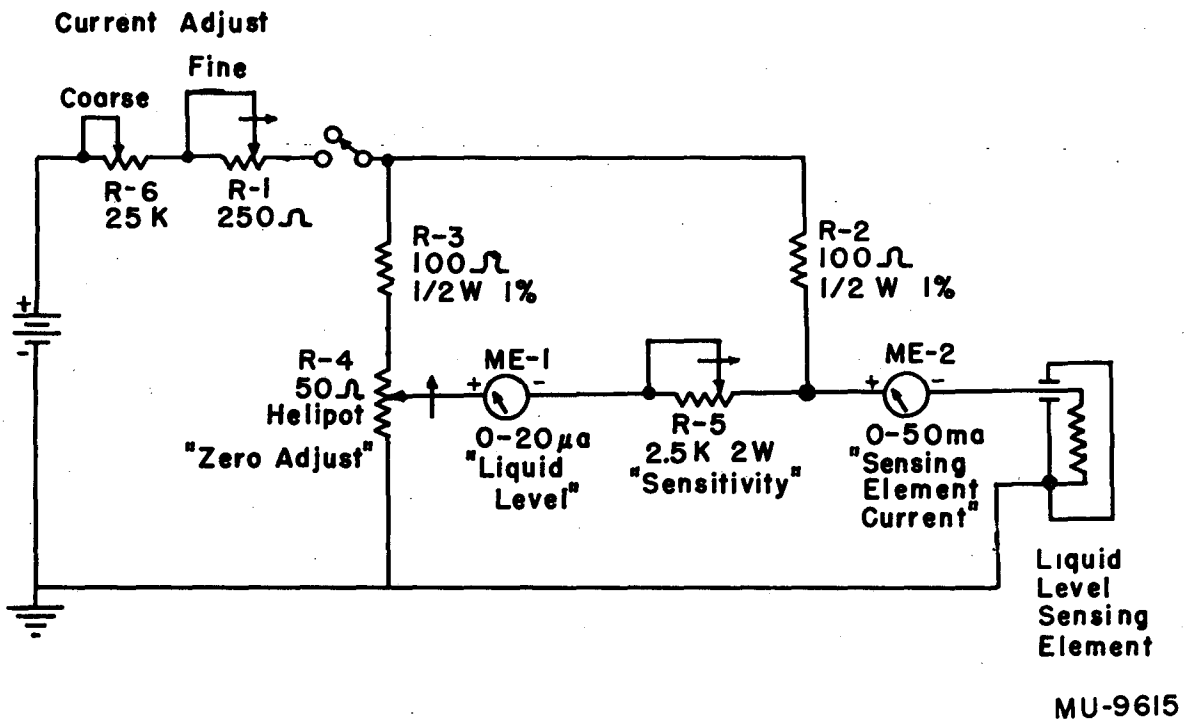

Fig. 21. Circuit diagram for liquid-level indicator.

bridge. Record the Helipot reading, R_1.

(c) Gradually increase the current and plot bridge unbalance versus sensing-element current, Curve A in Figs. 22 and 23.

(d) Plot bridge unbalance versus current with the sensing element completely in contact with the gas, Curve B in Figs. 22 and 23.

(e) Note the current I_1 at which the bridge gives full scale in the gas, and from the plot read the corresponding reading in the liquid, $L_{liq.}$. Extrapolate curve B for the gas until $L_{gas} = L_{liq} + 2$ (the 2 being the full-scale reading desired.)

(f) Reduce the current until the reading in the gas is the same as $L_{liq.}$ mentioned under (e).

(g) Adjust the Helipot R-4 until bridge is balanced (zero) and record the Helipot reading R_2.

(h) Set the Helipot at the intermediate value $(R_1 + R_2)/2$ and adjust the current to obtain full-scale deflection in the gas.

(i) Record the current I_2. This is the correct operating current for the sensing element.

The instrument is then adjusted to read correctly at the two ends of the scale for the given liquid and gas phases.

The above procedure is especially advantageous when the heat-transfer properties of the liquid phase change slowly with pressure, temperature, or composition, since it is then possible to prepare a family curves of bridge unbalance versus current for the liquids, and variations in the properties of the gas phase can be taken care of by individual calibrations under the different conditions. Step (h) of the calibration procedure gives rise to some error, especially at the higher pressures, when the deflection-versus-current curves are more nearly parallel and a higher operating current is required.

The linearity of the sensing element is satisfactory, as can be seen in Fig. 24, which compares the platinum ribbon with 1-mil platinum wire, showing that, as predicted, the ribbon gives a more linear response. The data were obtained in the system acetone-air at room temperature, with the power dissipated by the wire about four times as great as the power dissipated by the ribbon.

Also shown in Fig. 24 is the response of the 1-mil platinum

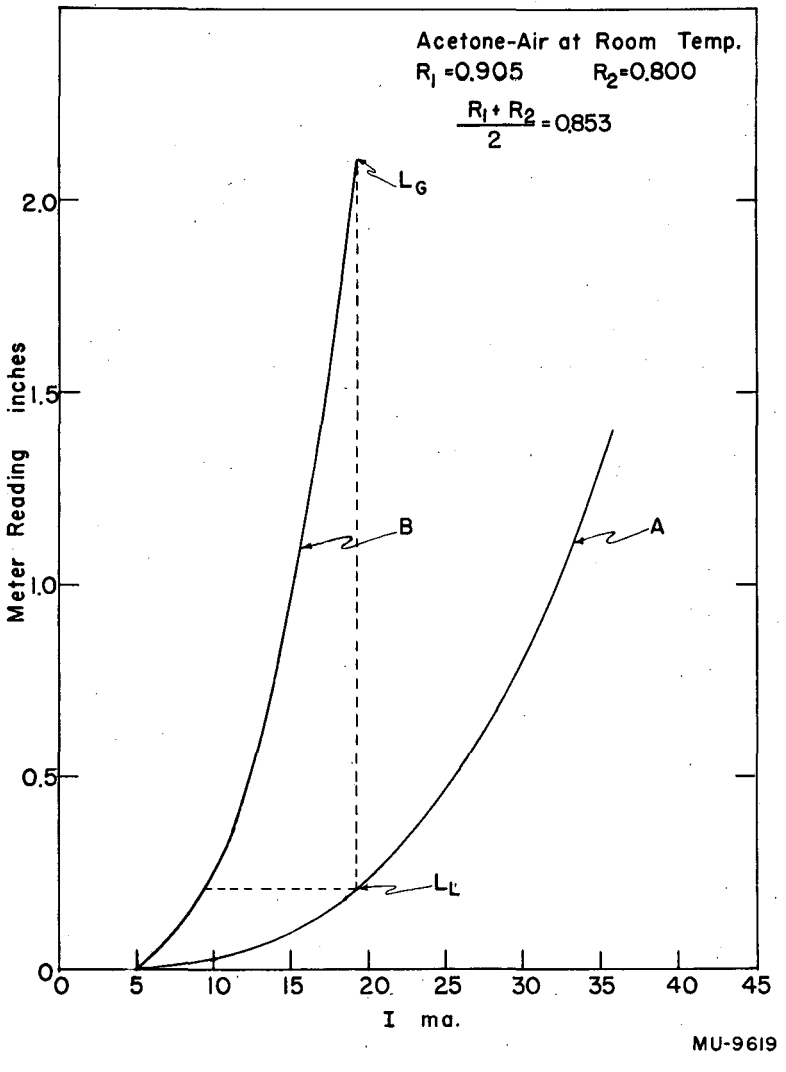

Fig. 22. Curve for calibration of liquid-level indicator, acetone-air at room temperature.

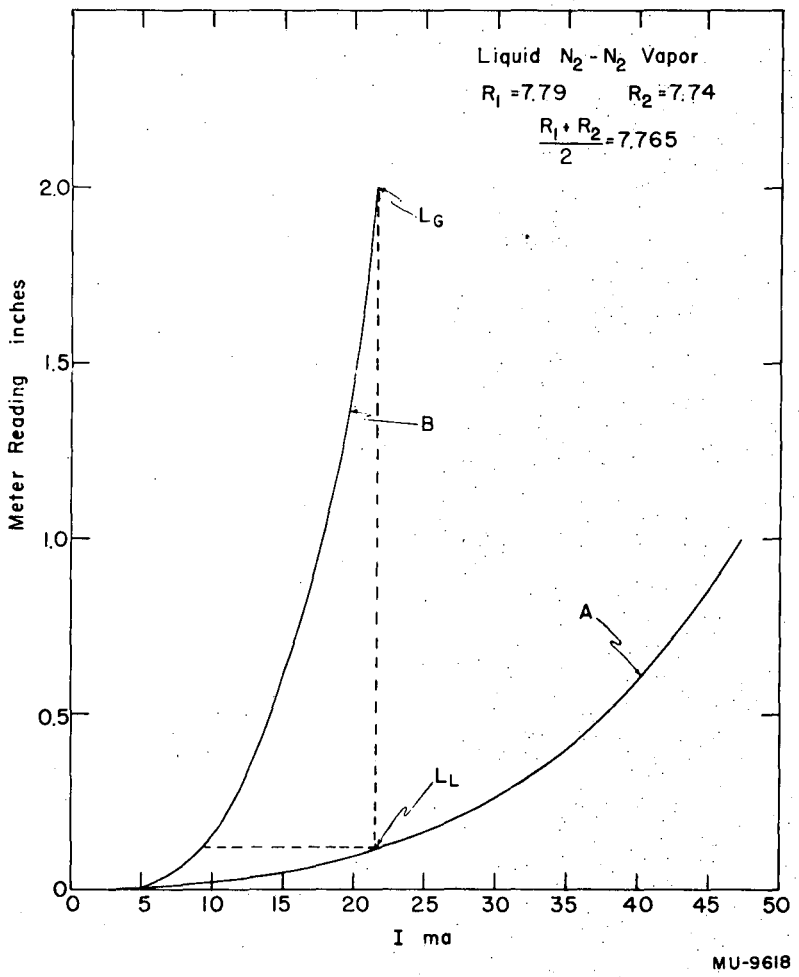

Fig. 23. Curve for calibration of liquid-level indicator, liquid nitrogen-nitrogen vapor at 1 atmosphere.

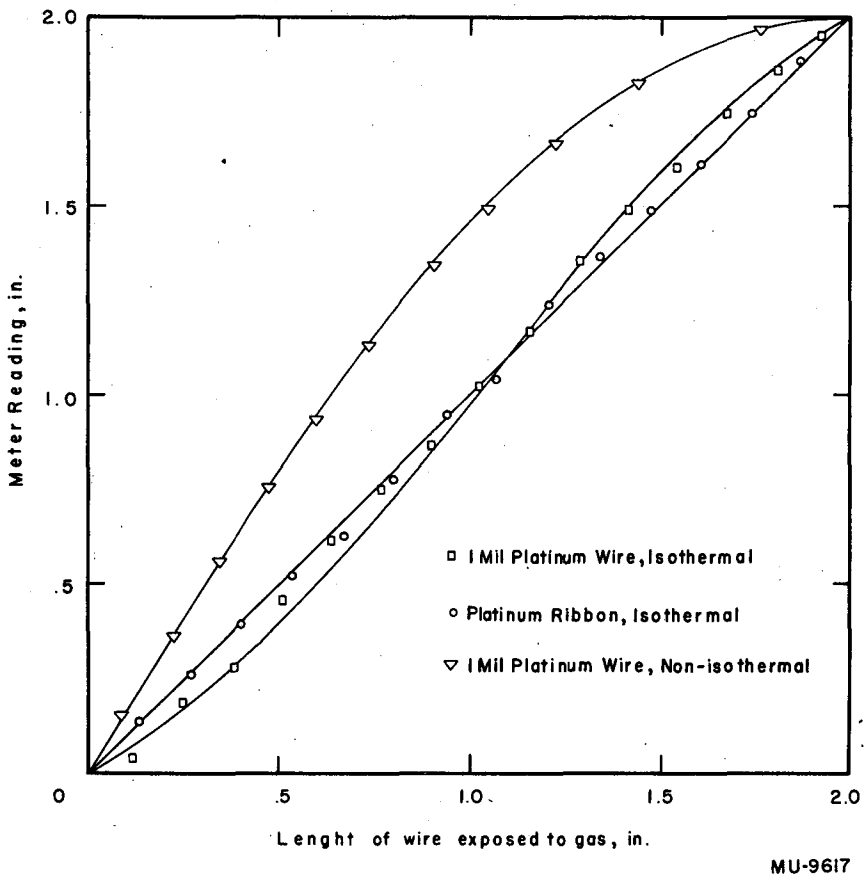

Fig. 24. Linearity of liquid-level indicator.

wire under nonisothermal conditions such as would be obtained in measuring the level of liquid nitrogen in an open container, where appreciable temperature gradients exist in the gas phase. The deviations from linearity are then quite appreciable.

The scatter in the experimental data shown is due to variations in the operating current, and a part of the deviations from linearity could be adscribed to the difficulty in obtaining a perfectly taut filament out of such fine wire.

The power dissipation of the liquid-level indicator under operating conditions at liquid nitrogen temperatures was about 3.4 milliwats per inch or 6.8 milliwatts for the total length.

The calibrating procedure given above was found to be fairly reliable at low pressures or for operation with pure nitrogen vapor. Thus reliable results were obtained with pure nitrogen at 100 psig; however, the addition of hydrogen to the vapor phase increased the heat-transfer coefficient of the vapor to the point where the above calibrating procedure was not reliable at operating pressures of about 300 psig, with hydrogen concentrations in the vapor of the order of 75%.

Liquid-level indicator for PV-3. The liquid-level indicator in PV-3, used during sampling, is a simple "on-off" device using as sensing element a Globar type 304B resistor, chosen because of its large temperature coefficient of resistance in the region -100° to -200° C. The Globar resistor was ground to an outside diameter of 1/16 inch for ease of assembly inside the pressure vessel, and its resistance was measured with a bridge very similar to that shown in Fig. 21.

The adjustment of the bridge to obtain a liquid sample free from vapor bubbles was rather critical and merits discussion in more detail, with Fig. 21 as a reference for the circuit diagram and Fig. 25 for the flow diagram.

When a sample is taken, the liquid flows up into PV-3, pushing ahead of it the vapor contained in the tubes and valves, and it is desired to close the liquid-sample valves V-8 and V-9 when the liquid level in PV-3 is high enough to cover the Globar, but not before, thus flushing the vapor bubbles from the line. Therefore the meter should read full scale when the Globar is completely immersed in the liquid, but should

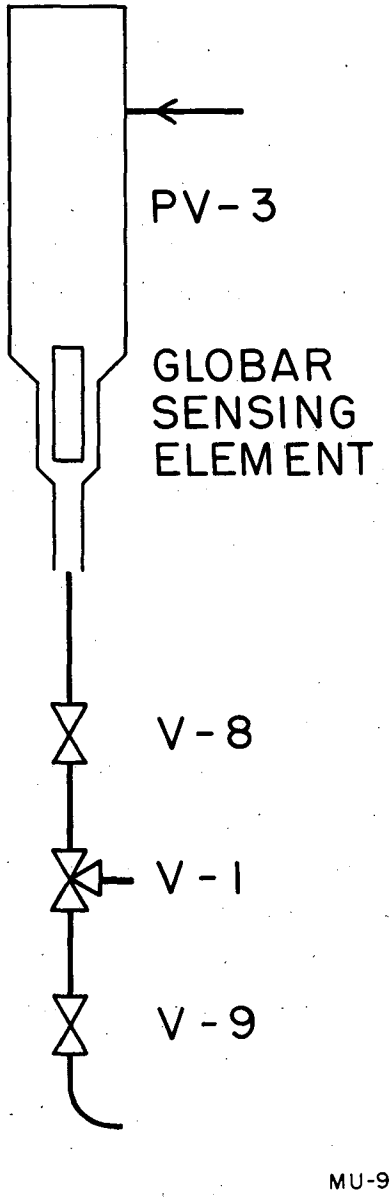

Fig. 25. Flow diagram of liquid-sampling section.

not give full-scale readings in the moving vapor or when a slug of liquid wets the globar.

The adjustment of the circuit constants is best made by trial with the given liquid and vapor phases, after the pressure in the equipment is brought to operating value, before a run is made. This also insures that an adequate amount of liquid is present in the equilibrium cell to take a sample after the run is made.

The bridge is operated at maximum sensitivity by decreasing R-5, and R-4 is adjusted to zero the bridge very shortly after the current is turned on, before the Globar reaches its equilibrium temperature in contact with the vapor. With this adjustment, the meter reading will be negative when the Globar is in contact with stagnant vapor. Now the flows in the equipment are adjusted for sampling, as described elsewhere, and the valves are closed after the meter goes off scale, indicating that liquid is present in PV-3. After the valves are closed the meter should remain off scale for at least 30 seconds, indicating that the Globar is covered with liquid. If this is not the case the value of R-4 is changed, because the meter indication was due to vapor flow or to a slug of liquid.

The adjustment of the circuit constants becomes increasingly difficult at the higher pressures, in the vicinity of the critical point of the mixture, because the liquid and vapor phases have nearly the same thermal properties. The upper limit of applicability of the liquid-level indicator in PV-3 is not known; however, it gave reliable indications at 95°K and about 1200 psig for hydrogen-nitrogen mixtures containing more than 70% H_2 in the vapor phase.

Time for Approach to Equilibrium

The time required for a given approach to equilibrium in a recirculation type apparatus is short, and can be calculated if we assume that all the vapor is concentrated in a reservoir and that there is perfect mixing of the gas in the reservoir.

For a leaktight system, a material balance (Fig. 26) yields

$$m_1 x + m_2 y = C = \text{total moles of comp. 1}, \tag{9}$$

$$m_1 + m_2 = C_1, \tag{10}$$

where

m_1 is the number of moles in the liquid phase,

m_2 is the number of moles in the vapor phase,

C and C_1 are constants,

x = composition of the liquid, mol fraction,

y = composition of the vapor, mol fraction.

The above material-balance equations neglect the small amount of vapor of composition y_1 in the tubing between the liquid and vapor reservoirs.

In addition, we can write the following relations between the vapor and liquid compositions:

$$y^* = Kx \tag{11}$$

and

$$E = \frac{y_1 - y}{y^* - y}, \tag{12}$$

where

y^* is the vapor in equilibrium with a liquid of composition x;

E is the Murphree plate efficiency, which is the ratio of actual enrichment to the enrichment obtained in ideal contacting;

K is the vapor-liquid equilibrium constant.

From Eq. (11) and (12) we have

$$y_1 = EK x + (1 - E) y. \tag{13}$$

From Eq. (9),

$$y = C/m_2 - m_1 x/m_2. \tag{14}$$

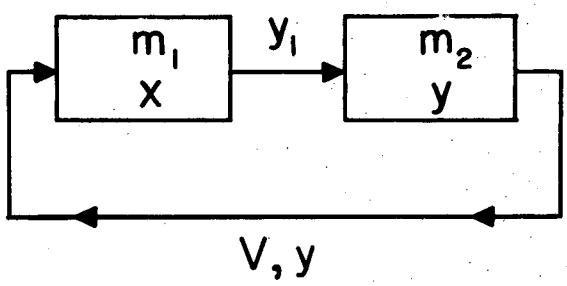

MU-9835

Fig. 26. Recirculation equipment, block diagram.

Combining Eqs. (13) and (14), we get

$$y_1 = \frac{C}{m_2}(1 - E) + \left[EK - (1 - E)\frac{m_1}{m_2}\right] x. \qquad (15)$$

Now we can write the equations describing the transient behaviour of the system. For the liquid,

$$Vy - Vy_1 - m_1 \frac{dx}{dt} = 0. \qquad (16)$$

For the vapor,

$$Vy_1 - Vy - m_2 \frac{dy}{dt} = 0. \qquad (17)$$

However, it can be shown that Eq. (16) and (17) are not independent, since they are related by the material balance, Eq. (9). Therefore we can work with either one of them; let us take Eq. (16).

We can substitute the values of y and y_1 obtained in Eq. (14) and (15), obtaining

$$\frac{dx}{dt} + \frac{VE}{m_1}\left(K + \frac{m_1}{m_2}\right) x = \frac{VEC}{m_1 m_2}, \qquad (18)$$

An equation which can be easily solved if it is assumed that m_1 and m_2 are constant, giving

$$s = \frac{b}{a} + A e^{-at}, \qquad (19)$$

where

$$a = \frac{VE}{m_1 m_2}(m_2 K + m_1),$$

$$b = VEC/m_1 m_2,$$

$$\frac{a}{b} = \frac{C}{m_2 K + m_1} \quad ;$$

A is the integration constant.

A can be evaluated from the following boundary conditions:

$$t = 0 \qquad x = x_o$$

$$t = \infty \qquad x = x_e$$

where x_e is the final equilibrium composition at steady state, so that

$$x = x_e + (x_o - x_e) e^{-at}. \qquad (20)$$

The value of a can be further simplified by writing Eq. (9) for the equilibrium compositions,

$$m_1 x_e + m_2 K x_e = C,$$

therefore we have

$$x_e = \frac{C}{m_1 + m_2 K}$$

and a becomes

$$a = \frac{VEC}{m_1 m_2 x_e} \quad . \tag{21}$$

The assumption of perfect mixing in the gas reservoir is very conservative, since shorter equilibrium times would be obtained for "slug" flow.

We can now apply Eq. (20) to two typical cases to find the order of magnitude of time required to reach equilibrium.

The total volume of the recirculation equipment used was 600 ml, of which 500 were located in the main water bath, at 35°C. The design pumping rate of the vapor is 200 ml/min and the volume of the liquid phase is smaller than 23 ml.

If we assume that the Murphree plate efficiency of contacting is 50%, and that owing to leaks of mercury in the pumping system the actual pumping rate is 100 ml/min, the following results are obtained in the H_2 - N_2 system for $x - x_e = 0.0001$;

P (atmos)	T (°K)	t (min)
5	79	6.6
70	109	14.3

Thus, the time required to approach the equilibrium composition within 0.01% is at the most 15 min, which is a relatively short time for equilibrium measurements of this nature.

EXPERIMENTAL RESULTS

The time available for taking data in the vapor-liquid-equilibrium equipment was rather limited, therefore the following results include only the 90° and 95° K isotherms up to a pressure of about 700 psia. The results are listed in Table II and are plotted in a P-x-y diagram in Fig. 27. This type of diagram is difficult to read accurately because the lines expressing liquid compositions fall practically on top of each other. Also, because of the large curvature of the vapor composition line, it is difficult to smooth the data.

The K-value-type plot presented in Fig. 28 is convenient for numerical calculations not requiring a high degree of accuracy, but is not sensitive enough to show the scatter in the data presented here.

What is desired is a method of plotting the data so that the small amount of scatter may be readily detectable, and preferably one that would not combine the liquid and vapor compositions in a complex function, but deal with them independently, to avoid compounding the the errors.

Liquid Compositions

One of the common ways of smoothing liquid compositions is to plot the vapor pressure of mixtures of constant composition in a reference-substance-type plot,[29] but this method is not applicable to systems like the H_2 - N_2 system, where one of the components is a gas very much above its critical temperature, because in this case the lines have slopes very different from those of the reference substance. Thus, while the total pressure increases with temperature for pure nitrogen and for mixtures containing less than 8% H_2, it is practically independent of temperature for mixtures containing 8% H_2, and decreases with an increase in temperature for richer mixtures.

However, the concentration of hydrogen in the liquid increases almost linearly with pressure at constant temperature indicating that Henry's law should be followed rather closely.

Table II

Liquid-vapor equilibrium data
H_2 - N_2 System

Run No.	T (° K)	P (psia)	$P-P^{\circ}_{N_2}$ (psi)	x (mol fractions) H_2	y	$K = \frac{y}{x}$	$\frac{x}{P-P^{\circ}_{N_2}} \times 10^4$	$\frac{yp}{P-P^{\circ}_{N_2}}$
	90.00	52.14 *	0	0	0			
10	90.02	259.0	206.8	---	0.7324	---	---	0.9173
11-a	90.02	196.76	144.52	0.0248	0.6732	27.1	1.716	0.9165
11-b	90.01	188.20	136.02	0.0234	0.6619	28.3	1.720	0.9158
11-c	90.03	171.91	119.62	0.0207	0.6367	30.8	1.730	0.9150
11-d	90.02	164.42	112.18	----	0.6247	---	---	0.9156
11-e	90.03	142.74	90.49	----	0.5791	---	---	0.9135
11-f	90.04	148.07	95.76	0.0164	0.5903	36.0	1.713	0.9127
11-g	89.99	122.35	70.24	0.0119	0.5217	43.8	1.694	0.9087
11-h	90.01	88.96	36.76	----	0.3753	---	---	0.9082
18-a	90.01	146.00	93.80	0.0159	0.5855	36.8	1.695	0.9113
20-a	90.06	354.19	301.77	0.0534	0.7800	14.61	1.769	0.9155
20-b	90.04	666.51	614.21	0.1115	0.8304	7.447	1.815	0.9011
	95.00	78.43 *	0	0				
19-a	95.02	160.87	82.32	0.0149	0.4492	30.1	1.810	0.8778
19-b	95.00	380.24	301.81	0.0566	0.7005	12.38	1.875	0.8825
21-a	94.99	657.44	579.07	0.1121	0.7643	6.818	1.936	0.8677

* Vapor pressure of nitrogen by definition

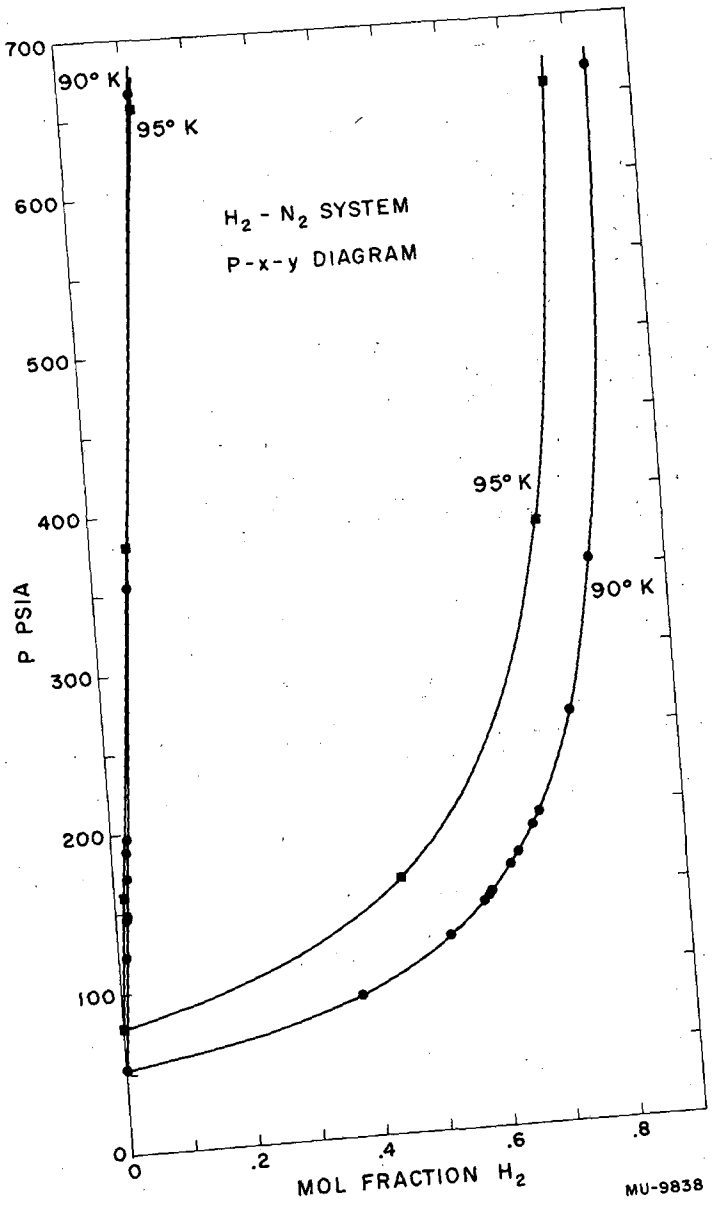

Fig. 27. Hydrogen-nitrogen system: P-x-y diagram.

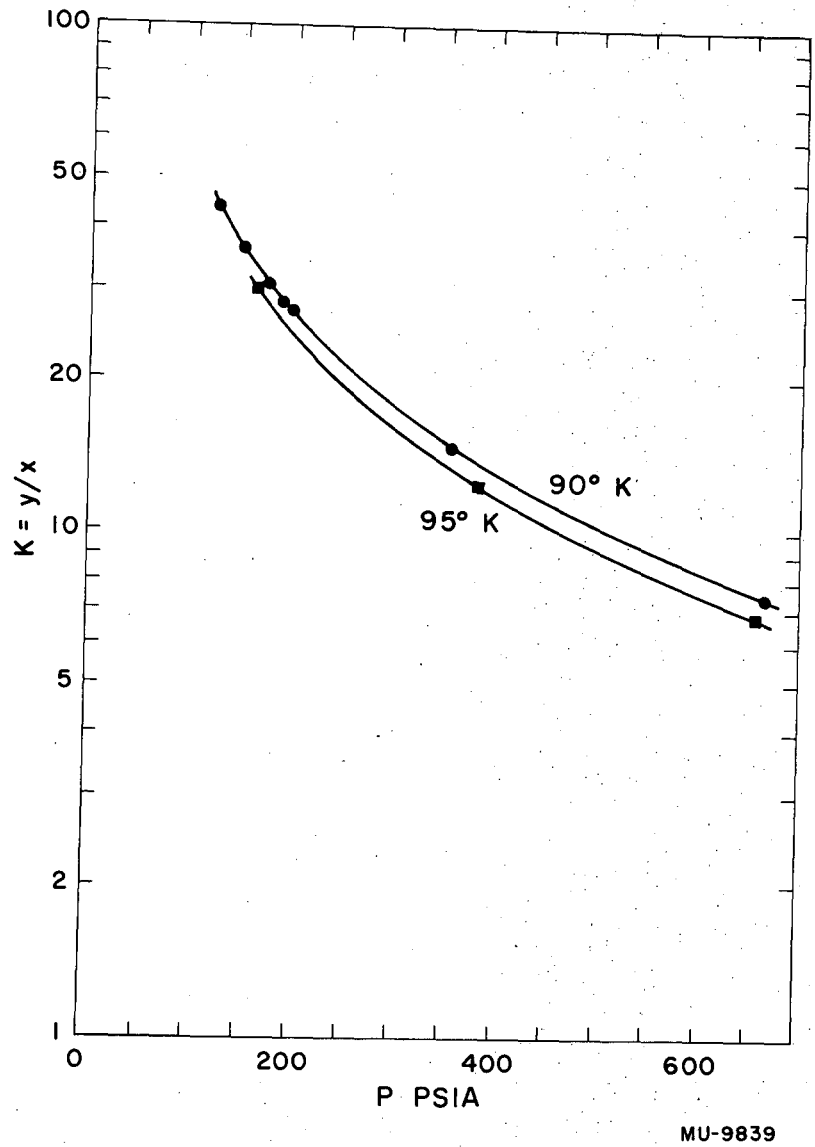

Fig. 28. Hydrogen-nitrogen system: K values.

Henry's law can be written as

$$x = k \bar{P}_{H_2}, \tag{22}$$

where x is the mol fraction of hydrogen in the liquid,

k is a constant,

$\bar{P}_{H_2}$ is the partial pressure of hydrogen in the vapor.

The partial pressure of hydrogen in the vapor can be expressed in terms of the total pressure and the partial pressure of nitrogen as

$$\bar{P}_{H_2} = P - \bar{P}_{N_2}, \tag{23}$$

and if Raoult's law applies to the liquid phase, the partial pressure of nitrogen can be expressed in terms of the liquid composition,

$$\bar{P}_{N_2} = P^{o}_{N_2} (1-x), \tag{24}$$

where $P^{o}_{N_2}$ is the vapor pressure of pure nitrogen. We can substitute this value in Eq. (22), obtaining

$$x = k\left[P - P^{o}_{N_2} (1-x)\right], \tag{25}$$

which can be further simplified to

$$x = k'(P - P^{o}_{N_2}), \tag{26}$$

which neglects the effect of the liquid composition. From Eq. (26) the value of k' is

$$k' = \frac{x}{P - P^{o}_{N_2}}. \tag{27}$$

The value of k' was used in the plots in preference to the value of k, because it is a parameter simpler to calculate and the ratio k'/k is practically constant at 1.009 throughout the pressure range investigated. The variation of k' with pressure and temperature is shown in Fig. 29. It can be seen that the solubility of hydrogen in liquid nitrogen, when expressed as mol fraction per psi partial pressure of hydrogen in the vapor, increases with both temperature and pressure. The shaded region around each line indicates the limits of error in the values of k' corresponding to an error of ± 0.01% in the composition of the liquid phase. k' was plotted versus $P - P^{o}_{N_2}$ instead the total pressure P,

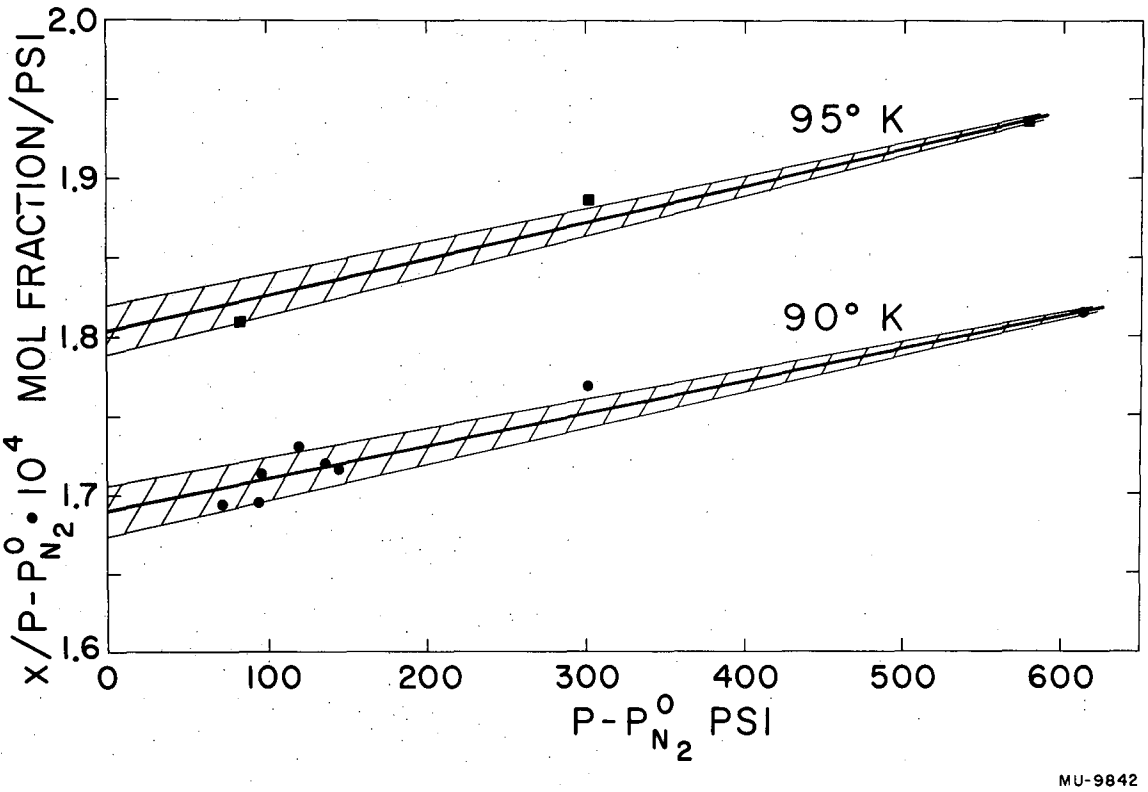

Fig. 29. Hydrogen-nitrogen system: liquid compositions.

to allow for comparisons of solubility at the same values of partial pressure of hydrogen.

Vapor Compositions

If the vapor phase were an ideal gas mixture, the following relationship would hold:

$$\bar{P}_{H_2} = yP = P - P^{o}_{N_2}(1-x), \tag{28}$$

which can be again simplified by neglecting the effect of liquid composition to obtain

$$\bar{P}_{H_2} = yP = P - \bar{P}_{N_2}. \tag{29}$$

Figure 30 shows the value of the function $yP/(P-P^{o}_{N_2})$, which differs from 1 even at the lowest pressures and has a strong temperature dependence. However, it is convenient for smoothing isothermal data because it varies relatively slowly with pressure, except near the critical point of the mixtures.

Temperature Scale

The temperatures of 90° and 95° K used in this work are defined in terms of the vapor pressure of pure nitrogen and NACA-NBS table of vapor pressure of nitrogen,[27] as follows;

Temperature (°K)	Vapor pressure (psia)
90.000	52.140
95.000	78.430

Comparison with Literature Valves

The vapor-liquid equilibrium for the H_2-N_2 system has been determined by several investigators, and some of their results are compared in Figs. 31 and 32. Verschoyle[46] used the equilibrium-bomb technique and investigated the vapor-liquid equilibrium between the triple point of nitrogen and 85.7° K.* The volume of his equilibrium bomb was only 9 ml, so that appreciable pressure changes must have

* The temperature values mentioned may differ from those cited by the original investigator because they were corrected to be in agreement with the values of vapor pressure of nitrogen given by the NACA-NBS tables.[27]

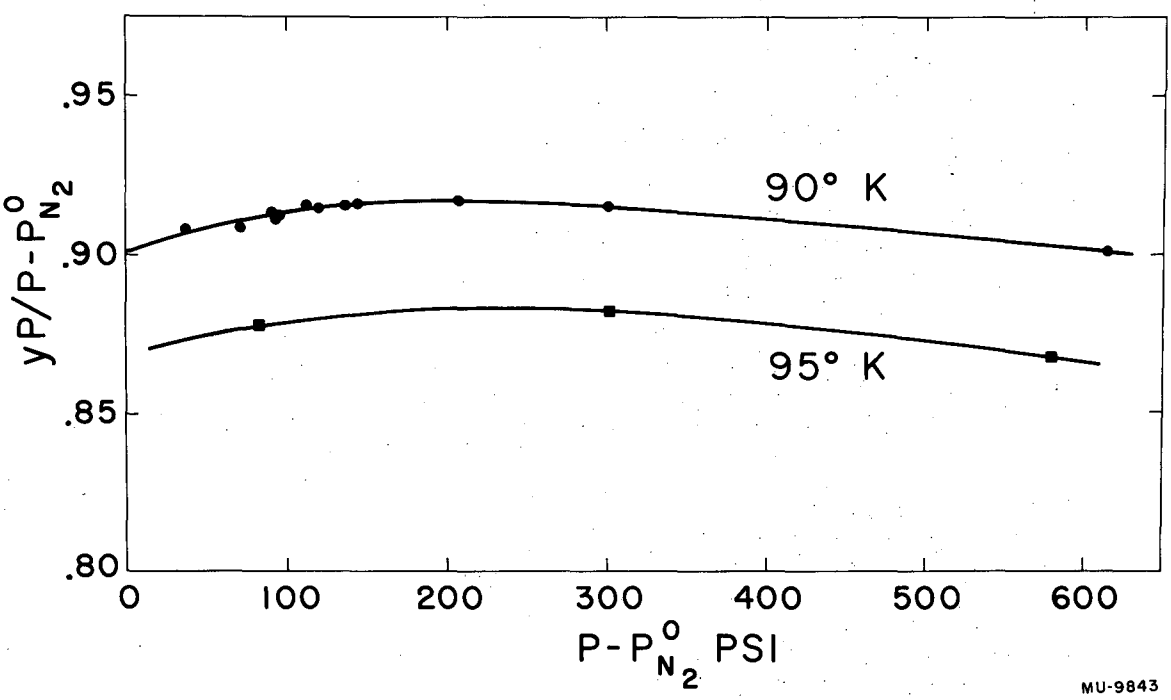

Fig. 30. Hydrogen-nitrogen system: vapor compositions.

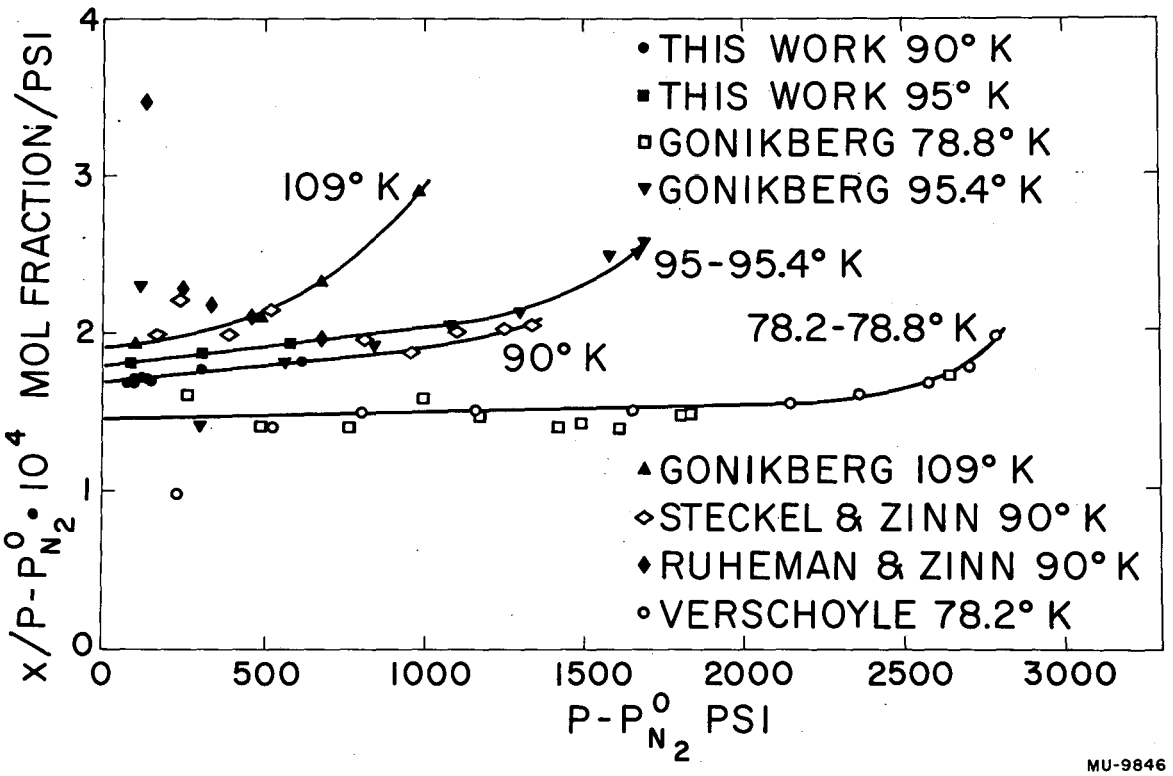

Fig. 31. Hydrogen-nitrogen system: liquid compositions; comparison with literature values.

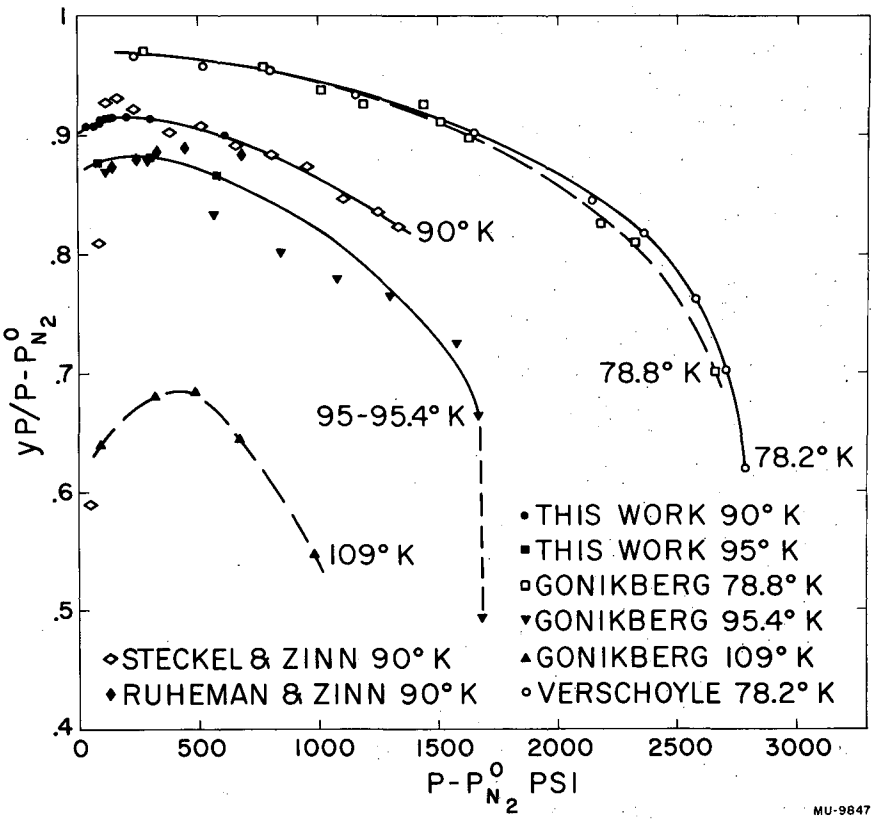

Fig. 32. Hydrogen-nitrogen system: vapor compositions; comparison with literature values.

occurred during the sampling of the vapor. This is confirmed by the very low values of hydrogen concentration in the liquid reported at the lower pressures, as can be seen in Fig. 31, which shows his 78.2° K isotherm. The same effect is noticed in his 85.7° K isotherm (not shown). His data at higher pressures, however, seem to be fairly reliable.

Ruhemann and Zinn[38] report data at 78°, 83°, and 90° K* and pressures up to 50 atmos (735 psia). They used a dynamic method in which a mixture of known composition is cooled to the desired temperature through a long cooling coil, and later the liquid and vapor phases are separated and sampled. Unfortunately their data were not tabulated and had to be read off a very small plot, therefore the following conclusions may be colored by a possible reading error. Their 90°K isothermal data can be seen to differ appreciably from the rest of the literature values. The same is true of their 78° and 83° K data (not shown).

Later data taken in the same equipment by Steckel and Zinn[40] seem to be of much higher quality, although subject to the same possible reading error mentioned above. Steckel and Zinn worked at 90°, 107.7°, and 109° K and pressures up to 95 atmos (1396 psia.). Their 90° K data agree fairly well with the data obtained in this work, especially at the higher pressures. Their 107.7° and 109°K data are not shown.

Gonikberg and his co-workers[11] used the dynamic method in an apparatus very similar to Dodge's.[8] They tried to duplicate the 78.2° and 85° data of Verschoyle, and also obtained data at 95.4° and 109°K. There is some question as to the actual temperature levels at which they obtained their data, because they used the vapor pressure of oxygen together with the vapor-pressure equation of Dodge and Davis[9] as their temperature reference; but when the temperature

---

* The temperature values mentioned may differ from those cited by the original investigator because they were corrected to be in agreement with the values of vapor pressure of nitrogen given by the NACA-NBS tables.[27]

calculated from the Dodge and Davis equation* is compared with the temperature as calculated from the vapor pressures of nitrogen reported, a small discrepancy exists.

Nominal temperature (°K)	Based on oxygen (°K)	Based on nitrogen** (°K)
79.0	78.81	78.96
86.1	86.06	86.17
95.4	95.45	95.37
109.0	108.95	108.46

It is not known whether the above discrepancies point to an error in the NBS tables or to an error in Gonikberg's vapor-pressure data. The agreement between Gonikberg's data at 95.4° K and the data reported in this work at 95.0°K is fair, considering the slight difference in temperature levels. Most of the discrepancy in the liquid-sample compositions occurs at low pressures, where the effect of errors in the analysis is more pronounced. The vapor compositions at about 600 psia differ by about 1.5%, but the discrepancy is smaller at the lower pressures. Goinkberg's data at 109° are also shown in Figs. 31 and 32.

---

* Corrected to agree with the NBS values of vapor pressure of oxygen.

** The temperature values mentioned may differ from those cited by the original investigator because they were corrected to be in agreement with the values of vapor pressure of nitrogen given by the NACA-NBS tables.[27]

Testing of the Data for Thermodynamic Consistency

The usual methods of testing the thermodynamic consistency of liquid-vapor equilibrium data cannot be applied to the thermodynamic analysis of the hydrogen-nitrogen system, or other systems where one of the components is above its critical temperature and the vapor phase cannot be considered ideal.

Thus, the "area condition" developed independently by Redlich[33] and by Herington,[15]

$$\int_0^1 \log \left(\frac{\gamma_1}{\gamma_2} \right) dx_1 = 0 \qquad (30)$$

where

γ_1 is the activity coefficient of component 1,

γ_2 is the activity coefficient of component 2,

x_1 is the liquid-phase composition, mol fraction,

cannot be applied because the liquid-phase composition does not extend throughout the entire range; besides, the function Q, related to the excess free energy of the mixture,

$$\frac{\Delta F^E}{RT} = Q = x_1 \log \gamma_1 + x_2 \log \gamma_2, \qquad (31)$$

from which Eq. (30) was derived, is not a definite function in the critical region.

The other criteria mentioned by Redlich et al.[34] cannot be applied to the hydrogen-nitrogen system because they are derived on the assumption of an ideal vapor phase and break down, even if some corrections are applied by the use of their "adjusted vapor pressure". Thus, their equation for testing isothermal data,

$$\frac{d \ln P}{dy_1} = \frac{y_1 - x_1}{y_1 \gamma_2}, \qquad (32)$$

breaks down because the slope $d \ln P/dy_1$ assumes infinite and negative values as the pressure is increased, but the right-hand side of the equation yields only finite, positive values.

Similar considerations apply to the methods derived by Kuo Tsung Yu,[22] Othmer[29,30] and various others, which are based

on ideal gas behavior. Other methods describing the limiting trend of activity coefficients in binary mixtures[13,17] are not of immediate applicability. Following the publication of equations based on the Benedict-Webb-Rubin equation of state for the calculation of the partial molal free energies and fugacities of components in mixtures,[1,2] thus making possible the calculation of liquid-vapor equilibria from the equations of state of the pure components, various attempts have been made to calculate the vapor-liquid equilibria for actual systems. Thus, Stotler and Benedict[41] correlated the nitrogen-methane vapor-liquid equilibrium data of Cines et al.[4], and Schiller and Canjar[39] calculated the nitrogen-carbon monoxide system and compared their results with the experimental data of Torocheshnokov.[44]

The calculations are quite involved and result in a fit to the data within about 2%, even after the method of combining constants was changed to fit some of the experimental points.

This method, then, could be used to obtain a rough check on the consistency of my data, but could not be trusted to give results of the same order of accuracy of the data; therefore some other testing procedure had to be devised.

The method finally devised is not entirely rigorous because it checks the limiting behavior of the activity coefficient of only one of the components; however, it is relatively simple and tested the consistency of the data within about 0.2%.

The activity coefficient of nitrogen in the liquid phase was calculated from the liquid-vapor equilibrium data and the equations developed by Redlich[34], by use of the "adjusted vapor pressure" calculated from the equation of state of Redlich and Kwong.[35] The calculations were considerably shortened by the use of the tables of derived functions from the equation of state, supplied by Redlich.[36]

The activity coefficient of a component in a mixture can be empirically expressed by a power series of the form

$$\log \gamma_2 = x_1^2 \left[B + C(x_1 - 3x_2) + D(x_1 - x_2)(x_1 - 5x_2) + \ldots, \right. \quad (33)$$

which simplifies to

$$\log \gamma_2 = Bx_1^2 \quad (34)$$

for nearly ideal solutions.

Thus, if the liquid phase is nearly an ideal solution, a plot of log γ_2 vs x_1^2 should give a straight line going through the origin. This is indeed the case for hydrogen-nitrogen mixtures, as can be seen in Fig. 33.

Actually, the line representing the activity coefficients at 95° K goes through the origin, while the line for 90° K is parallel to it and slightly displaced, having an intercept at x = 0 of 0.0024 corresponding to a value of γ_2 of 1.0055, but the values at low concentrations indicate a definite curvature towards the origin. Further, Fig. 34 shows the range of error in log γ_2 corresponding to an error of ± 0.1% in vapor composition, indicating that the vapor compositions are at most 0.2% in error, if we assume that such a simple equation of state as Redlich and Kwong's, together with the approximate integrations used to obtain the adjusted vapor pressure, can be expected to hold within that accuracy.

This method of plotting the data is particularly sensitive to errors in vapor composition, because the activity coefficient of nitrogen is obtained from

$$\gamma_{N_2} = \frac{K_{N_2}}{Pa/P} , \qquad (35)$$

where

K_{N_2} = vapor-liquid equilibrium constant of nitrogen
= (1-y)/(1-x),

Pa = adjusted vapor pressure of nitrogen,

P = total pressure,

and the values of (1-x) are very close to 1 whereas (1-y) is relatively small. Thus, any error in the vapor composition has a large effect in log γ_{N_2}. Likewise, a small error in the temperature at which the data were obtained has a large effect in log γ_{N_2}, because it affects directly the values of the adjusted vapor pressure.

The shift in the 90°K points, if real, could be explained by assuming that a small amount of liquid is entrained by the vapor as it leaves the equilibrium cell. Actually, if the ratio of moles of liquid entrained to total vapor flow is of the order of 0.0003, the shift in composition of the vapor is about 0.2%. Data on other systems

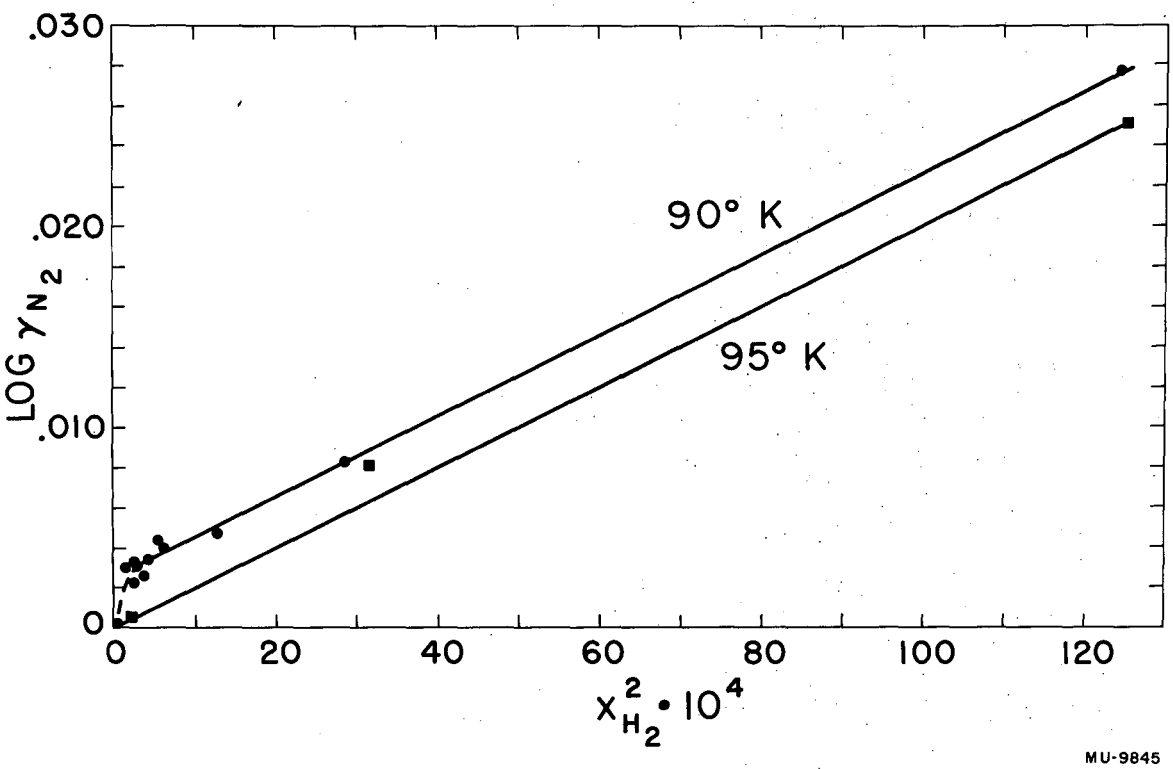

Fig. 33. Hydrogen-nitrogen system: activity coefficient of nitrogen in the liquid phase.

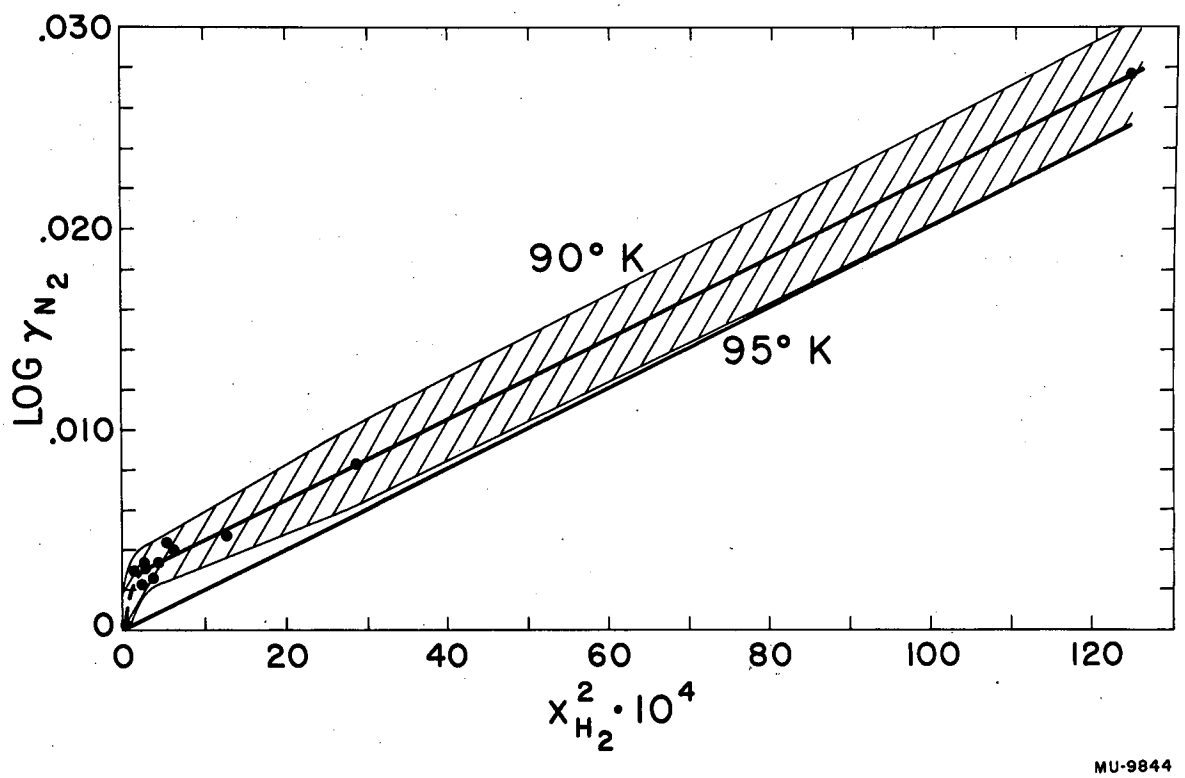

Fig. 34. Hydrogen-nitrogen system: effect of errors in vapor composition on the activity coefficient.

were also obtained,* however, and they do not show a systematic deviation when analyzed by similar techniques for thermodynamic consistency.

The value of the constant B calculated for best fit to the data going through the origin (95° K line) is 2.00.

---

* Arturo Maimoni and Donald N. Hanson, "Index of Refraction and Liquid-Vapor Equilibria for Deuterium-Nitrogen Mixtures," University of California Radiation Laboratory Report No. UCRL-3169, October, 1955.

ANALYSIS

Although the analysis of mixtures of hydrogen and nitrogen can be handled adequately by a number of standard gas-analysis techniques, a great deal of time was devoted to the development of a method that would be

(a) accurate, because it was desired to know compositions of the vapor phase to better than 0.1% and compositions of the liquid phase to better than 0.05%, in order to obtain accurate values of the liquid-vapor equilibrium constant;

(b) fast, or at least requiring little of the operator's time, which was almost an essential condition in view of the complexity and fast rate of approach to equilibrium of the main piece of equipment;

(c) essentially trouble-free, so that analysis could be run on a routine basis;

(d) flexible, to allow for changes in the systems that are to be run on the equipment.

The above considerations eliminated a number of possible analytical methods. Thus, while absorption and combustion analysis in an apparatus of the Orsat type is probably the most flexible of all the methods available for gas analysis, it is slow and requires constant operator attention. Also, obtaining the desired accuracies by this method is somewhat difficult, especially if those accuracies are to be obtained on a routine basis.

Among the physical methods the following were considered;
Mass spectrograph. Although a mass spectrograph was available for occasional analysis, especially on the purity of the gases used, it could not be used for routine analysis on a large number of samples. Also, obtaining the desired accuracies would be somewhat of a problem, since accurate calibration blends are required.
Density. Although there is a large density difference between hydrogen and nitrogen, an examination of the methods available for its measurement did not offer much promise, falling short on accuracy or on reliability.

Effusion. A method of analysis involving the difference in effusion rates[14] was examined with the above criteria in mind, but seemed too difficult to develop into an analytical tool of high accuracy, since it requires very accurate measurements of pressures of the order of 1 mm of mercury.

Among the methods that appeared most promising at the beginning of this investigation was the measurement of the velocity of sound. This method was investigated experimentally, using a sound interferometer operating at 500 kc. The experimental results showed this method to be capable of very high accuracy. However, it could not be developed to a trouble-free status suitable for routine analysis, and was abandoned.

The next method to be investigated experimentally was the measurement of thermal conductivity, a method that offered some early promise but was not reproducible enough to meet the standards of accuracy desired.

Finally an optical interferometer was purchased from Carl Zeiss, and it solved the analytical problem in a fairly satisfactory manner. The results of its calibration and details of the experimental technique are described in a later section.

Common to the calibration of the above analytical instruments was a gas-blending apparatus capable of producing synthetic mixtures in which the composition was known to ± 0.01%. The blending apparatus was developed in this laboratory and is described in the following section.

Blending Apparatus

An apparatus capable of preparing synthetic gas mixtures of any composition with a high degree of accuracy was necessary for the calibration of the analytical techniques. A number of alternative designs for such a piece of equipment have been reported in the literature, especially in the last few years, in connection with methods for calibrating infrared and mass spectrometers.

An early example of blending apparatus was that of Valentiner and Zimmer,[45] which was used in connection with the calibration of a gas interferometer. Their design is fairly complex, not well

adapted to vacuum techniques, and has some dead volume in the bores of stopcocks. The average scatter of their calibration data was about 0.5%, which probably originated in the blending apparatus.

Taylor and Young[42] and Busey et al.[3] describe mixing apparatuses that are better adapted to making blends of liquids of high vapor pressure or of easily condensible vapors than of the permanent gases.

Langer[23] measures the gases independently in the same gas buret, and transfers them to a sample reservoir. A small uncertainty in the composition of the blend results from the gas trapped in a fritted glass section, gas which cannot be removed when a second constituent is added to the mixture. He compares the a priori composition of a 9-component blend with the mass spectroscopic analysis of the same. The maximum deviation between the two sets of compositions is 0.79%, the minimum 0.01%; but it is difficult to ascertain whether the error originates in the blending apparatus or in the subsequent analysis.

Opler and Smith[28] describe a fairly simple blending apparatus, in which the gases are measured in two separate reservoirs and then blended. The same stopcocks are used for admission of the pure gases and removing the finished blend, however, and the small amount of pure constituent trapped in the bore introduces some uncertainty in the final composition. They do not quote any limits of accuracy. None of the above seemed suitable for this investigation, because it was desired to have a blending apparatus with an a priori accuracy of about 0.01%, and capable of maintaining this accuracy over the composition range of 4% to 96% of any component. Further, it was to be well adapted for making binary mixtures, although it was anticipated that a few multicomponent mixtures might be made in it.

The apparatus devised is shown diagramatically in Fig. 35 and was permanently mounted in an aluminum frame with "3-M" Bedding Compound,* as shown in Fig. 36. The apparatus has two calibrated burets in which the pure components are measured.

*Manufactured by Minnesota Mining and Manufacturing Co.

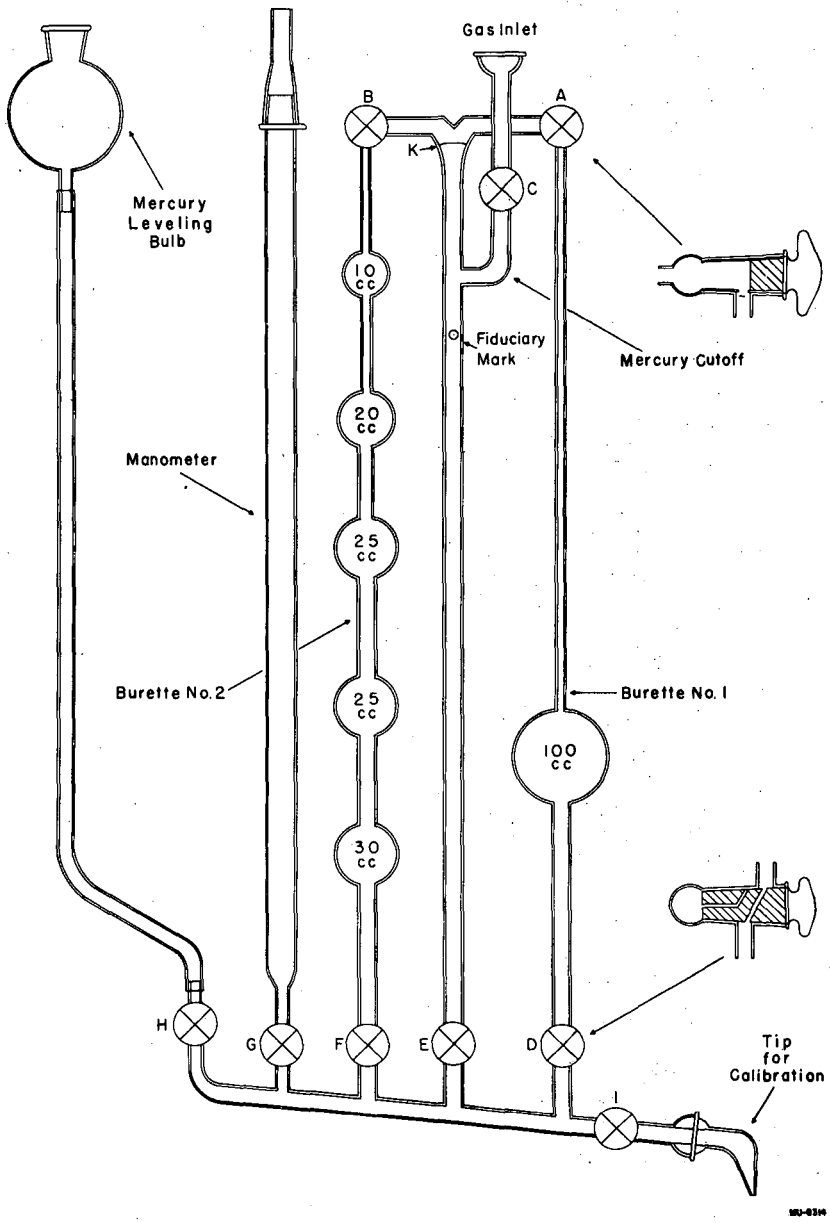

Fig. 35. Gas-blending apparatus.

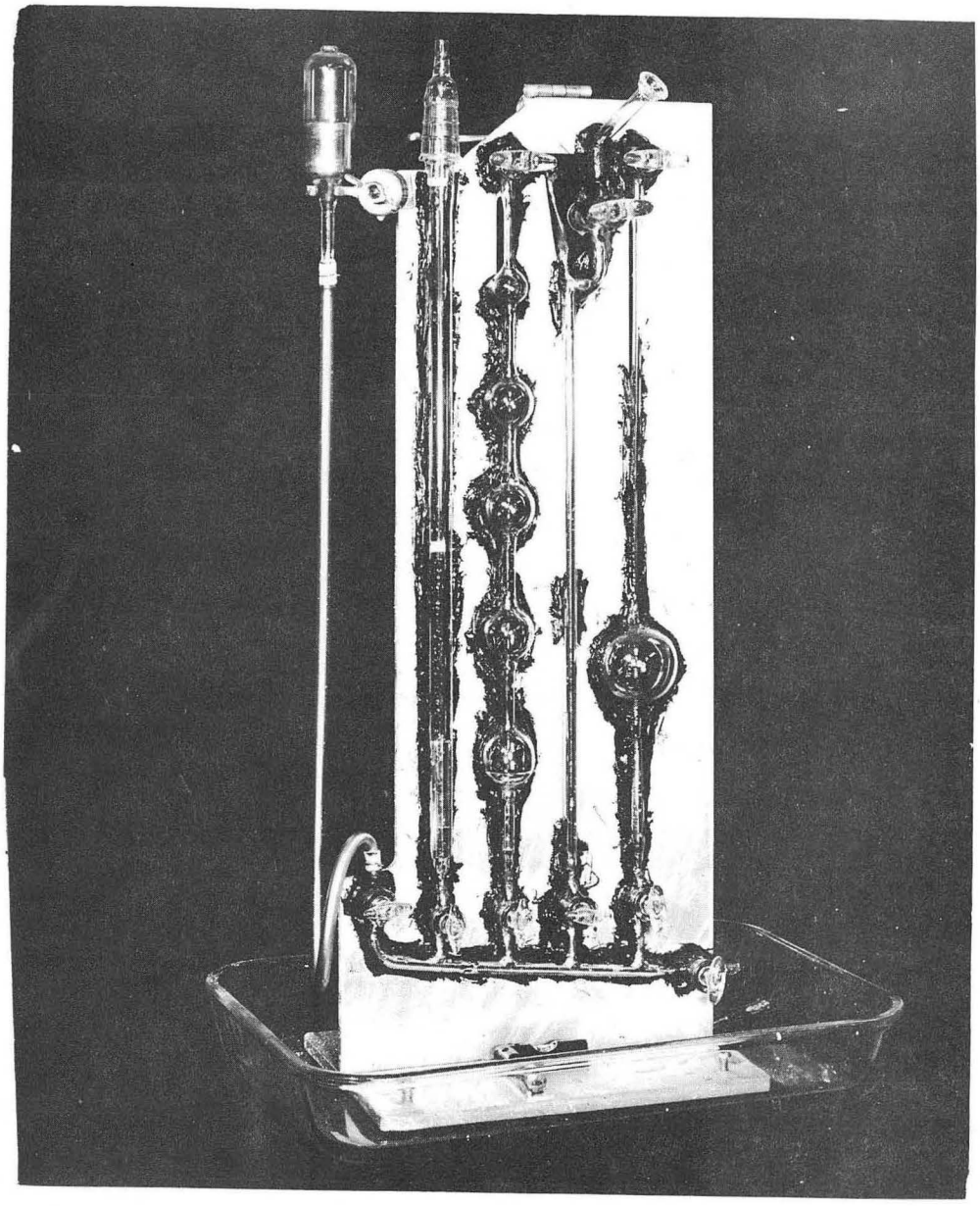

ZN-1302

Fig. 36. Gas-blending apparatus.

Each buret acts as one leg of a mercury manometer, the other leg being open to the atmosphere. After the pressure and the volume of the individual gases are determined, the burets are interconnected for blending.

The diameters of the tubes in the different sections of the burets were chosen so as to minimize the percentage error in the PV product. This point can be clarified further as follows; if a standard reading error of 0.1 mm is assumed, the diameter of the tubing is selected so that the percentage error in reading the volume is about the same as the percentage error in reading the pressure, taking into consideration the additional source of error introduced by the capillary correction. This point is discussed in more detail by Cook.[5]

A more detailed description of the blending apparatus follows, together with the experimental procedure used in making a blend.

Calibration

The volume calibration of the burets was obtained by weighing the mercury drained from the appropriate sections. To avoid gas bubbles, the apparatus was filled with mercury after the burets had been evacuated to less than 10 microns. A small volume uncertainty is present, due to small amounts of stopcock grease from stopcocks A and B that may extrude and adhere to the top sections of the burets; for this reason the above stopcocks were lubricated with a minimal amount of grease. Successive volume calibrations were internally consistent, and the volume uncertainty was below that required to produce an error in composition of 0.01%.

Blending

The apparatus is connected to the vacuum system manifold and pumped out before admission of the gases to be blended. The gas that is to be present in highest concentration in the final mixture is admitted to buret No. 1.

The mercury level in No. 1 is adjusted in the calibrated section above stopcock D, and the first gas is admitted. The pressure of the gas is adjusted to be very close to atmospheric. Stopcock A is closed and the system evacuated for admission of the second

constituent into buret No. 2. The mercury level in No. 2 is adjusted to obtain the proper volume ratio between the two gases. After the pressure in the system is below 5 microns, as shown by a vacuum thermocouple gauge in the vacuum-system manifold, the second gas may be admitted to buret No. 2. Stopcock B is now closed and the system is evacuated.

Once the pressure in the system is below 5 microns, stopcocks E and H are opened, letting the mercury rise in the intermediate tube until it is above stopcock C, which is now closed. The mercury level is allowed to rise until it reaches point K.

At this point the blending apparatus is charged and ready for the determination of the pressure and volume of the gases in the burets. This reading is accomplished by connecting each of the burets to the manometer tube, by opening stopcocks G and D or F. For certain volume and pressure ratios it is possible to open the three stopcocks simultaneously and adjust the amount of mercury in the system so that the mercury meniscus in each of the burets is in a calibrated section. For the apparatus described presently, mixtures containing about 6%, 17%, 41%, and 52% of either component could be read in this fashion. For other mixtures, the determination could not be carried out simultaneously.

The blending apparatus is disconnected from the vacuum system and immersed in a well-stirred water bath. This water bath was designed specifically for this purpose and was provided with long plate-glass windows, to allow accurate reading of the mercury levels.

The mercury levels and the position of the fiduciary mark (Fig. 35) are read with a cathetometer to the nearest 0.1 mm; the apparatus was always carefully leveled before a set of readings was taken.

The atmospheric pressure and temperature of the water bath are recorded and the blending apparatus is ready to be connected to the vacuum system for transfer of the blend to the apparatus to be calibrated.

Once the blending apparatus is connected, stopcocks G and either D or F are closed, stopcocks A and B opened, and the gas transferred back and forth between burets Nos. 1 and 2 for mixing.

The amount of time devoted to this particular operation is quite important. It was found that as much as 40 minutes was required for proper mixing and that shorter mixing times resulted in inconsistent results. This is probably the main drawback of this piece of equipment; however, it can be improved appreciably by the inclusion of another bulb of about 100 cc capacity, below the calibrated section of buret No. 1, to allow complete transfer of the gases from one buret to the other and to increase the amount of mixing in any given transfer. After the gases are properly blended, the mercury level in the central tube is lowered below the mercury cutoff, and the blend is introduced into the vacuum system manifold by opening stopcock C.

From the values of pressure and volume of the gases the value of the PV product was calculated, by use of the ideal gas law. The temperature of the water bath was noted to ascertain the mercury-density correction factor, but was not used to reduce the PV product to a standard temperature, since both gases are at the same temperature and the percent correction would be the same for both gases. The number of mols of each gas was computed from the PV product and the value of the actual molar volume of the gas.

For the gases used in this work--hydrogen and nitrogen--the above calculation procedure is justified, since the deviations from ideal gas behavior would introduce errors smaller than 0.01% in the final molal composition of the blend.

The pressure readings were corrected for the capillarity effects of the tubes of the burets. The diameter of the manometer tube, 18 mm i.d., was chosen to eliminate the need for any correction.

The hollow bore of stopcocks A and B was partially filled with sealing wax, to eliminate the dead volume and the possibility of having an unmixed pocket of gas. For the same reason the mercury level in the central tube is raised to point K.

This particular design of blending apparatus, in which the gases are measured in two independent burets, performed very satisfactorily after the effect of mixing time was ascertained and allowed for. It is believed that the average error in the composition of a blend was of the order of 0.01%, as evidenced by the data obtained in the calibration of the interferometer (which is described in the following section.)

GAS ANALYSIS BY OPTICAL INTERFEROMETRY

The possibility of using an optical interferometer for analysis was apparent once the manufacturer's claims (Carl Zeiss, Jena) were examined together with the known indices of refraction of the pure components. For a gas chamber 50 cm long, the limits of error claimed correspond to about 0.03% error in composition for the H_2 - N_2 system, an error that is within the accuracy tolerances specified.

It was also known that the index of refraction of a gas mixture is approximately linear with composition, although it was not known if the linearity could be assumed to hold within 0.03%, since all previous data on mixtures are of lower accuracy and very few extend over the entire range of composition.

Edwards[10] determined the sensitivity of his apparatus by filling both gas chambers with dry, CO_2-free air, and obtaining the interferometer reading while pressures were different in the two chambers. This reading, together with the known index of refraction of air, gave him the desired value of interferometer sensitivity. He then prepared a CO_2-air mixture containing 2.52% CO_2 and found that the calculated index of refraction agreed with that found experimentally.

Mohr[26] analyzed flue gases containing from 4% to 14% CO_2 for CO_2 and O_2, calibrating his interferometer by standard gas-absorption techniques. He declared his accuracy to be ± 0.5% and the index of refraction to be linear in this range.

Cuthbertson and Cuthbertson[7] measured the index of refraction of mixtures of O_2 and O_3, analyzing their mixtures either by the volume increase upon decomposition or by chemical absorption. The scatter of their data ran from 1% to 3%, and the range of compositions investigated was limited to about 7% O_3.

The best values for the dependence of index of refraction on composition are those of Valentiner and Zimmer.[45] They measured the index of refraction of synthetic gas mixtures, which they made by measuring accurately the amounts of pure components and mixing them inside their blending apparatus. Their data extend over the entire

composition range, with an average deviation of about 0.5%. They found a small deviation from linearity for the system H_2 - CO_2, which was almost completely masked by the scatter. Their data for the ternary system He-Ne-H_2 are linear, thus contradicting an earlier result of Ramsay and Travers[32] that had indicated deviations of the order of 3% for 50% mixtures of He - H_2.

Therefore the assumption of linearity of index of refraction with composition is seen to require a more careful investigation if uniform accuracies of the order of 0.03% are required.

Theory

Even though equipment for obtaining the index of refraction of gases has been described profusely in the literature, it is necessary at this time to describe some of the features of the Rayleigh-Haber-Zeiss interferometer, inasmuch as they have a bearing on the interpretation of the data.

As indicated in Fig. 37, light from the source A is collimated into a very narrow beam at the slit S_1, which is located at the focal point of L_1. The parallel beam emerging from L_1 is divided into two parallel beams B_1 and B_2, which after passing through the sample reservoirs C_1 and C_2 go through two glass plates P_1 and P_2, and are made to converge in the focal plane of L_2, where the two beams give rise to an interference pattern. Also shown in Fig. 37 is the distribution of light intensity in the focal plane of L_2 when a monochromatic light source is used and the length of the optical path of the two beams is identical. If a source of white light is used at A, the two central dips in light intensity appear black, while those farther removed from the center appear colored on a white background. If the light paths of B_1 and B_2 are not identical, the set of fringes will be displaced along the focal plane of L_2. In the Zeiss interferometer the set of interference lines is actually observed by means of a high-powered cylindrical lens, and only the upper part of the beams goes through the sample reservoirs; the lower part proceeds underneath C_1 and C_2 to an auxiliary compensating plate which directs it to L_2, giving rise to a set of fringes which is unaffected by the contents of the sample reservoirs and therefore

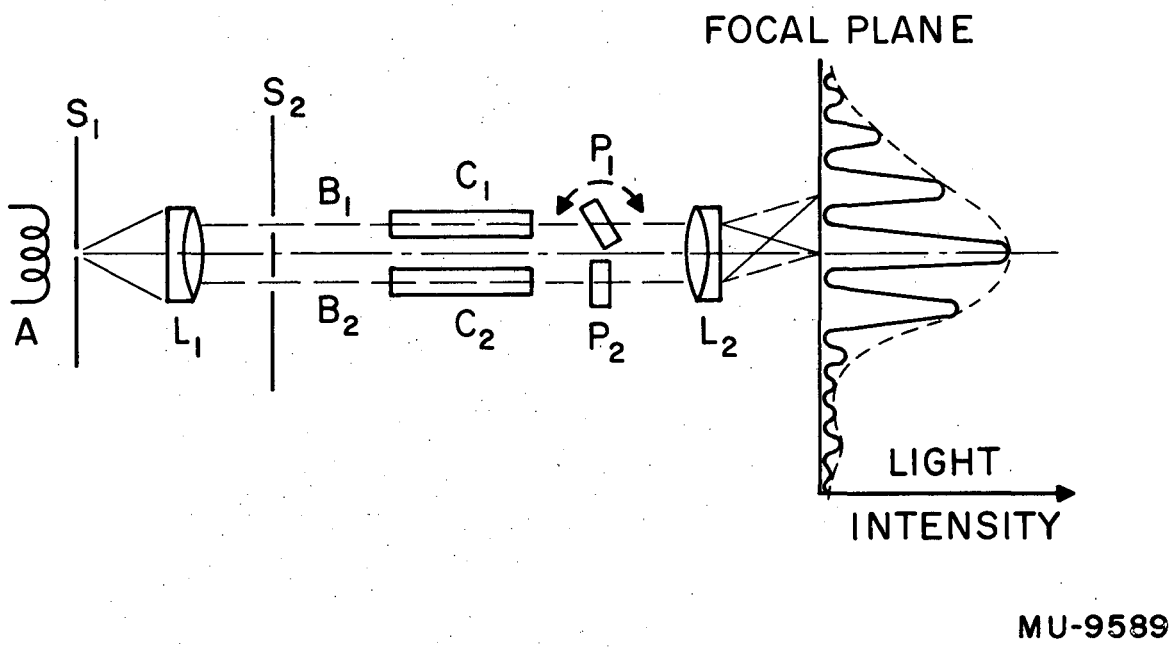

Fig. 37. Optical interferometer (diagram).

always maintains its fixed position and appearance and serves as reference. The appearance of the field of view in the ocular is indicated diagrammatically in Fig. 38.

The sample reservoirs contain the unknown and reference substances; for this work there were two parallel tubes 50 cm. long, sealed at both ends with optically flat windows.

The difference in the optical path of the beams B_1 and B_2 caused by differences in the index of refraction of the unknown and reference gases is compensated by changing the tilt in the glass plate P_1, which changes the thickness of glass through which the beam B_1 has to go. The inclination of P_1 is controlled by means of a graduated micrometer screw, from which readings can be obtained that are a function of the difference between the index of refraction of the unknown and that of the reference substance. The procedure for making a measurement consists of rotating the micrometer screw until the upper and lower set of spectra are made to coincide, reading the graduations on the micrometer, and subtracting from this value the reading obtained when both sample reservoirs are filled with the same substance, or are evacuated.

Absolute calibration of the interferometer

As the reading of the micrometer screw is a function of the refractive index difference, it is necessary to ascertain the nature of this function, or obtain what is called the absolute calibration of the interferometer. The optical path P is defined by

$$P = \Sigma\, nt \tag{36}$$

where

n = index of refraction

t = thickness

and, for monochromatic light, a maximum in light intensity is obtained when

$$P_2 - P_1 = h\lambda \tag{37}$$

where λ is the wavelength and h the band number; and a minimum in light intensity when

$$P_2 - P_1 = (h + 1/2)\,\lambda. \tag{38}$$

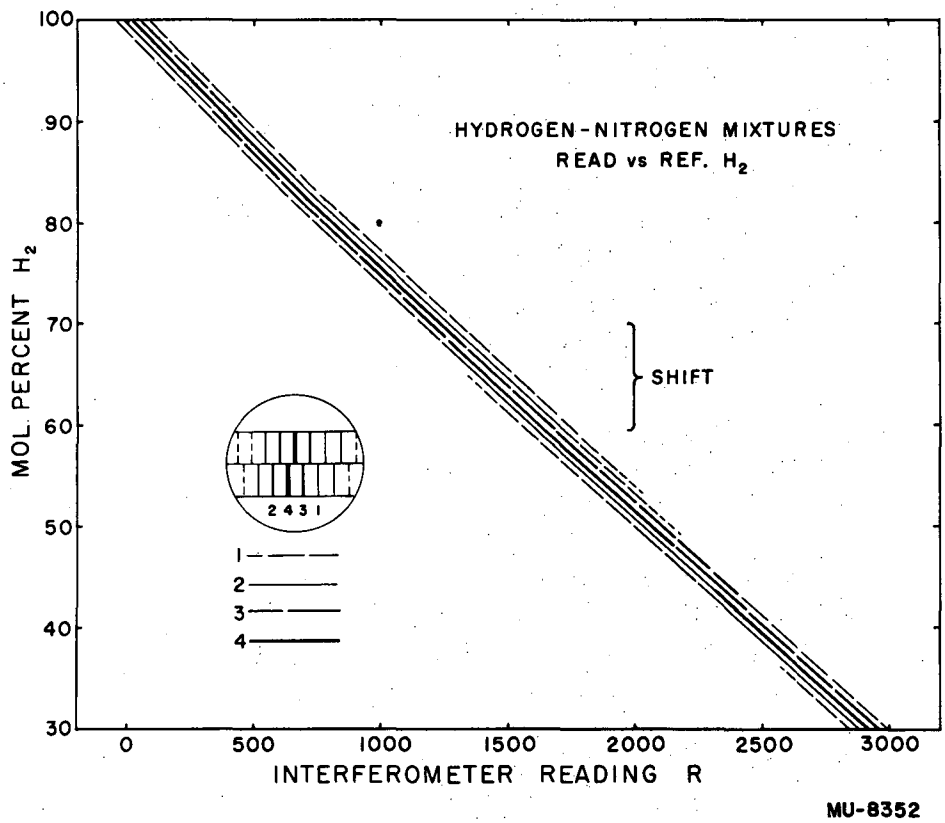

Fig. 38. Band shift for hydrogen-nitrogen mixtures read versus reference hydrogen.

When white light is used, the minimums corresponding to h=0 appear black, those corresponding to $h = \pm 1$ are colored but readable, while all the higher-order lines are very faint or completely indistinguishable. With monochromatic light all the minimums or bands present the same appearance, i.e., black on a colored background, and the zero-order band cannot be distinguished.

The absolute calibration is done with monochromatic light (5461 Å). It consists of obtaining the micrometer readings that correspond to the successive bands that pass through the ocular as the screw is rotated, and is usually expressed in the form of a calibration table in which values of band number h are listed versus the corresponding values of $R - R_o$; where R_o is the reading corresponding to the zero-order band--obtained with white light when both chambers are evacuated. These readings correspond to equal increments in thickness of the compensating glass plate P_1, and correspondingly to equal increments in index of refraction difference between the unknown and reference substances, since

$$\Delta h\lambda = n_g \Delta t = l\Delta n = f(R) \qquad (39)$$

Although the band-number calibration thus obtained holds only for a particular value of λ, it can be used with white light if only a measure of equal increments in index of refraction difference is required.

Molar refraction

The Lorentz-Lorentz molar refraction is known to give a very good approximation to the changes in index of refraction with pressure, temperature, and composition, and was used to reduce all the interferometer readings to standard conditions. It is defined by

$$N = \frac{n^2 - 1}{n^2 + 1} \quad \frac{M}{\rho} , \qquad (40)$$

where N is the molar refraction,

n is the index of refraction,

M is the molecular weight,

ρ is the density.

The density can be expressed in terms of the ideal gas density given by

$$\rho = \frac{P}{rT} M, \tag{41}$$

where P = pressure,

T = absolute temperature,

r = gas constant, expressed in appropriate units,

to obtain

$$N = \frac{n^2 - 1}{n^2 + 2} \frac{rT}{P}, \tag{42}$$

which can be simplified by the introduction of

$$e = n - 1. \tag{43}$$

Since e is a very small quantity compared with unity ($e = 299.8 \times 10^{-6}$ for nitrogen), its square can be neglected, so that we obtain

$$N \cong \frac{2}{3} e \frac{rT}{P}, \tag{44}$$

or

$$e \cong \frac{3}{2} \frac{NP}{rT}. \tag{45}$$

The interferometer, however, measures

$$h = a(e_r - e_g) \tag{46}$$

where a = interferometer sensitivity,

e_r = n-1 for the reference gas,

e_g = n-1 for the unknown gas,

whereas we are interested in the values of

$$h_0 = a \left[(e_0)_r - (e_0)_g\right], \tag{47}$$

where the subscript 0 refers to some standard reference state like $0^{\circ}C$, 760 mm of mercury. The values of h can be transformed into values of h_0 by

$$\left[(e_0)_r - (e_0)_g\right] = e_r \frac{Tr}{273} \cdot \frac{760}{P_r} - e_g \frac{Tg}{273} \cdot \frac{760}{Pg}, \tag{48}$$

and for the particular case in which $P_r = P_g = P$; $T_r = T_g = T$, Eq. 48 can be simplified to

$$\left[(e_0)_r - (e_0)_g\right] = \frac{760}{273}\ \frac{T}{P}\ (e_r - e_g)$$

$$= 2.7822\ \frac{T}{P}\ (e_r - e_g)$$

$$= 2.7822\ \frac{T}{P}\ \frac{h}{a}\ . \qquad (49)$$

Therefore

$$h_0 = 2.7822\ \frac{T}{P}\ h. \qquad (50)$$

This last equation expresses the functional relationship between the values of h, P, T, and h_0 and was used to bring all data to the same standard conditions.

If $P_r \neq P_g$ but $T_r = T_g = T$, then

$$h_0 = 2.7822\ \frac{T}{P}\ h + \left(1 - \frac{P_r}{P_g}\right)(e_0)_r\ a. \qquad (51)$$

Thus, if the pressures in the two gas chambers are not identical, an appreciable correction has to be applied, which involves the absolute values of interferometer sensitivity and index of refraction of the reference gas.

Equation (51) can be used, however, to determine either the absolute sensitivity or the absolute value of e_0 for a gas, if the other value is known. Thus, for determining the value of the sensitivity both chambers are filled with a gas of known index of refraction the pressure in both chambers is determined, and since $h_0 = 0$,

$$a = \frac{2.7822\ Th}{(P_r - P_g)\ (e_0)_r}\ . \qquad (52)$$

Experimental Procedure

The experimental procedure recommended by the manufacturers was modified to allow the use of relatively small gas samples and of vacuum techniques. The interferometer was connected to the vacuum system manifold, and reference gas cylinders as shown in Figs. 39 and 40. Figure 40 also shows the gas-blending apparatus connected to the interferometer.

The procedure for making a measurement is as follows. The system is first evacuated until the vacuum thermocouple gauges Nos. 9 and 10 show a pressure smaller than 5μ, at which point the

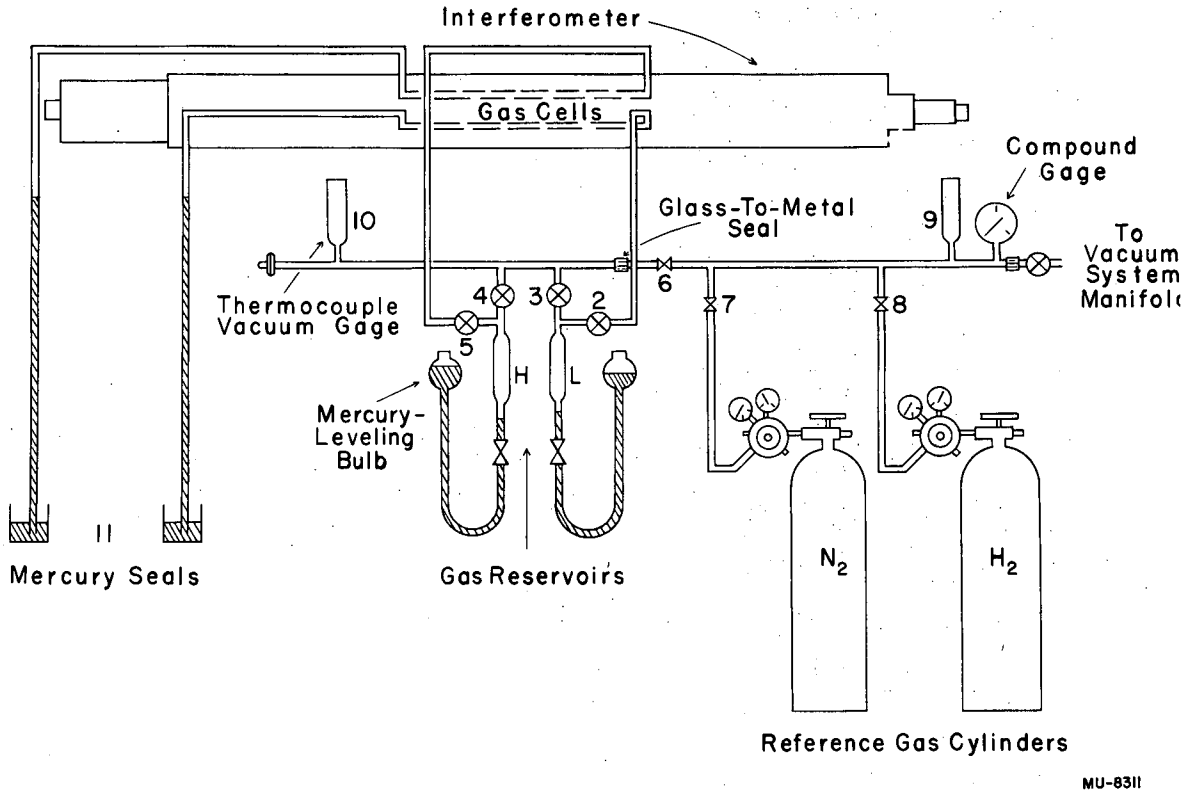

Fig. 39. Optical interferometer; flow diagram.

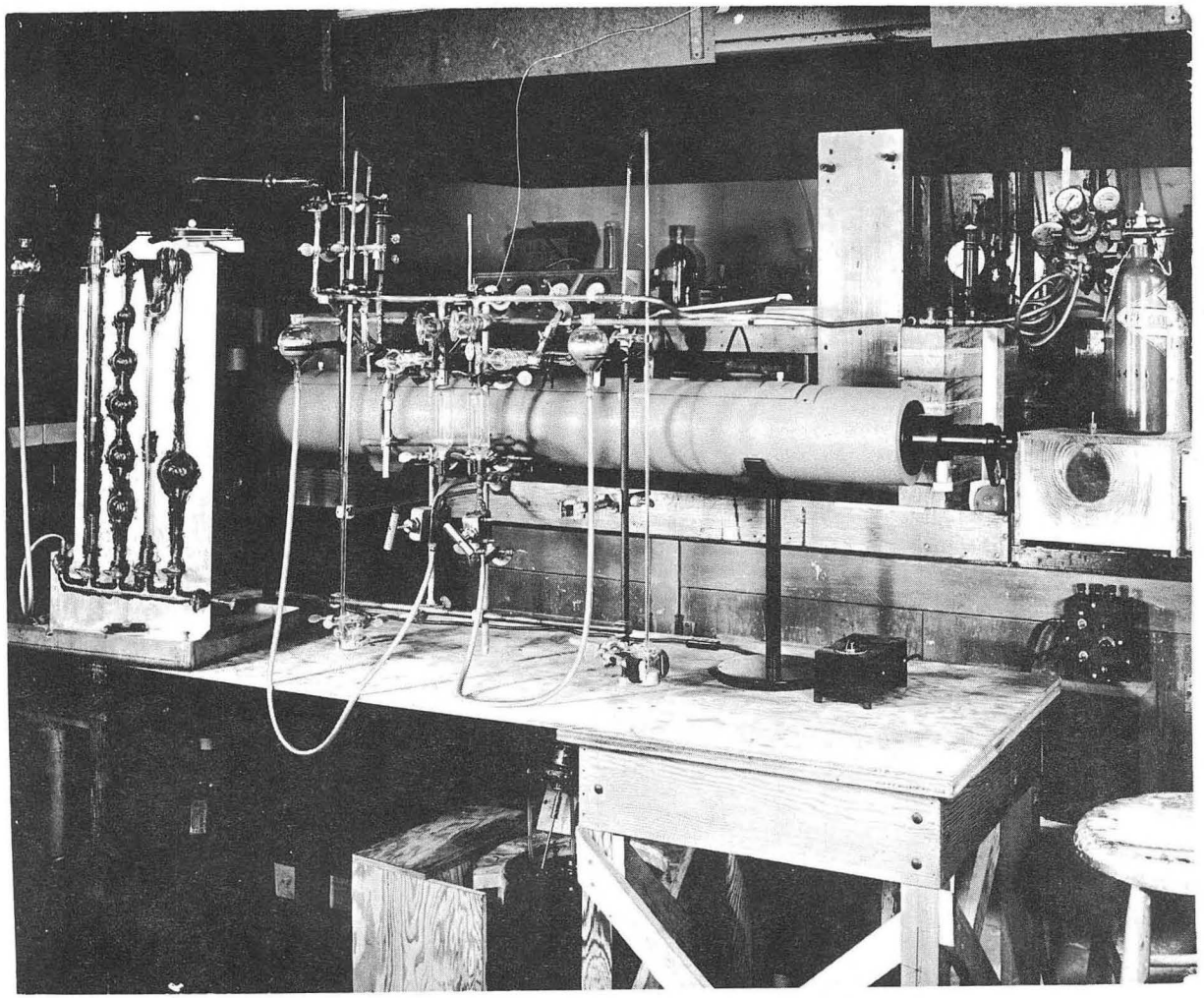

ZN-1303

Fig. 40. Optical interferometer with blending apparatus

gas sample may be introduced into the system. The hydrogen content of the sample determines the reference gas and chamber to be used. Take the case of a sample that is known to contain about 50% H_2, and is to be read against nitrogen gas as reference. The sample is introduced into chamber L, for a gas of low index of refraction, while the reference nitrogen is introduced into chamber H, for a gas of high index of refraction. If the amount of sample is not sufficient to bring up the pressure in L to atmospheric pressure, additional gas may be pumped out from the line by manipulating stopcocks Nos. 2 and 3 and the mercury level in L. The pressure in the gas cell is shown by the height of the mercury column over the mercury seals No. 11. When the gas cell is at atmospheric pressure, and enough gas is left in L for the purging procedure that is to be described, stopcock No. 3 is closed and the line is evacuated for admission of the reference gas into chamber H. Chamber H is filled by closing stopcock No. 1 and opening valve No. 7 by the reference nitrogen cylinder.

When both chambers have been filled with gas, a waiting period of about 1 minute is allowed for the gases to reach approximately the same temperature in the gas cells. The pressure is then raised in chamber L by admitting mercury, until the gas bubbles out through the mercury seal. The pressure in L is now above atmospheric, the mercury seal is lowered until the gas inside the chamber is directly connected with the atmosphere through the long glass capillary (about 1 mm in diameter), which minimizes the diffusion of air into the interferometer tubes. The same procedure is repeated for the gas in chamber H, and a period of 2 minutes is allowed for temperature equilibration before reading the interferometer.

The interferometer reading is obtained by lining up all the clearly visible bands of the upper spectra with the most prominent band of the reference spectrum, denoted band 4 in Fig. 38. For each of the successive bands in the upper spectra there is a corresponding reading which is identified by the subscripts 1, 2, 3, or 4, according to the relative intensity of the lines, 4 corresponding to the blackest line, 1 to the most colored, 2 and 3 for intermediate degrees

of blackness. The reading of any individual band is accomplished by rotating the micrometer screw (always in the same direction, to minimize the possible effects of backlash in the mechanism).

The above procedure is carried out for two reasons: to compensate for possible errors in the absolute calibration of the interferometer, and to obtain a set of independent readings of the same quantity, readings which are later brought to a common basis in the calculations. The distribution of color in the different bands of the upper spectrum is valuable in the identification of the zero order band as is described under band shift.

After a preliminary set of readings is taken, the mercury is allowed to rise in chamber H, thus purging the gas in the gas cell with the gas contained in H. A new reading is taken on the zero-order band. The same procedure is followed with the gas contained in reservoir L. This purging procedure allows for the detection of any lack of homogeneity of the gases in the chambers due to incomplete evacuation, slow leak, diffusion, or--in the case of the calibration blends--lack of homogeneity due to incomplete mixing in the blending apparatus.

While the reference and unknown gases are being purged, the necessary pressure and temperature readings are made.

After the readings are taken, the mercury seals are raised until the tips of the capillary tubes are under mercury, and stopcocks Nos. 1, 3, and 4 are opened so as to pump out all of the gas in the system. After the pressure has decreased to below 100 microns a new reading is taken, to establish the reading corresponding to the zero-order band when both chambers are evacuated. This zero reading is fairly constant, although it seems to be somewhat dependent on room temperature.

Band Shift

The use of white light allows for the easy identification of the zero-order interference band, whereas this identification is impossible to make with monochromatic light. For this reason white light is used almost universally when the interferometer is used for analytical purposes. However, owing to the difference in the

dispersive powers of the glass in the compensating plate and the substances in the sample reservoirs, the distribution of energy in the upper spectra shifts gradually with increasing difference in index of refraction, changing the chromaticity of the different bands until the zero-order band no longer corresponds to the two dips in light intensity that appear black (cf. Fig. 37) but may be displaced from it by one or more bands; i.e., the zero-order interference fringe is now colored.

The position of the zero-order band was determined during the calibrations of the interferometer with gas blends of known composition, by purging the blend with reference gas while following the position of one of the bands by rotating the micrometer screw. For the above example, where the unknown sample was in chamber L, the procedure would be as follows. Stopcocks 1, 3, and 4 are closed after the introduction of the gases in the chambers. Valve No. 7 is opened until the reference gas pressure, indicated in the compound gauge, is slightly above atmospheric. Valve No. 6 is closed and cock No. 3 opened. Valve No. 7 is opened. Then valve No. 6 is opened slightly while the movement of the bands in the interferometer field is followed. The band shift is established by the change in the relative color intensity of the band, thus, for the above example, if the blackest band is followed, it will gradually become more colored, and when both chambers are filled with essentially the same gas--reference nitrogen--the band will be found to lie one band to the left of the blackest band, which for this case is known to be the zero-order interference band. Figures 38 and 41 show the pattern of relative color intensity of the different bands versus composition and interferometer reading, and were used to determine the position of the zero-order band for unknown samples. This method of obtaining and plotting the band shift is very similar to the one recommended by Karagunis et al.[20] and allows for the identification of the zero-order band regardless of how colored it may be.

Pressure and Temperature Measurement

Barometric pressure was read on a Fortin-type U.S. Signal Corps barometer, and tabulated corrections provided by the manufacturer

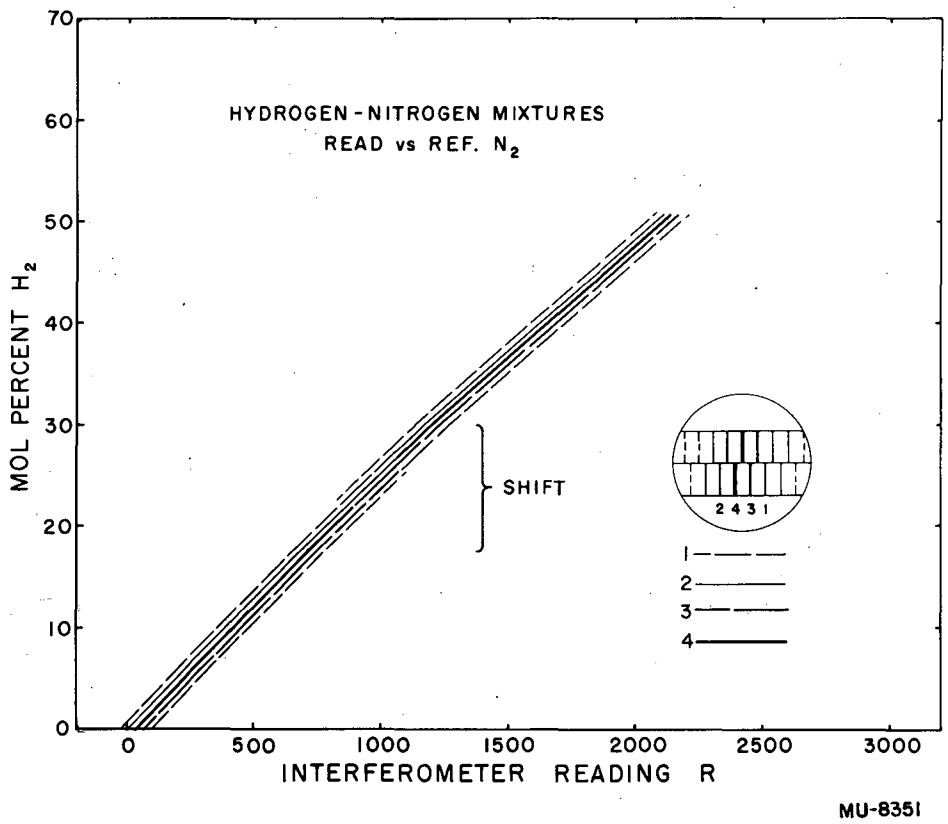

Fig. 41. Band shift for hydrogen-nitrogen mixtures read versus reference nitrogen.

were made for temperature and local gravity. The error in the pressure measurement is of the order of ± 0.1 mm of mercury.

Temperature was measured by means of a copper-constantan thermocouple, 5 feet of which were wound around the gas cells inside the interferometer case with the assembly insulated with 2 inches of fiberglass insulation. The latter made for very slow changes in the temperature of the gas cells, while winding the thermocouple wire around them minimized the effects of thermal conduction along the thermocouple wire. The thermocouple was read with a type K-2 Leeds and Northrup potentiometer, and was calibrated at the sodium sulphate point and against a Bureau of Standards certified thermometer. The error in temperature measurement was smaller than 0.01° C.

Sample Calculation

It was already mentioned that readings were taken on all the clearly visible bands, and that all the readings were brought to a common basis. To illustrate this point, and also to show the reproducibility of the different readings, the results and calculations on synthetic blend No. 70 are shown here.

Blend 70 was made in the blending apparatus, was known to contain 51.71% H_2, and was read against nitrogen as reference gas. The interferometer readings follow(P=738.6 mm of Hg; T=294.50 K):

R_2	R_4	R_3	R_1
2125.8	2162.2	2199.0	2235.6
2125.8	2162.0	2198.0	2235.7
2125.5	2161.7	2198.3	2235.9
2125.7	2161.8	2198.5	2235.6
	2162.2	2198.3	
	2162.1		
After purging with reference nitrogen		2199.5	
		2199.0	
		2199.0	
		2199.0	
After purging blend		2198.5	
		2199.5	
		2198.8	
		2198.9	
		2199.3	
		2198.5	
		2198.9	
		2199.1	
		2199.0	

After the above set of readings was completed, the chamber containing the blend was purged with reference nitrogen to determine the band shift. The band designated above as R_3 was kept fixed in position in the interferometer field by rotating the micrometer screw, and was found to become gradually blacker, becoming the zero-order fringe when both chambers were filled with reference nitrogen. The values of R_4 when both chambers were evacuated, designated as R_0, follow:

R_0
24.3
24.8
24.8
24.8
24.8

From the values of $R - R_0$ the corresponding values of band number h were calculated from the table of absolute calibration of the interferometer. The values of h were brought to a common basis with the following set of empirical values of the difference in h values between the different bands;

$$h_1 - h_4 = -2.09,$$

$$h_2 - h_4 = -1.04,$$

$$h_4 - h_4 = 0,$$

$$h_3 - h_4 = +1.05,$$

$$h_1 - h_4 = +2.10.$$

Thus the calculations proceed as follows

Band	$R-R_0$	h	correction	h'	
R_2	2100.9	66.02	+ 2.09	68.11	
R_4	2137.3	67.06	+ 1.04	68.10	
R_3	2173.5	68.14	---	68.14	$h'_{aver.} = 68.12_5$
R_1	2210.9	69.20	- 1.05	68.15	

The value of h_0 is now obtained by substituting the above into Eq. 50:

$$h_0 = 2.7822 \frac{294.50}{738.6} 68.12_5 = 75.57.$$

The results obtained with the above blend are representative of the results obtainable with the interferometer; they show a small drift

in the values of R_3 with purging, but the amount of drift is within the limits of reproducibility stated by the manufacturer and represents a possible composition error of 0.01%. Before the details of the blending technique were perfected much larger drifts were found, as large as 0.44 band numbers or 13.2 drum divisions.

Results

The results of calibrating the interferometer with gas blends of known compositions are presented in Figs. 38, 41, 42, and 43 and in Tables III and IV. Figures 38 and 41 present the general trend of interferometer readings versus gas composition, and were used mostly in the determination of band shift and as a help in selecting the zero-order interference fringe. It may be observed that the lines presented in Figs. 38 and 41 have a slight curvature, which is due entirely to the lack of linearity in the relationship between interferometer readings and band numbers.

If a plot were made of composition versus band number, it would appear as a straight line having the following equations:

H_2 - N_2 mixtures read versus reference hydrogen,

$$x_c = 0.99774 - .0068616\ h_0; \qquad (53)$$

H_2 - N_2 mixtures read versus reference nitrogen,

$$x_c = 0.0068476\ h_0 - 0.00014. \qquad (54)$$

The values of $x-x_c$, that is, mol fraction hydrogen in the synthetic mixture as obtained in the blending apparatus minus mol fraction calculated from the above expressions, are presented in Figs. 42 and 43.

In Figs. 42 and 43 distinction is made between the points obtained before the blending technique was perfected and the later values. While only two of the later values show deviations larger than 0.001, most of the earlier blends fall outside this range. The points in Figs. 42 and 43 show the combined errors in making the blend in the blending apparatus and errors in reading the interferometer, so that it is actually difficult to assign a definite value to either one of the two sources; however, the scatter for most of the "good" points is less than 0.0005.

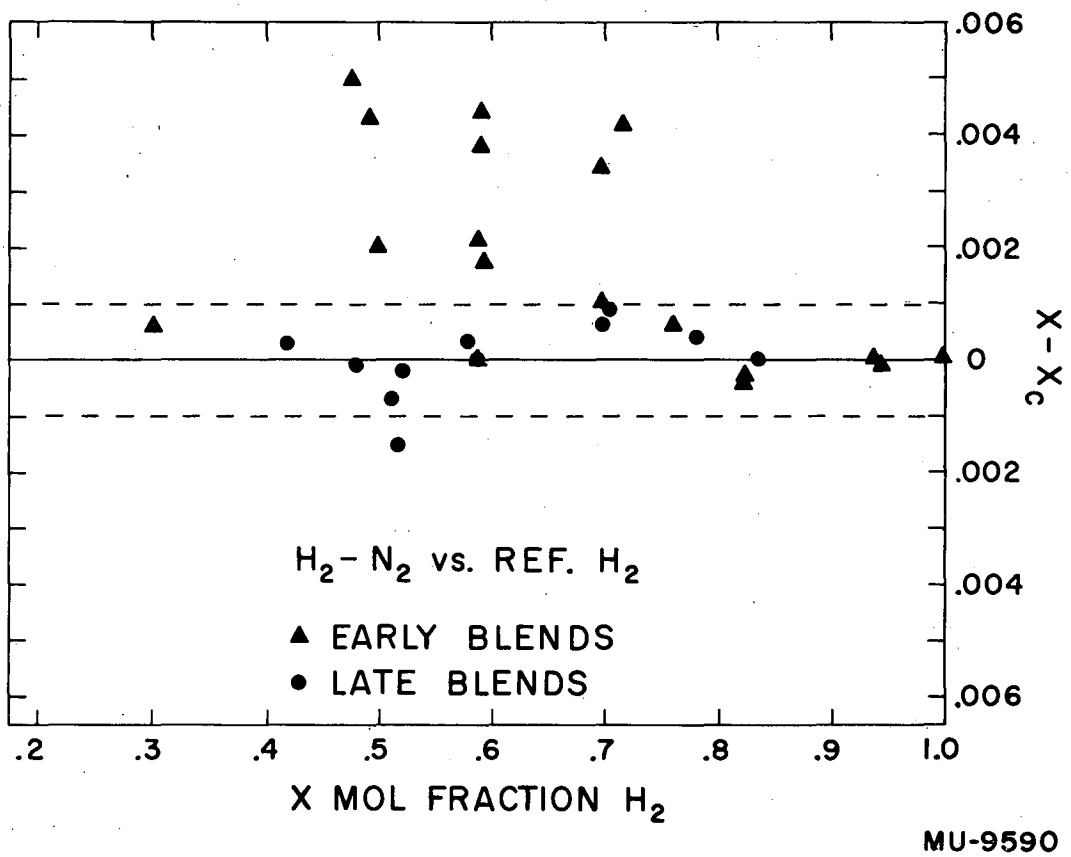

Fig. 42. Values of $x-x_c$ versus composition for hydrogen-nitrogen mixtures read versus reference hydrogen.

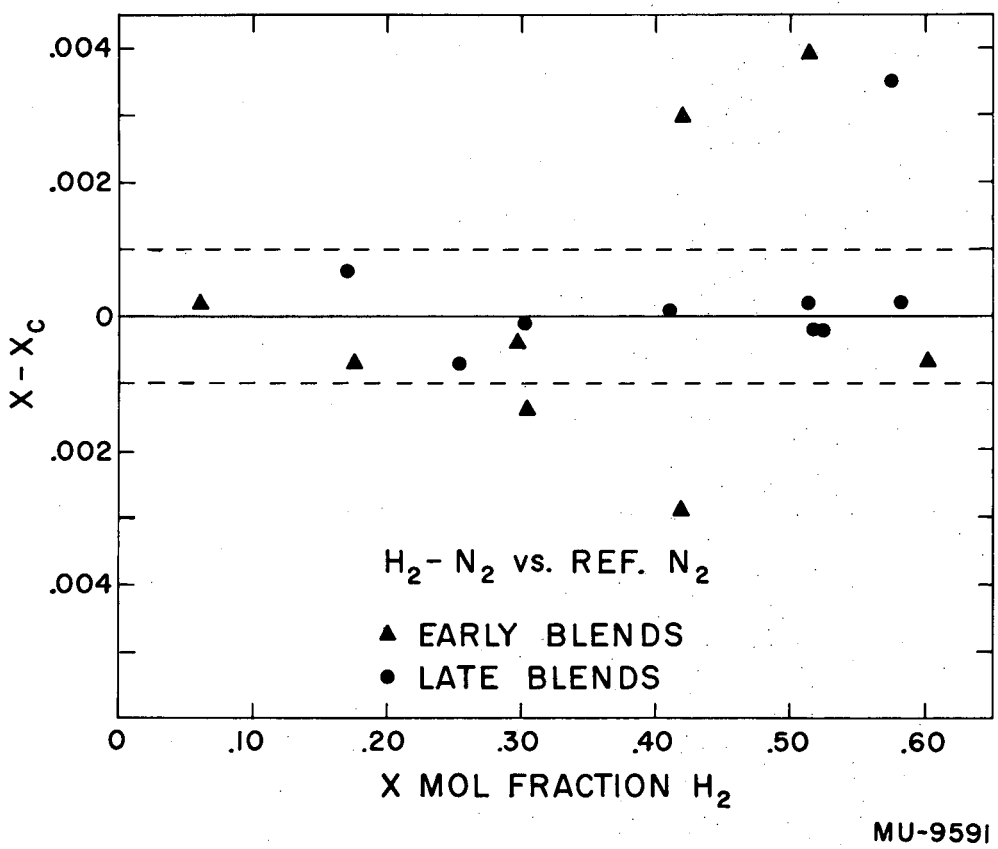

Fig. 43. Values of $x-x_c$ versus composition for hydrogen-nitrogen mixtures read versus reference nitrogen.

Table III

H_2 - N_2 vs reference hydrogen; values of h_0

Blend	x	h_0	x_c*	$x - x_c$
	1.0000	- .33	1.0000	0
10	.5946	59.39	.5902	+ .0044
11	.8233	25.36	.8237	- .0003
12	.5003	72.79	.4983	+ .0020
13	.7015	41.80	.7109	- .0094
14	.4840	75.60	.4790	+ .0050
17	.3021	101.47	.3015	+ .0006
20	.5955	58.87	.5938	+ .0017
21	.5893	59.83	.5872	+ .0021
22	.6990	44.03	.6956	+ .0034
23	.7200	41.09	.7158	+ .0042
24	.9432	7.93	.9433	- .0001
25	.9384	8.65	.9384	.0000
26	.8197	25.89	.8201	- .0004
27	.6984	43.77	.6974	+ .0010
28	.5990	58.67	.5952	+ .0038
29	.4957	73.79	.4914	+ .0043
73	.5156	70.05	.5171	- .0015
76	.5099	71.00	.5106	- .0007
77	.5204	69.54	.5206	- .0002
78	.4802	75.41	.4803	- .0001
79	.5799	60.93	.5796	+ .0003
80	.7020	43.23	.7011	+ .0009
81	.5871	59.85	.5871	.0000
82	.8346	23.77	.8346	.0000
83	.4173	84.63	.4170	+ .0003
84	.5873	59.81	.5873	.0000
86	.7002	43.45	.6996	+ .0006
87	.7805	31.71	.7801	+ .0004

* $x_c = .997736 - .0068616\ h_0$

Table IV

$H_2 - N_2$ vs reference nitrogen; values of h_0

Blend	x	h_0	x_c*	$x - x_c$
15	.5020	71.84	.4918	+.0102
16	.4217	61.16	.4187	+.0030
18	.3015	44.26	.3029	-.0014
19	.1744	25.59	.1751	-.0007
30	.0607	8.86	.0605	+.0002
31	.2971	43.47	.2975	-.0004
32	.5079	75.09	.5140	+.0039
35	.6007	87.85	.6014	-.0007
41	.4160	61.19	.4189	-.0029
69	.4119	60.16	.4118	+.0001
70	.5171	75.57	.5173	-.0002
71	.2525	37.00	.2532	-.0007
72	.5219	76.26	.5221	-.0002
74	.5788	84.04	.5753	+.0035
75	.5137	75.01	.5135	+.0002
85	.5818	84.95	.5816	+.0002
92	.1707	24.85	.1700	+.0007
93	.3038	44.40	.3039	-.0001

* calculated from $x_c = .0068476\ h_0 - .000137$

Discussion of Sources of Error

The assumption of idea gas behavior as applied in Eqs. (42) through (52) introduces some error in the values of h_0; however, for the gases used (H_2, N_2) and the usual range of temperatures and pressures (15° to 30° C, 740 to 750 mm Hg), the degree of error introduced is well below the limit of accuracy of the interferometer with 50-cm-long gas chambers.

The tolerances of error in the measurements of temperature and pressure are not very stringent provided the gases in the two chambers are at exactly the same pressure and temperature (see Eq. (51)). For H_2 - N_2 mixtures, with 50-cm-long gas chambers, it is necessary to measure concentrations below 60% H_2 against nitrogen gas as reference, and mixtures containing more than 40% H_2 against hydrogen gas as reference, thus obtaining a certain amount of overlapping in the region near 50%.

For mixtures containing 60% H_2 read versus reference nitrogen, the value of h_0 is about 89, and the errors in temperature and pressure corresponding to an error of 0.01% in composition are 0.045°C and 0.12 mm of mercury. For lower values of h_0 the allowable tolerances are correspondingly increased, as evidenced in Eq. (50). Thus the errors in the measurment of pressure and temperature are almost negligible compared with the lack of reproducibility in the interferometer readings, which at best is about 0.5 units in drum reading or about 0.02% in composition.

The interferometer is very satisfactory as an analytical instrument, however, and allows for fast accurate analysis of gas mixtures.

The time required for analysis is of the order of 30 min per sample, but most of that time is actually involved in pumping out the lines and involves no loss of operator time.

Discussion of Results in View of Molar Refraction Theory and Virial Coefficients

When discussing the experimental results obtained, I pointed out that the results could be expressed in terms of a straight line, within the limits of experimental error.

The equation of that line is of the type

$$x_c = sh_0 + b. \qquad (55)$$

It was interesting to note that the values of the coefficients s were different in the two equations; they were 0.0068616 for the data read versus reference hydrogen and 0.0068476 for the data read versus reference nitrogen, showing a discrepancy of 0.204% in the absolute values of the slopes.

This discrepancy could have been partially explained by assuming slightly different lengths for the two gas chambers, but the difference between the two tubes required to account for the discrepancy would be 0.5 mm. An alternate explanation for the difference between the two slopes is the possibility that the lines of index of refraction versus composition may have a small degree of curvature due to deviations from ideal gas-mixing behavior.

It is fortunate that for this case the second virial coefficients of the pure components and the interaction coefficient have been experimentally determined, thus making it possible to calculate the density of the mixtures as a function of composition, values which can be substituted into the molar-refraction equations to obtain correct values of index of refraction of the mixture.

Molar refraction theory predicts that the molar refraction of a mixture is a linear combination of the molar refractions of the pure components. For a binary mixture

$$N_M = N_1 x_1 + N_2 x_2 \qquad (56)$$

Where N_M is the molar refraction of the mixture, N_1, N_2 molar refraction of the pure components. For a gas mixture

$$e_M \frac{M_M}{\rho_M} = e_1 \frac{M_1}{\rho_1} x_1 + e_2 \frac{M_2}{\rho_2} x_2 \qquad (57)$$

If the components are ideal gases and mix without interaction, the above can be simplified to

$$(e_M)_I = e_1 x_1 + e_2 x_2 \qquad (58)$$

where the subscript I applies to ideal mixtures.

Combining Eqs. 57 and 58, we have

$$\left[e_M - (e_M)_I\right] = e_1 x_1 \left[\frac{\rho_M}{M_M} \cdot \frac{M_1}{\rho_1} - 1\right] + e_2 x_2 \left[\frac{\rho_M}{M_M} \cdot \frac{M_2}{\rho_2} - 1\right] \tag{59}$$

Expression which can be simplified by making the substitution

$$\frac{\rho}{M} = \frac{1}{V} , \tag{60}$$

where V is the molar volume, to obtain

$$\left[e_M - (e_M)_I\right] = e_1 x \left[\frac{V_1}{V_M} - 1\right] + e_2 x_2 \left[\frac{V_2}{V_M} - 1\right] . \tag{61}$$

The values of the molar volume of the mixture can be calculated from the virial equation

$$\frac{PV}{RT} = 1 + \frac{B}{V} , \tag{62}$$

where the second virial coefficient is given by

$$B_M = B_1 x_1^2 + 2 B_{12} x_1 x_2 + B_2 x_2^2 . \tag{63}$$

The following values have been given in the literature for the second virial coefficients:

Reference	B_{H_2}	B_{N_2}	B_{12}
Keyes[21]	+14.54	-2.78	
Hildebrand[16]	+14.5	-6.2	+13.7
calculated from data in Perry[31]	+13.7	-10.5	
Lunbeck and Roerboom[25]	+13.70	-4.71	+13.5 +11.5
Theoretical[25]			+11.5
Values used in the calculations	$+14.1_1$	-6.0_5	$+13.3_3$

The values of V obtained from Eq. (62) were combined with the following values of e obtained from the International Critical Tables:[18]

$$\lambda = 5461\ \text{Å}$$

$$H_2: \qquad e = n-1 = 139.65 \cdot 10^{-6},$$

$$N_2: \qquad e = n-1 = 299.77 \cdot 10^{-6},$$

$$e_{N_2} - e_{H_2} = 160.12 \cdot 10^{-6},$$

to obtain the values of $e_M - (e_M)_I$ presented in Fig. 44.

Thus, additivity in the molar refraction, when combined with the proper density values for the mixtures, predicts a small deviation from linearity for the index of refraction. The maximum deviation, of $8.3 \cdot 10^{-8}$ index of refraction units, occurs at 45% H_2, and should be large enough to be reflected in a difference in the slopes of the lines expressing composition versus refractive index. This is indicated in Fig. 45, which shows the over-all pattern of index of refraction versus composition, in which the deviations from linearity are greatly exaggerated.

At this point, however, the information available is not sufficient to show if the deviations from linearity predicted from molar refraction agree with the experimental data, since the absolute sensitivity of the interferometer is not known with sufficient accuracy to convert e values in h values. Alternatively, if the point of intersection of the lines of slopes s_1 and s_2 (Fig. 45) were known, the calculated and experimental values could be brought to the same basis. However, since the maximum deviation from linearity occurs at 45% H_2 and the fit of Eqs. (53) and (54) to the data is good at this concentration, it was decided to assume that the lines intersect at $x = 0.45$. This is the only assumption that was necessary for the following calculations. From this assumption and the slopes given in Eq. (53) and (54), it is possible to calculate the value of $h_2 - h_1$, from which the values of interferometer sensitivity a and average slope s follow. Thus, the values of s was found to be 0.0068553, with a corresponding value of interferometer sensitivity of 0.91102 band

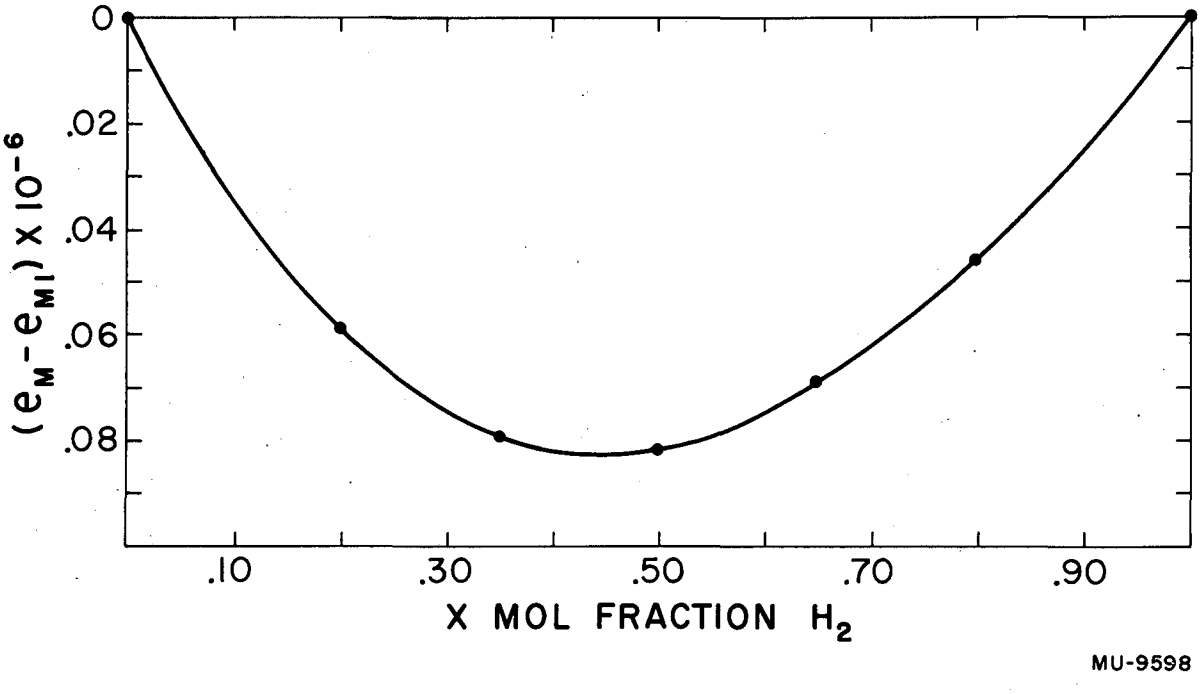

Fig. 44. Theoretical values of $e_M - (e_M)_I$.

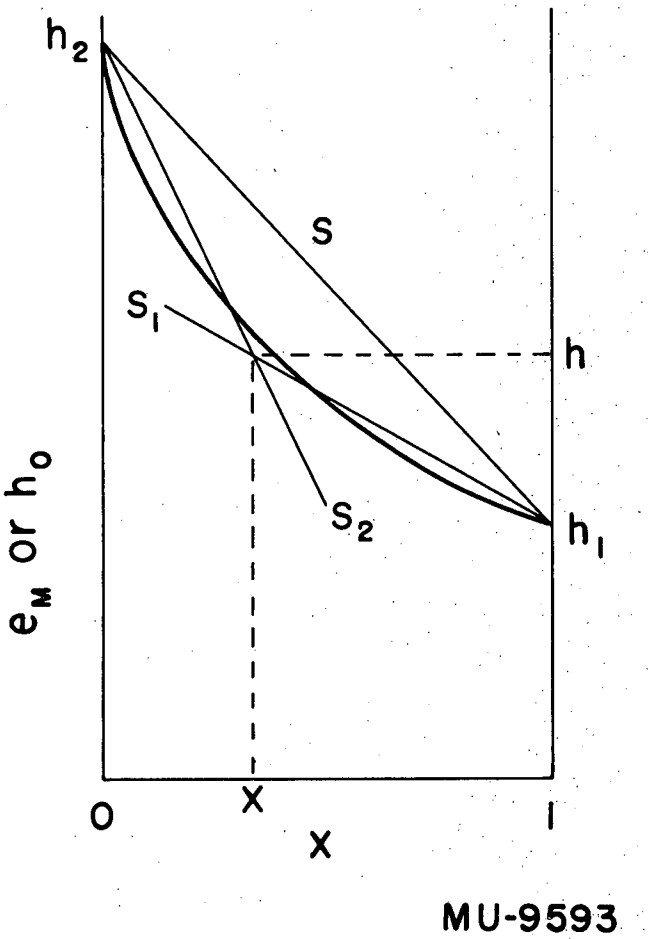

Fig. 45. Index of refraction versus composition, diagrammatic.

numbers per index of refraction difference 10^6. Once s is known, values of h corresponding to the different concentrations of the synthetic mixtures can be calculated and compared with the experimental findings, giving Fig. 46, which shows values of $h - (h_M)_I$ for the experimental blends, and the values of $h_M - (h_M)_I$ obtained from Fig. 44 and the interferometer sensitivity. The agreement between the two sets of values is quite good.

It may be concluded that, at least for the H_2 - N_2 system, the assumption of additivity of molar refraction is a very good approximation to fact, and that the probable deviation corresponds to an error of less than 0.01% in composition.

ACKNOWLEDGMENT

This work was done under the auspices of the U. S. Atomic Energy Commission.

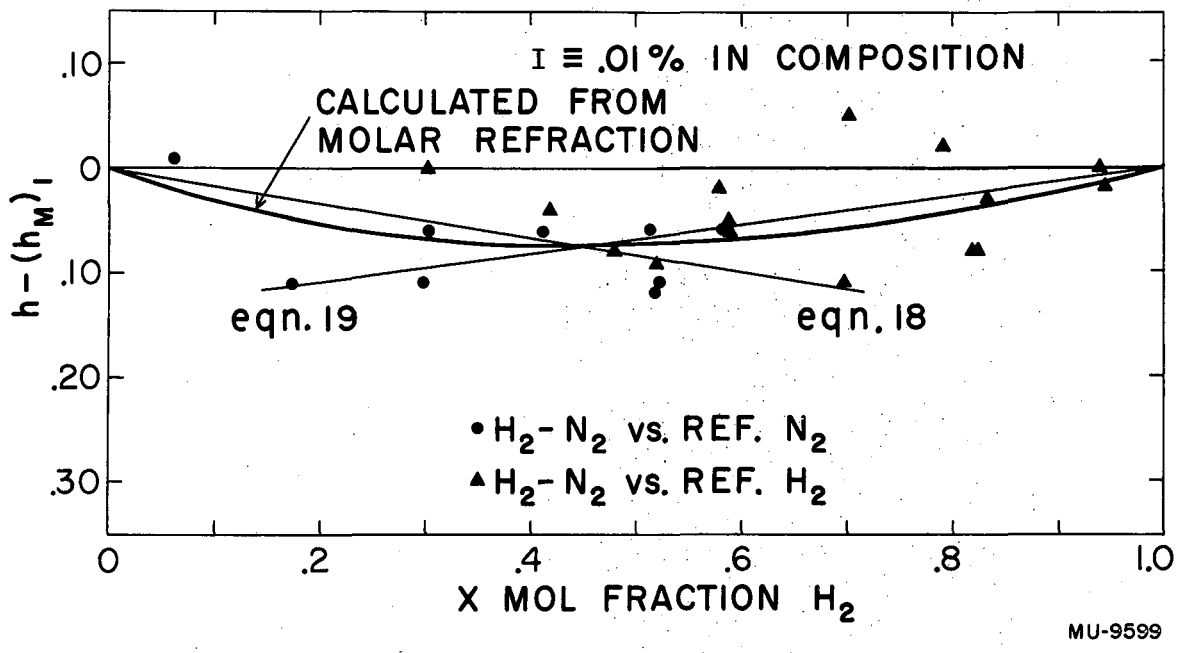

Fig. 46. Comparison of theoretical and experimental values of h - $(h_M)_I$.

LITERATURE CITED

1. M. Benedict, G. B. Webb, and L. C. Rubin, Chem. Eng. Prog. 47, 419 (1951).
2. M. Benedict, G. B. Webb, and L. C. Rubin, Chem. Eng. Prog. 47, 449 (1951).
3. R. H. Busey, G. L. Barthauer, and A. V. Metler, Ind. Eng. Chem. Anal. Ed. 18, 407 (1946).
4. M. R. Cines, J. T. Roach, R. J. Hogan, and C. H. Roland, Chem. Eng. Prog. Symposium Ser. No. 6, 49, 1 (1953).
5. M. W. Cook, "Solubility of Hydrogen in Nonpolar Solvents," University of California Radiation Laboratory Report No. UCRL-2459, 1954.
6. W. S. Corak and A. Wexler, Rev. Sci. Instr. 24, 994 (1953).
7. C. Cuthbertson and M. Cuthbertson, Phil. Trans. Roy. Soc. (London) A213, 1 (1914).
8. B. F. Dodge and A. K. Dunbar, J. Am. Chem. Soc. 49, 591 (1927).
9. B. F. Dodge and H. N. Davis, J. Am. Chem. Soc. 49, 610 (1927).
10. J. D. Edwards, J. Am. Chem. Soc. 39, 2383 (1927).
11. M. G. Gonickberg, V. G. Fastovskii, and I. G. Gurech, Acta Physicochim. U.R.S.S. 11, 865-82 (1939).
12. R. Griffiths, "Thermostats," Chas. Griffin, London, 1951.
13. R. Haase, Z. Naturforsch, 8a, 380 (1953).
14. F. E. Harris and L. K. Nash, Anal. Chem. 22, 1552 (1950).
15. E. F. G. Herington, Nature 160, 610 (1947).
16. J. H. Hildebrand and R. L. Scott, "The Solubility of Non-Electrolytes," Am. Chem. Soc. Monograph No. 17, 3rd ed. Guinn, New York
17. A. Huber, Monatsh. Chem. 84, 372 (1953).
18. International Critical Tables, Vol. VII, p. 7, McGraw-Hill New York, 1930.
19. J. E. Jacobs and R. R. Wilson, Electronics 24, 172, 176, 180, 184, 188, 192, 196 (October 1951).

20. G. Karagunis, A. Hawkins, and G. Damkoler, Z. physik. Chem A151, 433 (1930).

21. F. G. Keyes, "Gas Thermometer Corrections Based on an Objective Correlation of Available Data for H_2, He and N_2," in "Temperature," Reinhold Publ. Co., New York, 1941, p. 45-59.

22. Kuo Tsung Yu and J. Corill, Chem. Eng. Progr. Symposium Ser. No. 2, 48, 38-45 (1952).

23. A. Langer, Rev. Sci. Instr. 18, 101 (1947).

24. M. Lounsbury, Rev. Sci. Instr. 22, 533 (1951).

25. R. J. Lunbeck and J. H. Roerboom, Physica 17, 77 (1951).

26. O. Mohr, Z. angew. Chem. 25, 1313 (1912).

27. NACA-NBS. Table of Vapor Pressure of Nitrogen. Table 11.50 (1950).

28. A. Opler and E. S. Smith, Anal. Chem. 25, 686 (1953).

29. D. F. Othmer, Ind. Eng. Chem. 32, 841 (1940).

30. D. F. Othmer, L. G. Ricciardi, and M. S. Takar, Ind. Eng. Chem. 45, 1815 (1953).

31. J. H. Perry (Editor in Chief), Chemical Engineers Handbook, 3rd ed., McGraw-Hill New York 1950, p. 205.

32. Ramsay and Trovers, Proc. Roy. Soc. (London) 62, 225 (1897).

33. O. Redlich and A. T. Kister. Ind. Eng. Chem. 40, 345 (1948).

34. O. Redlich, A. T. Kister, and C. E. Turnquist. Chem. Eng. Progr. Symposium Ser. No. 2, 48, 49-61 (1952).

35. O. Redlich and J. N. S. Kwong, Chem. Rev. 44, 233 (1949).

36. O. Redlich, Personal communication (1954).

37. C. S. Robinson and E. R. Gilliland, "Elements of Fractional Distillation," 4th Ed., McGraw-Hill, New York, 1950, p. 3-15.

38. M. Ruhemann and N. Zinn, Physik. Z. Sowjetunion 12, 389 (1937).

39. F. C. Schiller and L. N. Canjar, Chem. Eng. Progr. Symposium Ser. No. 6, 49, 25 (1953).

40. F. Steckel and N. Zinn, Zhur. Khim. Prom. 16, No. 8, 24 (1939).

41. H. H. Stotler and M. Benedict, Chem. Eng. Progr. Symposium Ser. No. 6, 49, 25 (1953).

42. R. C. Taylor and W. S. Young, Ind. Eng. Chem. Anal. Ed. 17, 811 (1945).

43. J. L. Thomas, "Temperature, its Measurement and Control in Science and Industry," Reinhold, New York, 1941, p. 159.

44. N. Torocheshnokov, Tech. Phys. U.S.S.R. 4, No. 5, 365 (1937).

45. S. Valentiner and O. Zimmer. Ber. deut. physik. Ges. Verhandlungen 15, 1301 (1913).

46. T. T. H Verschoyle, Phil. Trans. Roy. Soc. (London) A230, 189 (1931).

47. A. Wexler and W. S. Cox, Rev. Sci. Instr. 22, 941 (1951).

48. W. P. White, J. Am. Chem. Soc. 56, 20(1934).

49. W. E. Williams, Jr. and E. Maxwell, Rev. Sci. Instr. 25, 111 (1954).